excelencia UAM CSIC+

UAM UNIVERSIDAD AUTONOMA DE MADRID

Applications of nanostructured porous silicon in biomedicine

Raúl J. Martín Palma

Departamento de Física Aplicada
Universidad Autónoma de Madrid
(rauljose.martin@uam.es)

FACULTAD DE CIENCIAS

www.uam.es

Outline

- Introduction: What is Nanotechnology? Examples and applications.
- What is porous silicon? Why is it interesting?
- How is porous silicon fabricated?, how does it look like?
- Key properties.
- Applications: From photonics to biomedicine.
- Summary

What is Nanotechnology?

“Nanotechnology is the understanding and control of matter at dimensions between approximately 1 and 100 nanometers, where unique phenomena enable novel applications. Encompassing nanoscale science, engineering, and technology, nanotechnology involves imaging, measuring, modeling, and manipulating matter at this length scale.”

(http://www.nano.gov/html/facts/whatIsNano.html, Accessed 03 June 2009)

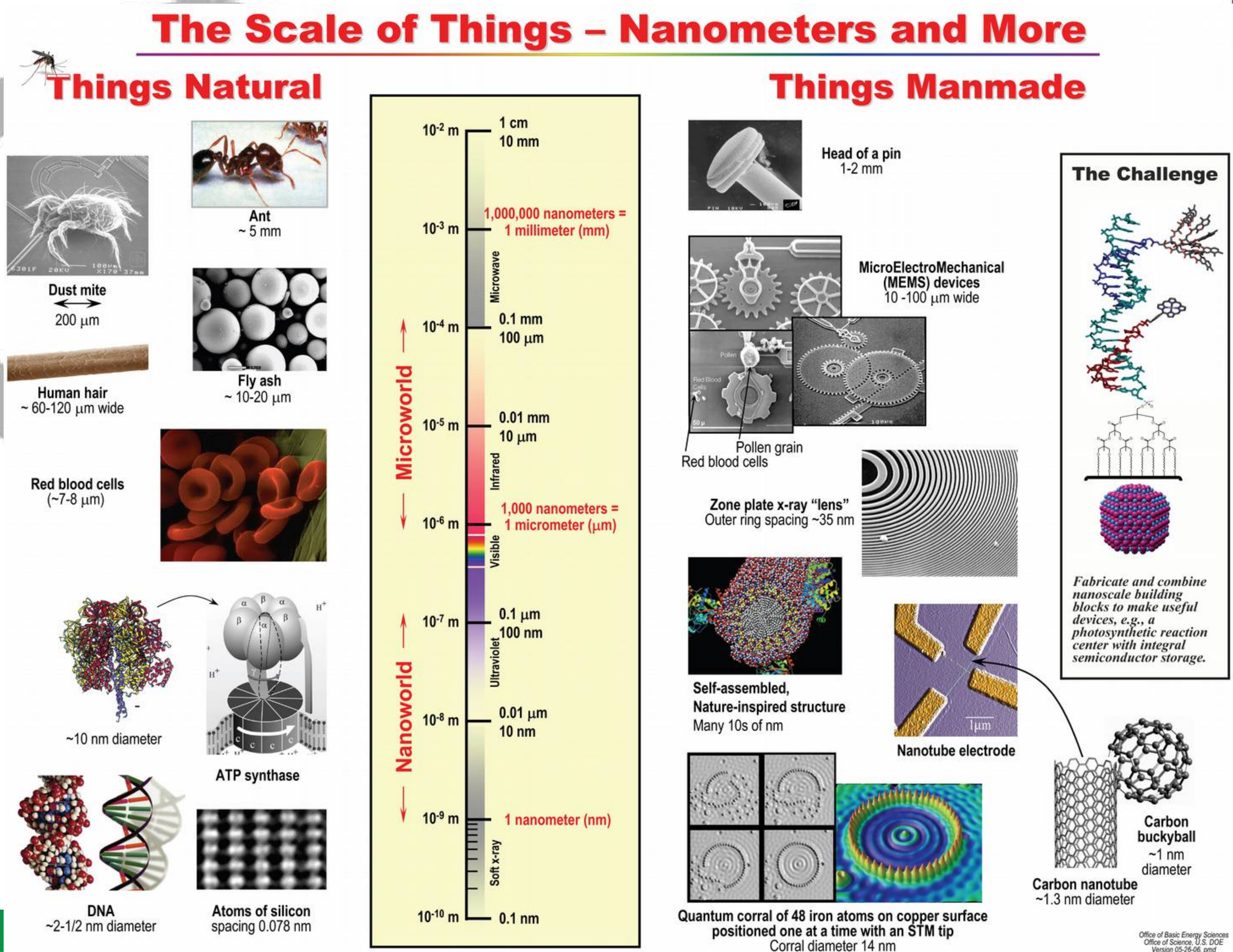

The Scale of Things – Nanometers and More
Things Natural
Things Manmade
Dust mite
200 µm
Ant
~ 5 mm
Human hair
~ 60-120 µm wide
Fly ash
~ 10-20 µm
Red blood cells
(~7-8 µm)
~10 nm diameter
ATP synthase
DNA
~2-1/2 nm diameter
Atoms of silicon
spacing 0.078 nm
10-2 m
1 cm
10 mm
10-3 m
1,000,000 nanometers =
1 millimeter (mm)
Microwave
10-4 m
0.1 mm
100 µm
Microworld
10-5 m
0.01 mm
10 µm
Infrared
10-6 m
1,000 nanometers =
1 micrometer (µm)
Visible
10-7 m
0.1 µm
100 nm
Ultraviolet
Nanoworld
10-8 m
0.01 µm
10 nm
10-9 m
1 nanometer (nm)
Soft x-ray
10-10 m
0.1 nm
Head of a pin
1-2 mm
MicroElectroMechanical
(MEMS) devices
10 -100 µm wide
Pollen grain
Red blood cells
Zone plate x-ray "lens"
Outer ring spacing ~35 nm
Self-assembled,
Nature-inspired structure
Many 10s of nm
Nanotube electrode
1µm
Quantum corral of 48 iron atoms on copper surface
positioned one at a time with an STM tip
Corral diameter 14 nm
Carbon nanotube
~1.3 nm diameter
Carbon
buckyball
~1 nm
diameter
The Challenge
Fabricate and combine
nanoscale building
blocks to make useful
devices, e.g., a
photosynthetic reaction
center with integral
semiconductor storage.
Office of Basic Energy Sciences
Office of Science, U.S. DOE
Version 05-26-06, pmd
www.uam.es

Examples

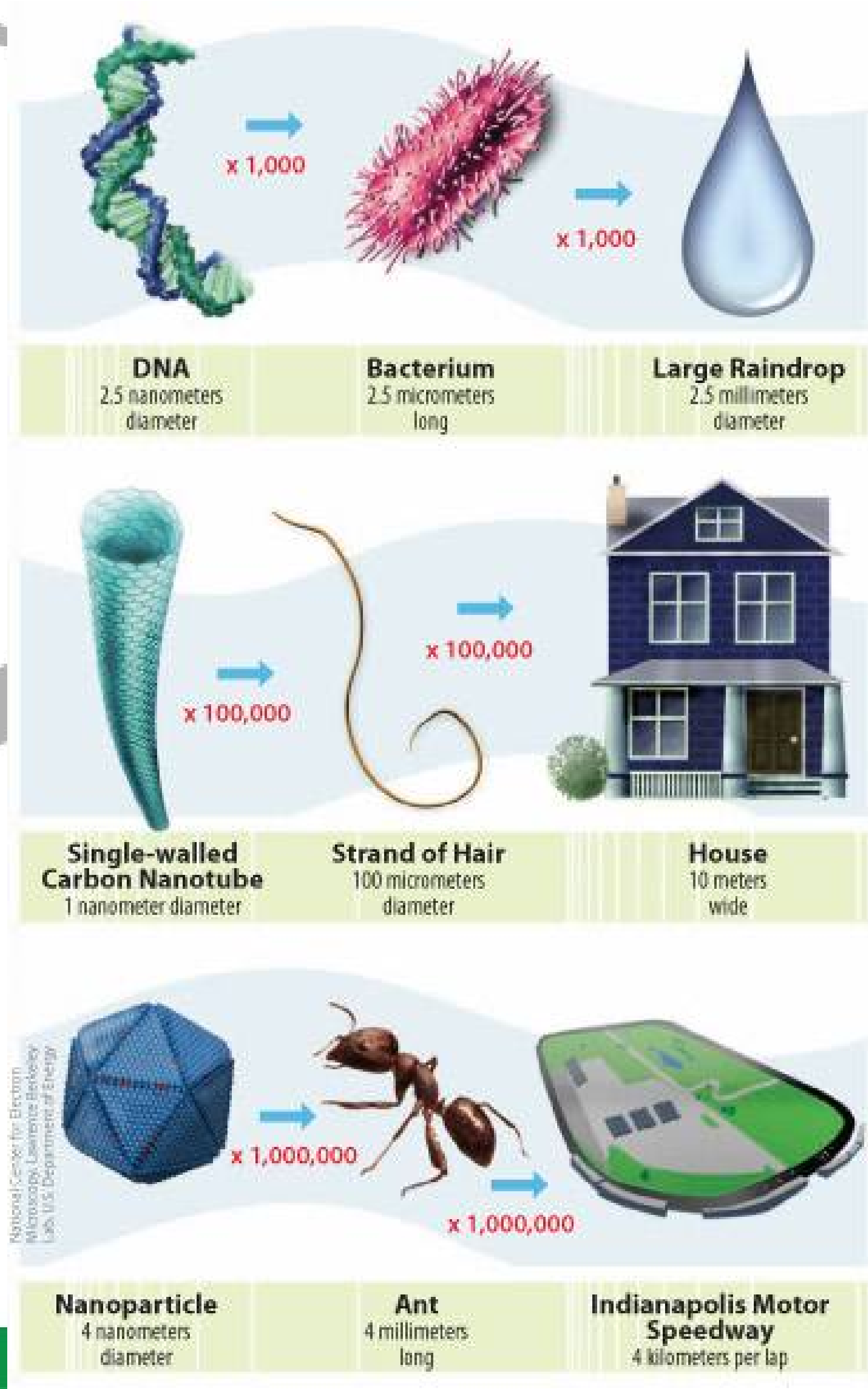

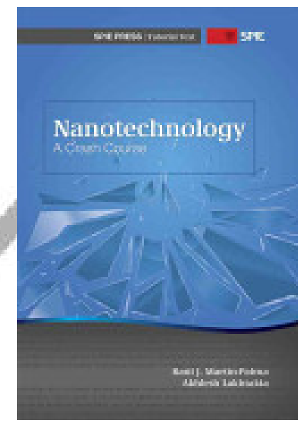

Martín-Palma & Lakhtakia
SPIE Press 2010

Nanotechnology Applications and Products

Drug-Delivery Techniques

Dendrimers are a type of nanostructure that can be precisely designed and manufactured for a wide variety of applications, including treatment of cancer and other diseases. Dendrimers carrying different materials on their branches can do several things at one time, such as recognizing diseased cells, diagnosing disease states (including cell death), drug delivery, reporting location, and reporting outcomes of therapy.

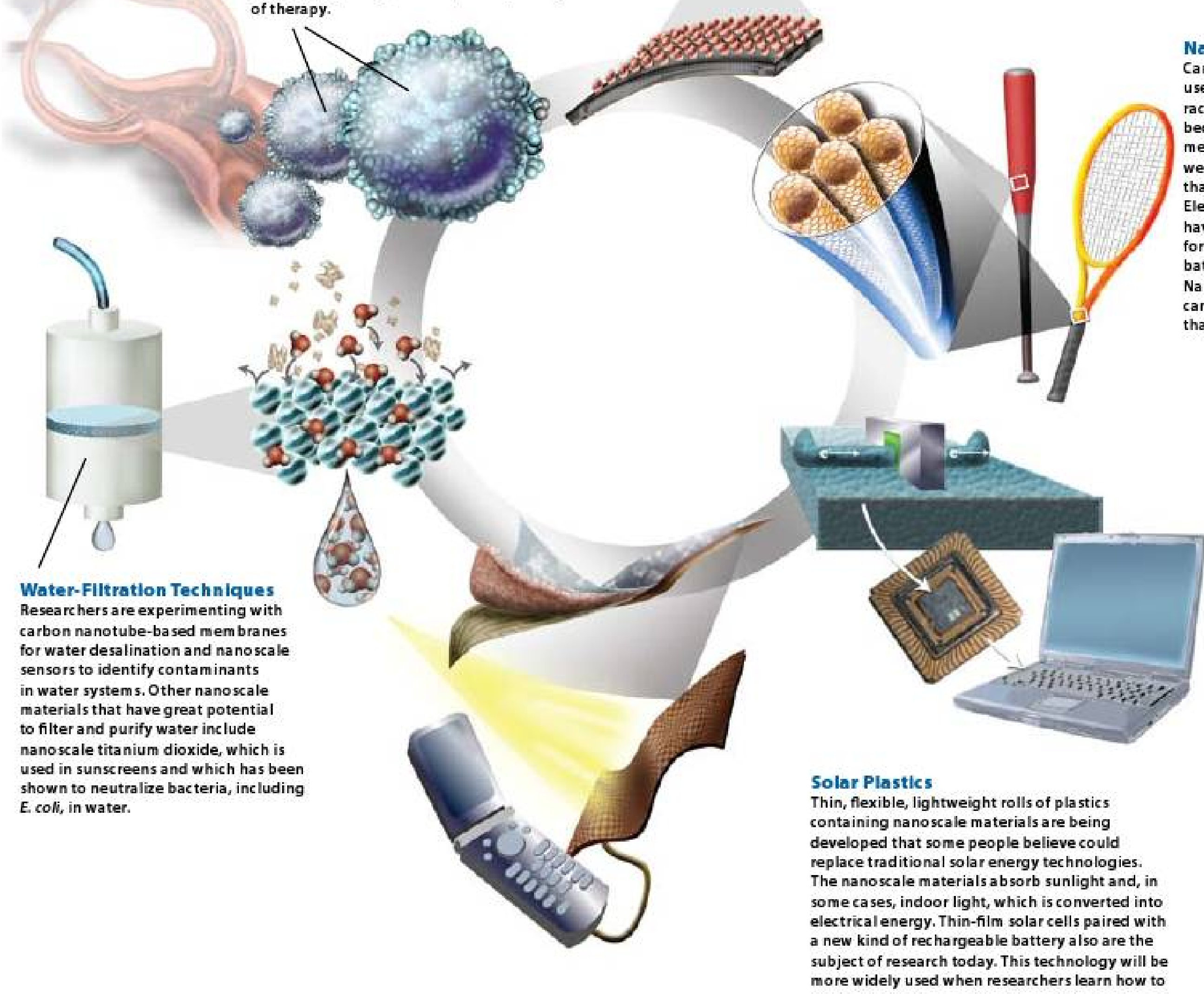

Nanofilms

Different nanoscale materials can be used in thin films to make them water-repellent, anti-reflective, self-cleaning, ultraviolet or infrared-resistant, anti-fog, anti-microbial, scratch-resistant, or electrically conductive. Nanofilms are used now on eyeglasses, computer displays, and cameras to protect or treat the surfaces.

Nanotubes

Carbon nanotubes (CNTs) are used in baseball bats, tennis racquets, and some car parts because of their greater mechanical strength at less weight per unit volume than that of conventional materials. Electronic properties of CNTs have made them a candidate for flat panel displays in TVs, batteries, and other electronics. Nanotubes for various uses can be made of materials other than carbon.

Nanoscale transistors

Transistors are electronic switching devices where a small amount of electricity is used like a gate to control the flow of larger amounts of electricity. In computers, the more transistors, the greater the power. Transistor sizes have been decreasing, so computers have become more powerful. Until recently, the industry's best commercial technology produced computer chips having transistors having 65-nanometer features. Recent announcements indicate that 45-nanometer feature technology soon will be here.

Water-Filtration Techniques

Researchers are experimenting with carbon nanotube-based membranes for water desalination and nanoscale sensors to identify contaminants in water systems. Other nanoscale materials that have great potential to filter and purify water include nanoscale titanium dioxide, which is used in sunscreens and which has been shown to neutralize bacteria, including *E. coli*, in water.

Solar Plastics

Thin, flexible, lightweight rolls of plastics containing nanoscale materials are being developed that some people believe could replace traditional solar energy technologies. The nanoscale materials absorb sunlight and, in some cases, indoor light, which is converted into electrical energy. Thin-film solar cells paired with a new kind of rechargeable battery also are the subject of research today. This technology will be more widely used when researchers learn how to capture solar energy more efficiently.

Silicon in the field of photonics

- Advantages:
    - Is abundant.
    - Tremendous base technology that has developed around it.
    - Superior mechanical and thermal properties.
    - Possibility to form an excellent passivating oxide.
    - Technology is much less hazardous to the environment than other technologies.

- Drawbacks:
    - Si is lacking the properties necessary to emit light efficiently: Cannot be used for optically active or optoelectronic applications.

It is of great importance to develop a technology that allows optical and electronic devices to be easily and inexpensively integrated on Si wafers.

Light emission from nanostructured porous silicon

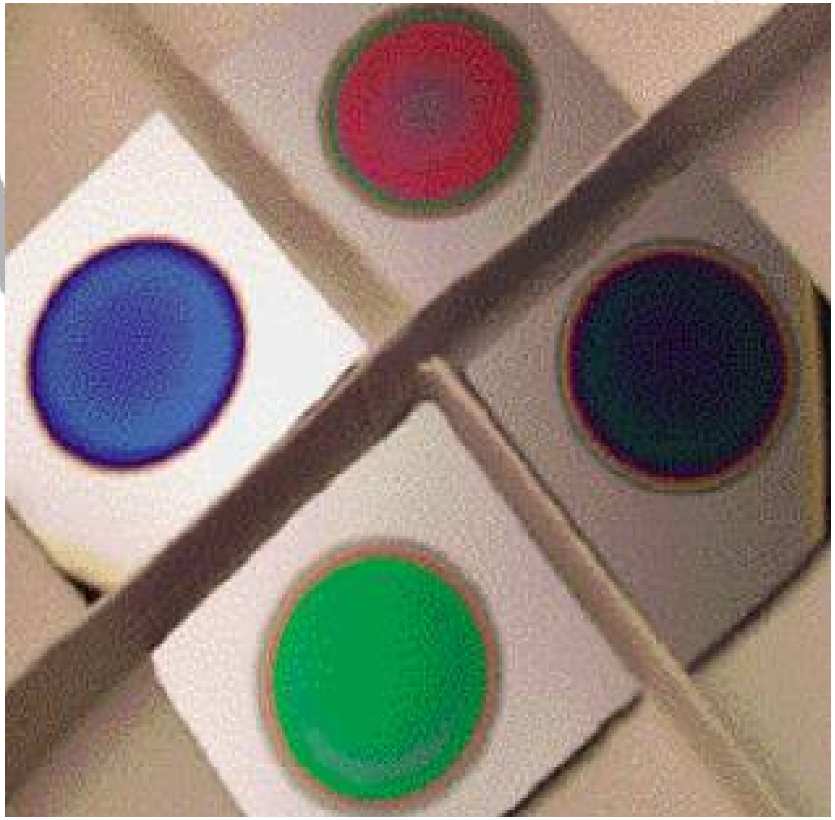

G. Marsh, Materials Today, January 2002.

- Emission energy well above the bandgap of bulk Si.
- The energy (color) can be tuned throughout the visible (NIR) spectrum.
- Quantum efficiency comparable to that of direct-bandgap (compound) semiconductors.

Nanostructured porous silicon

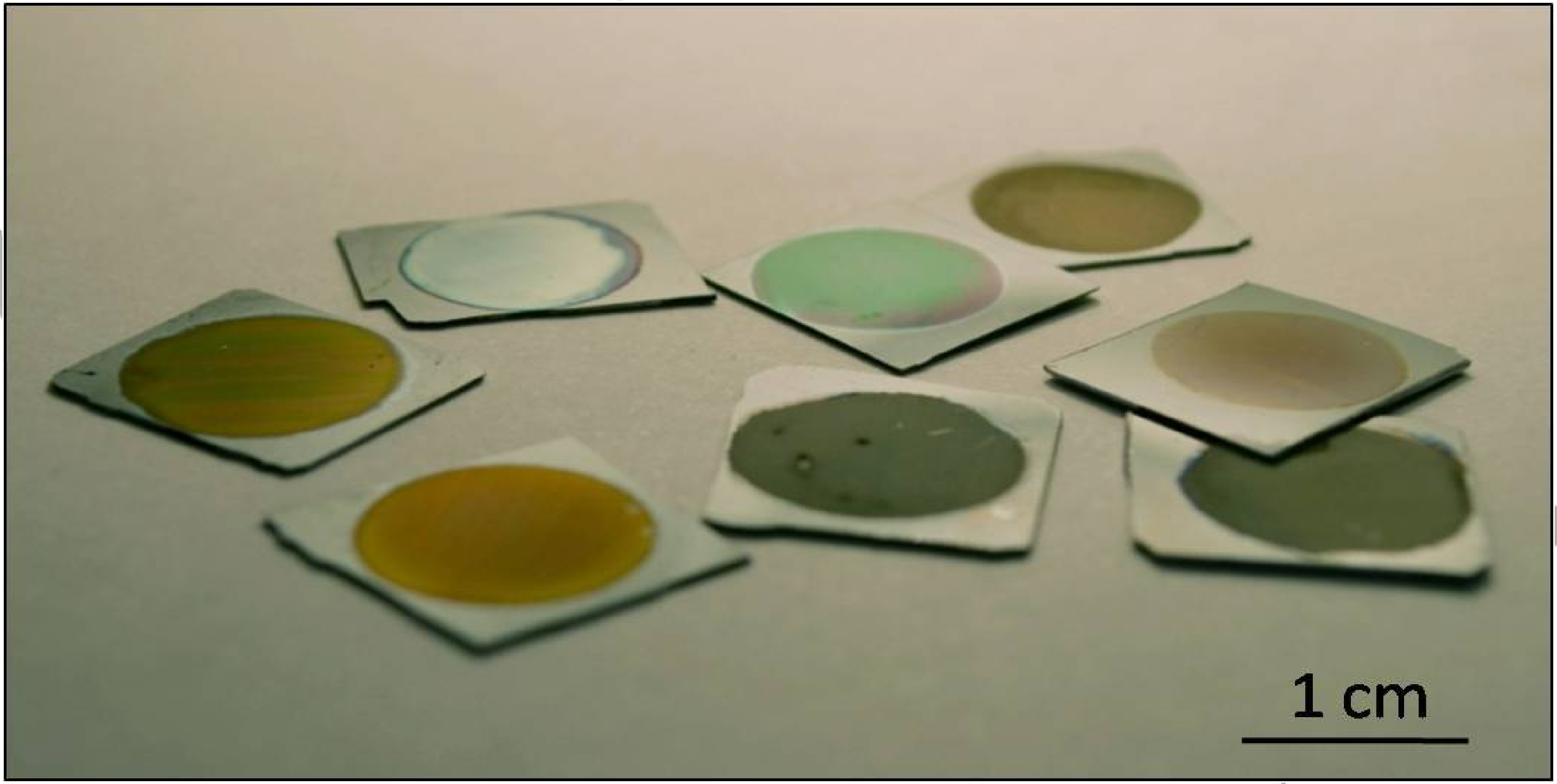

J. Hernández-Montelongo, Á. Muñoz-Noval, J.P. García-Ruíz, V. Torres-Costa, R.J. Martín-Palma, and M. Manso-Silván, Frontiers in Bioengineering and Biotechnology 3, 60 (2015).

What is porous silicon?

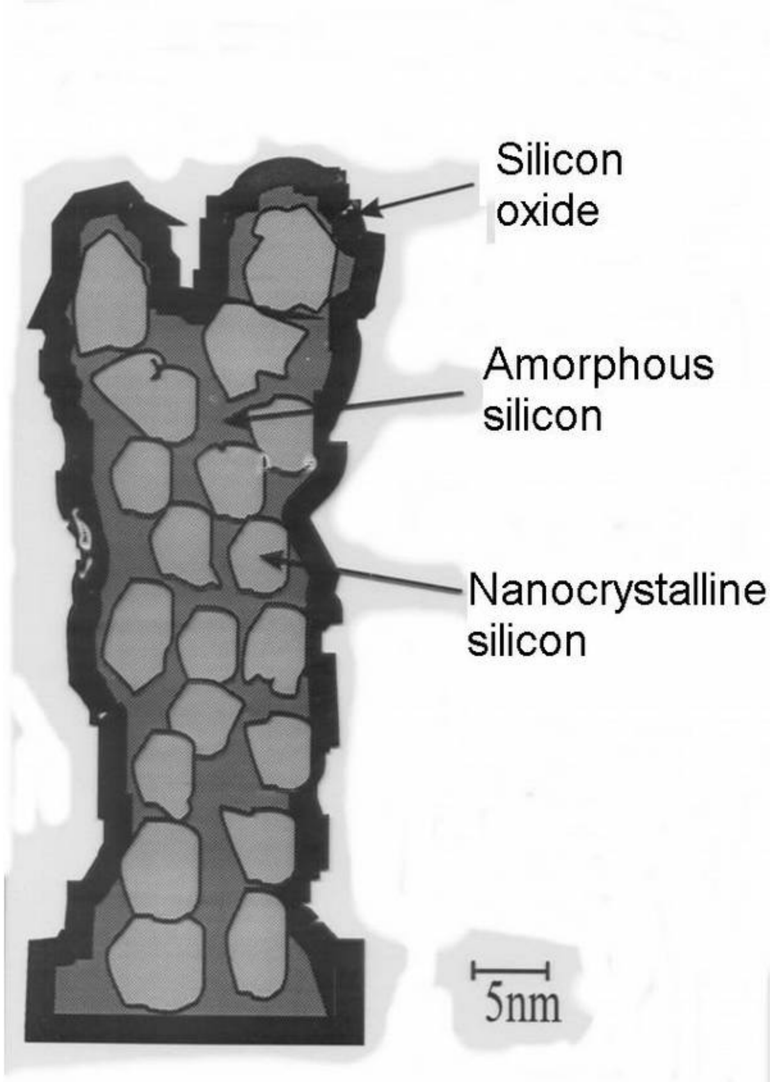

Network of nanometer-sized Si regions surrounded by void space

Shows quantum size effects

Emission in the visible: Quantum confinement

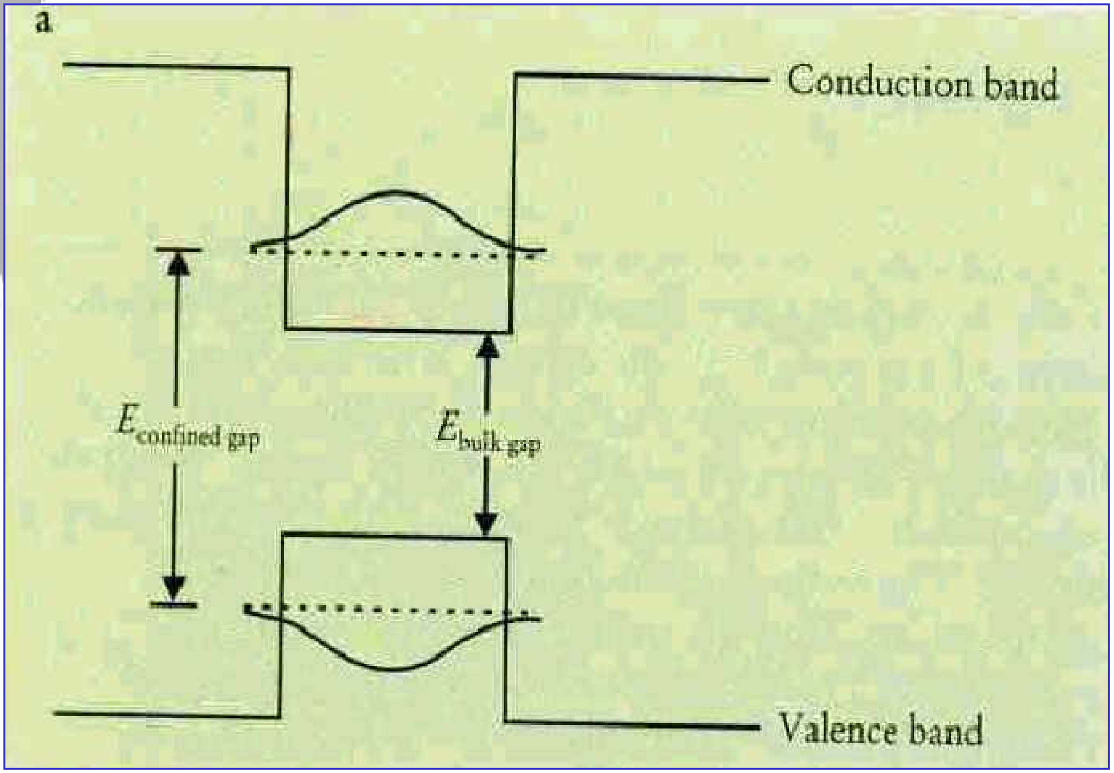

Semiconductor quantum well:

Electrons and holes are confined spatially by potential barriers (surface of nanocrystals, Si/SiO_2 interface, ...).

The lowest energy optical transition from the VB to the CB increases in energy, effectively increasing the bandgap.

Simple effective-mass approximation:

$$E_{confined-gap} = E_{bulk-gap} + \frac{h^2}{8} \times \left[\frac{1}{w_x^2} + \frac{1}{w_y^2} + \frac{1}{w_z^2} \right] \times \left[\frac{1}{m_c^*} + \frac{1}{m_v^*} \right]$$

More sophisticated calculations:

- Nonparabolicity of the CB.
- Detailed shape of the VB.
- Influence of the neighboring bands.
- Excitonic contributions.

Tunability of color: Quantum confinement

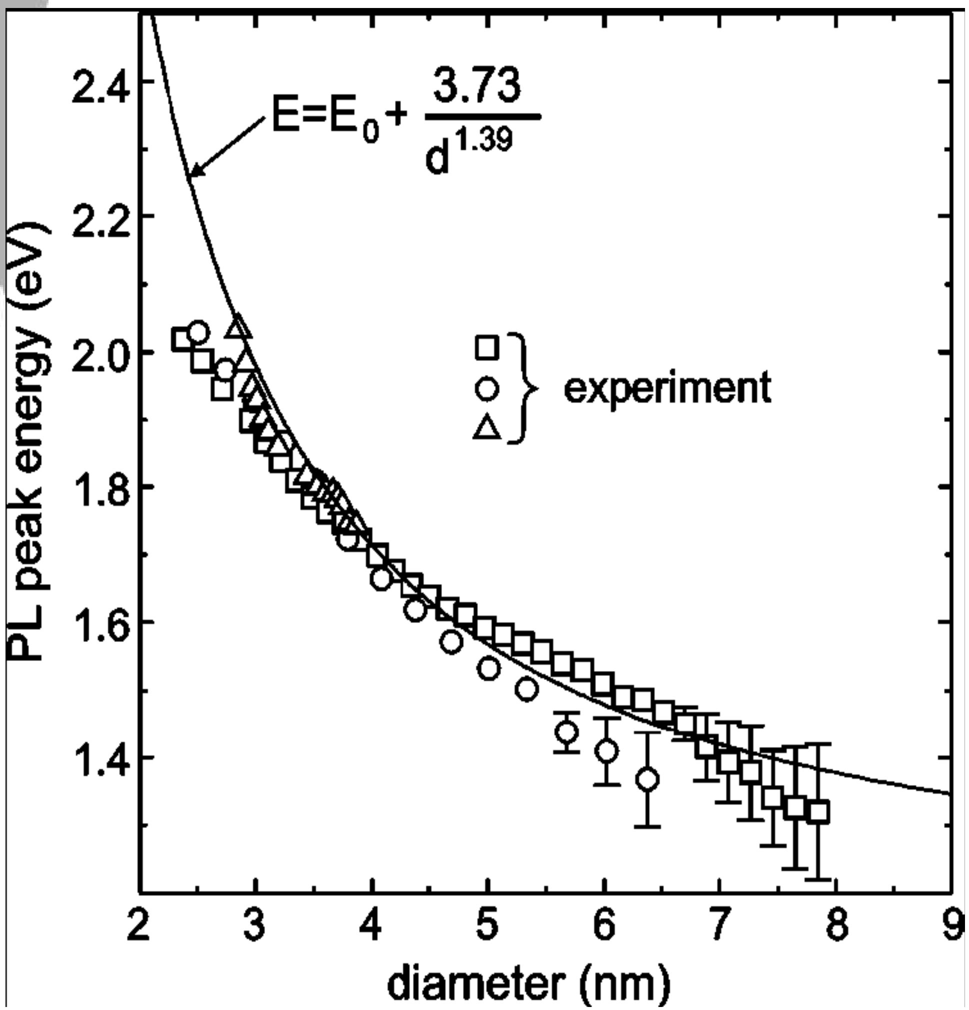

The size of the confined bandgap grows as the characteristic dimensions of the crystallite decreases.

↓

The emission spectrum shifts to higher energy as the particle size decreases.

Visible PL and tunability are a consequence of quantum size effects.

G. Ledoux *et al.*, APL 80,4834 (2002).

Increased quantum efficiency

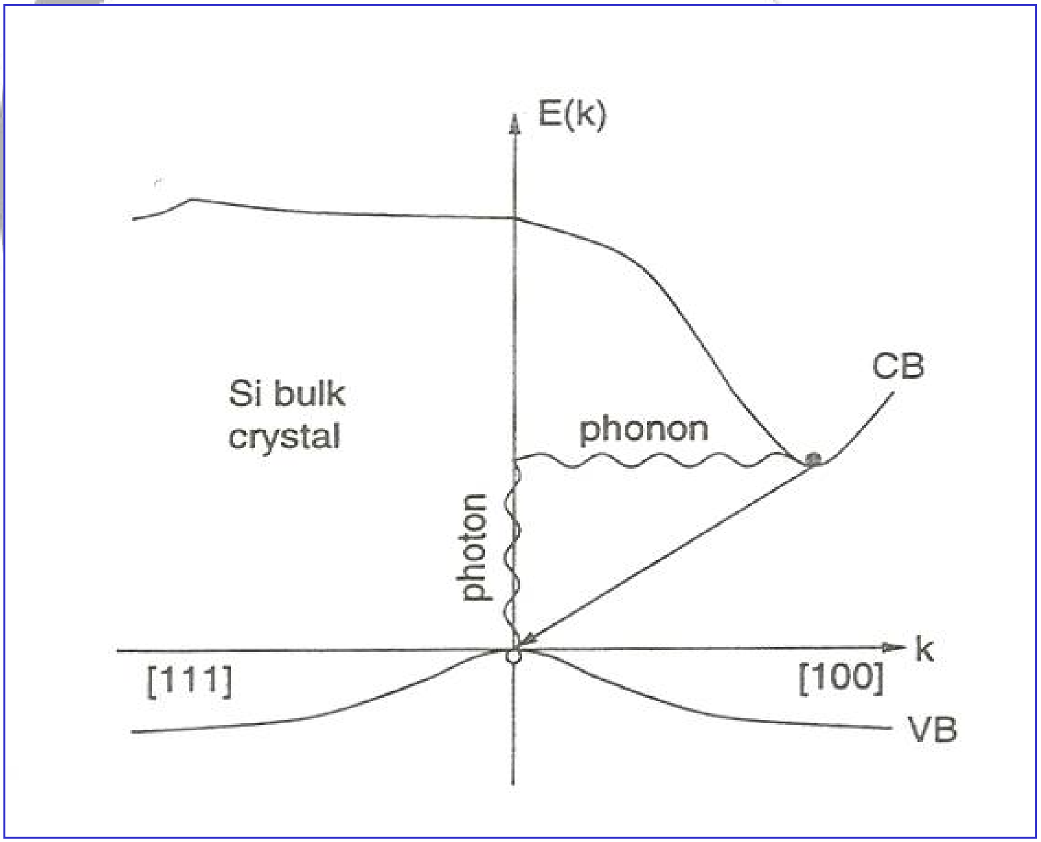

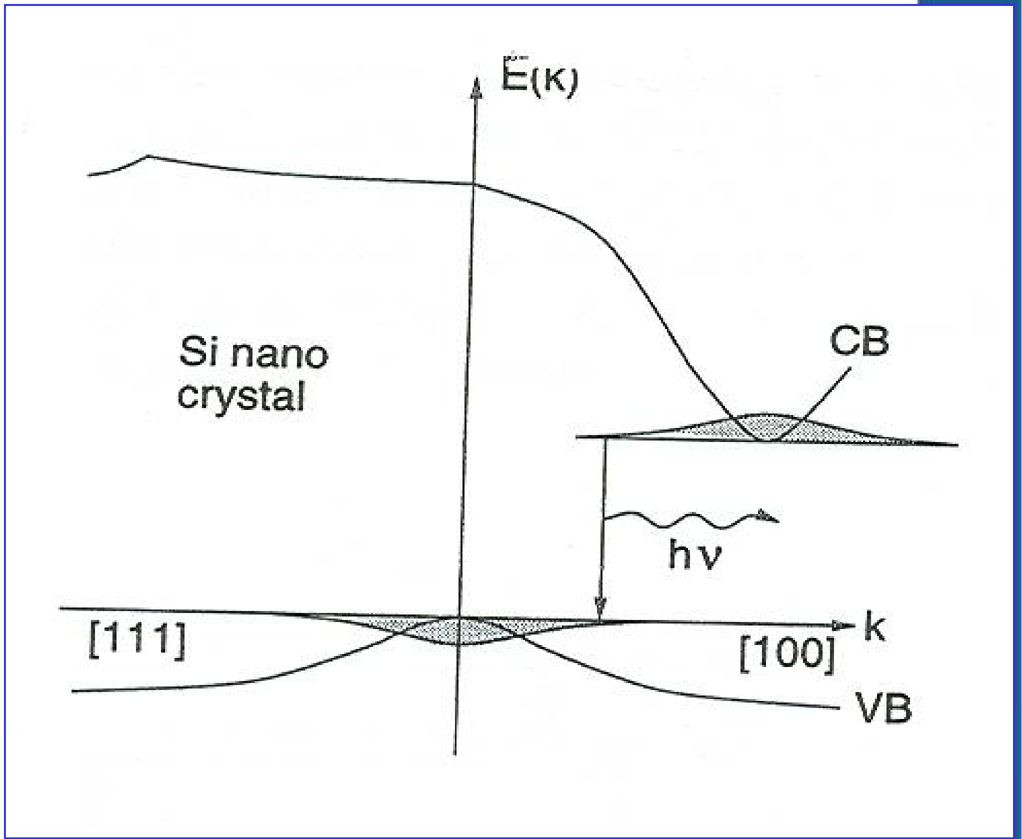

Poor optoelectronic behavior caused by the indirect bandgap:

The extreme of the bands are located at different *k* values → A transition process requires a change of the wave vector → Interation with phonons → Less efficient process

Heisenberg uncertainty principle: $\Delta x \Delta p \geq \hbar/2$

↓

Increased probability distribution

↓

Increased radiative recombination rate

History

- Discovered by Uhlir in 1956 at Bell Labs. Bulk Si was transformed into a porous material when subjected to an electrochemically forced dissolution process in HF: A. Uhlir, Bell System Tech. J. 35, 333 (1956).
- First practical application: dielectric in Si-on-insulator (SOI) technology (80’s).
- Canham reported an intense orange/red photoluminescence and at room temperature: L.T. Canham, Appl. Phys. Lett. 57, 1046 (1990).
- Electroluminescence demonstrated in 1992: N. Koshida and H. Koyama, Appl. Phys. Lett. 60, 347 (1992).

Fabrication

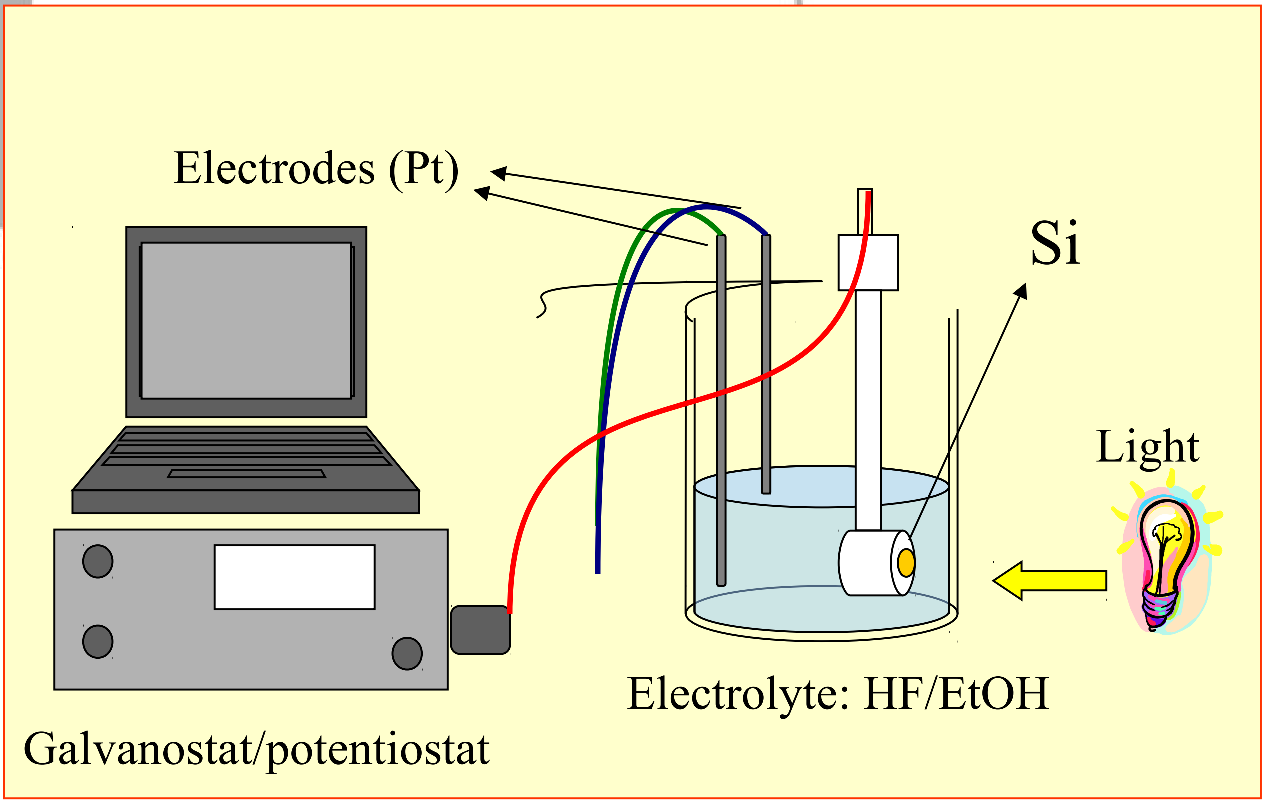

PS is formed by the electrochemical etch of Si in HF-based solutions. Chemical etching is also possible ...

The particular structure depends on:

- Formation method (chemical/electrochemical).
- Concentration of the components of the solution.
- Etching time.
- Current density (electrochemical).
- Post-formation process.
- Presence of light.
- Temperature.

Morphology

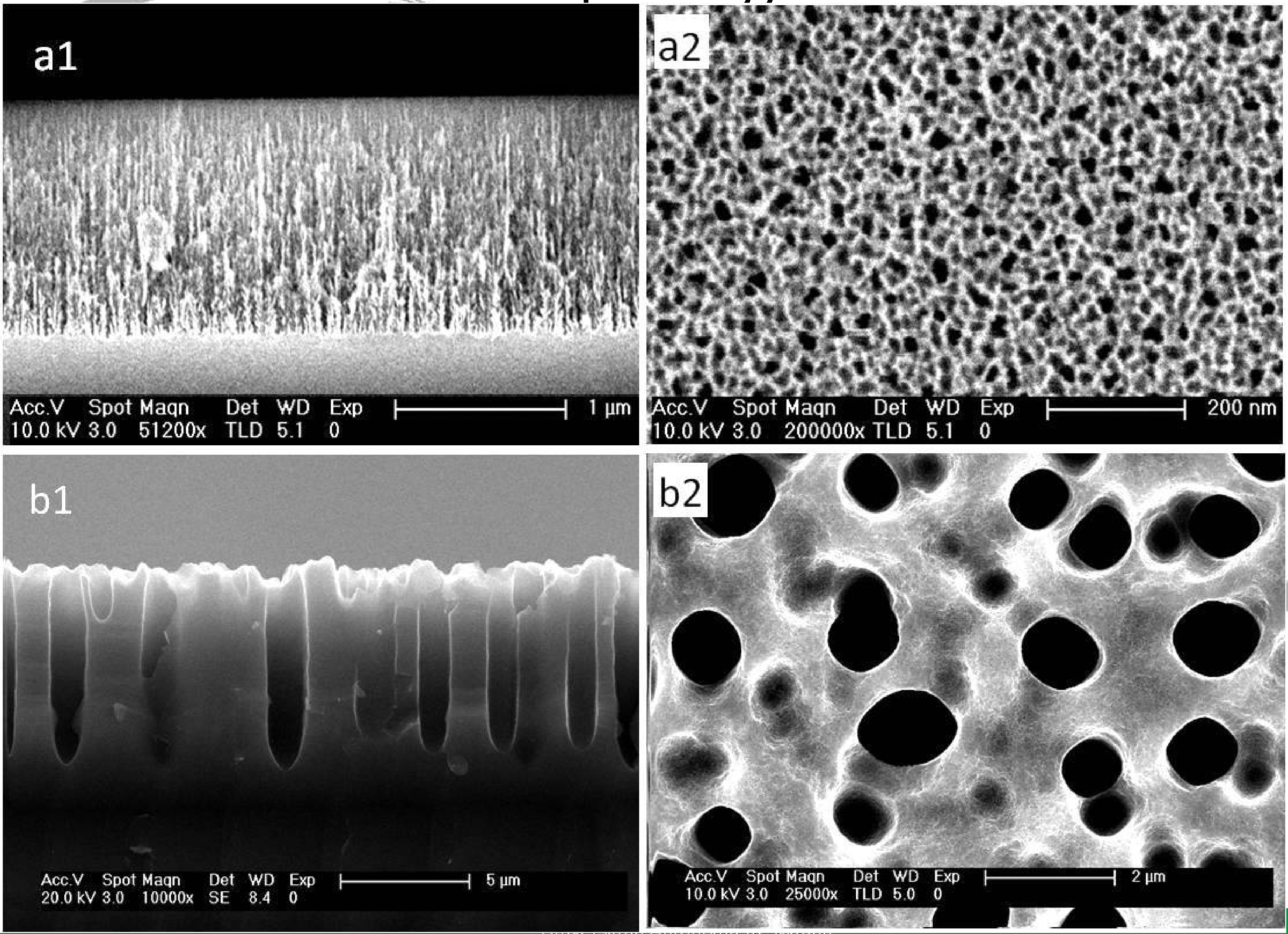

Nanostructured porous silicon-mediated drug delivery, R.J. Martín-Palma *et al.*, Expert Opinion on Drug Delivery 11(8), 1273 (2014).

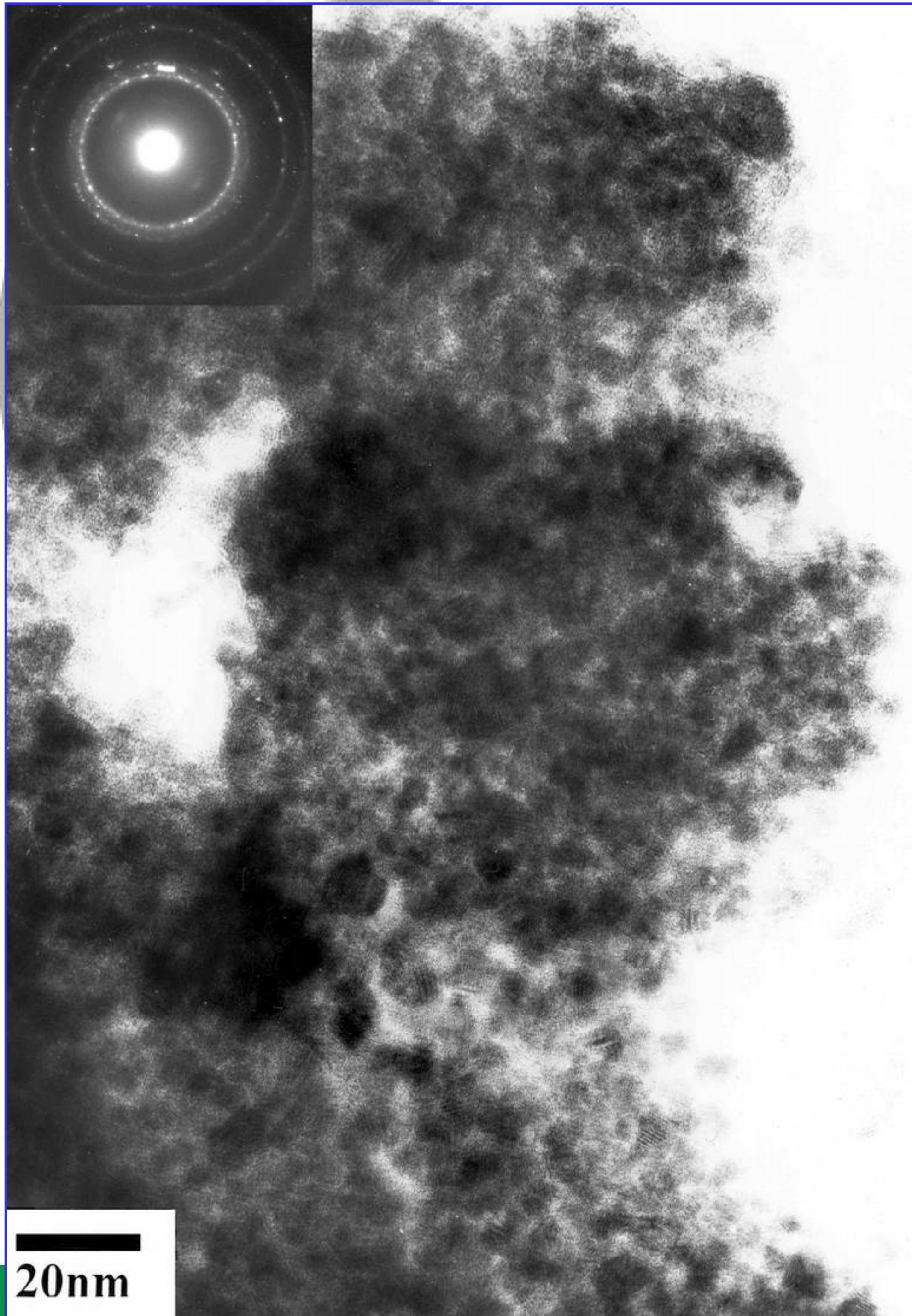

Morphology (cont'd)

NanoPS consists in an amorphous matrix with Si crystallites embedded in it that retain the substrate crystallinity:

- Round shape
- Characteristic dimensions: 20 - 80 Å
- No preferential orientation: Policrystalline diffraction pattern

R.J. Martín-Palma, L. Pascual, P. Herrero and J.M. Martínez-Duart, Applied Physics Letters 81, 25 (2002).

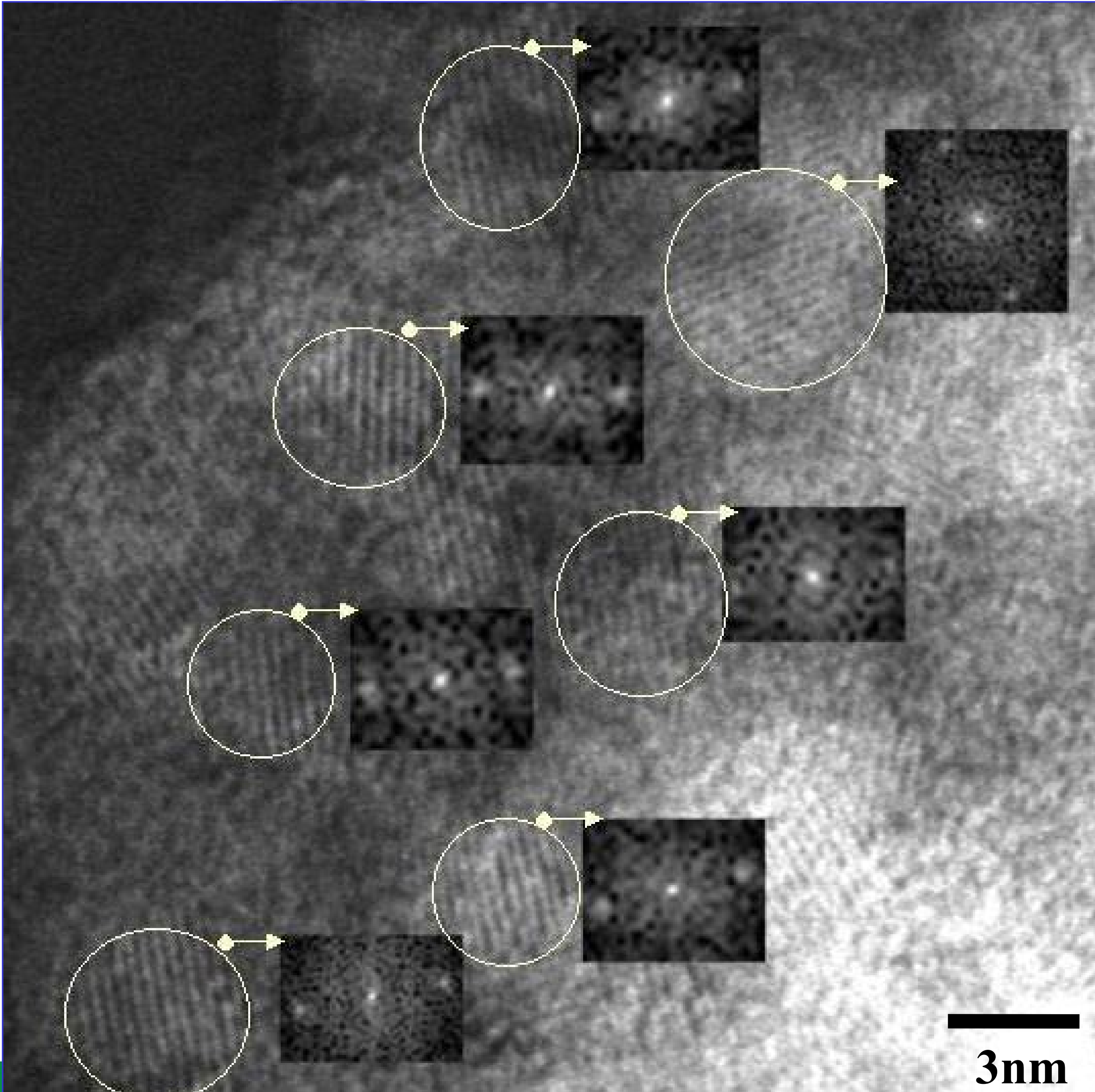

R.J. Martín-Palma, L. Pascual, P. Herrero and J.M. Martínez-Duart, *Applied Physics Letters* 81, 25 (2002).

Size of the individual Si crystallites

The size of the individual Si crystallites was directly determined.

↓

All the data were fitted to Gaussian distributions.

Individual Si crystallites:

20 Å – 80 Å

Center: 45.89 Å

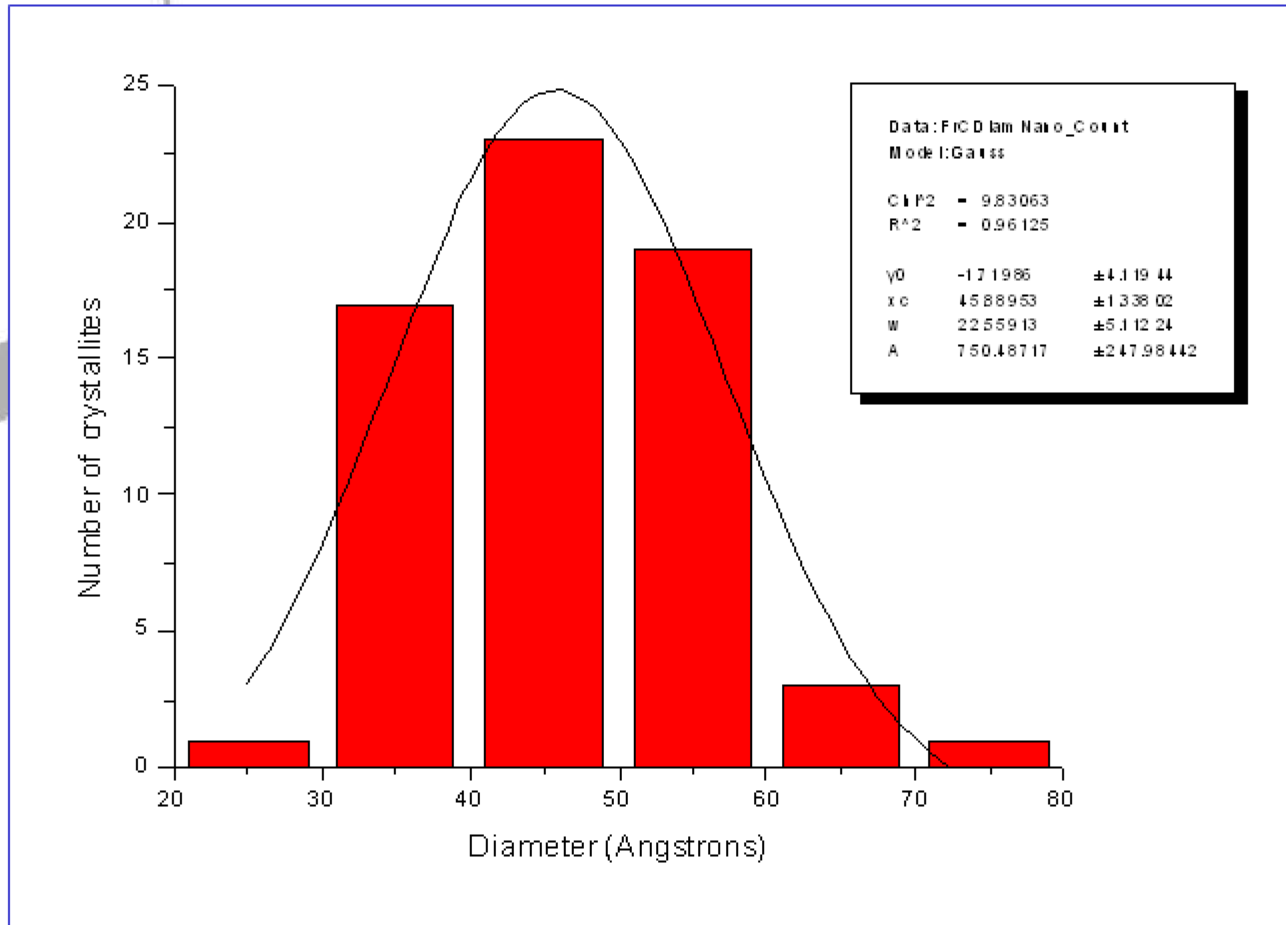

The size distribution affects the properties of PS

Photoluminescence

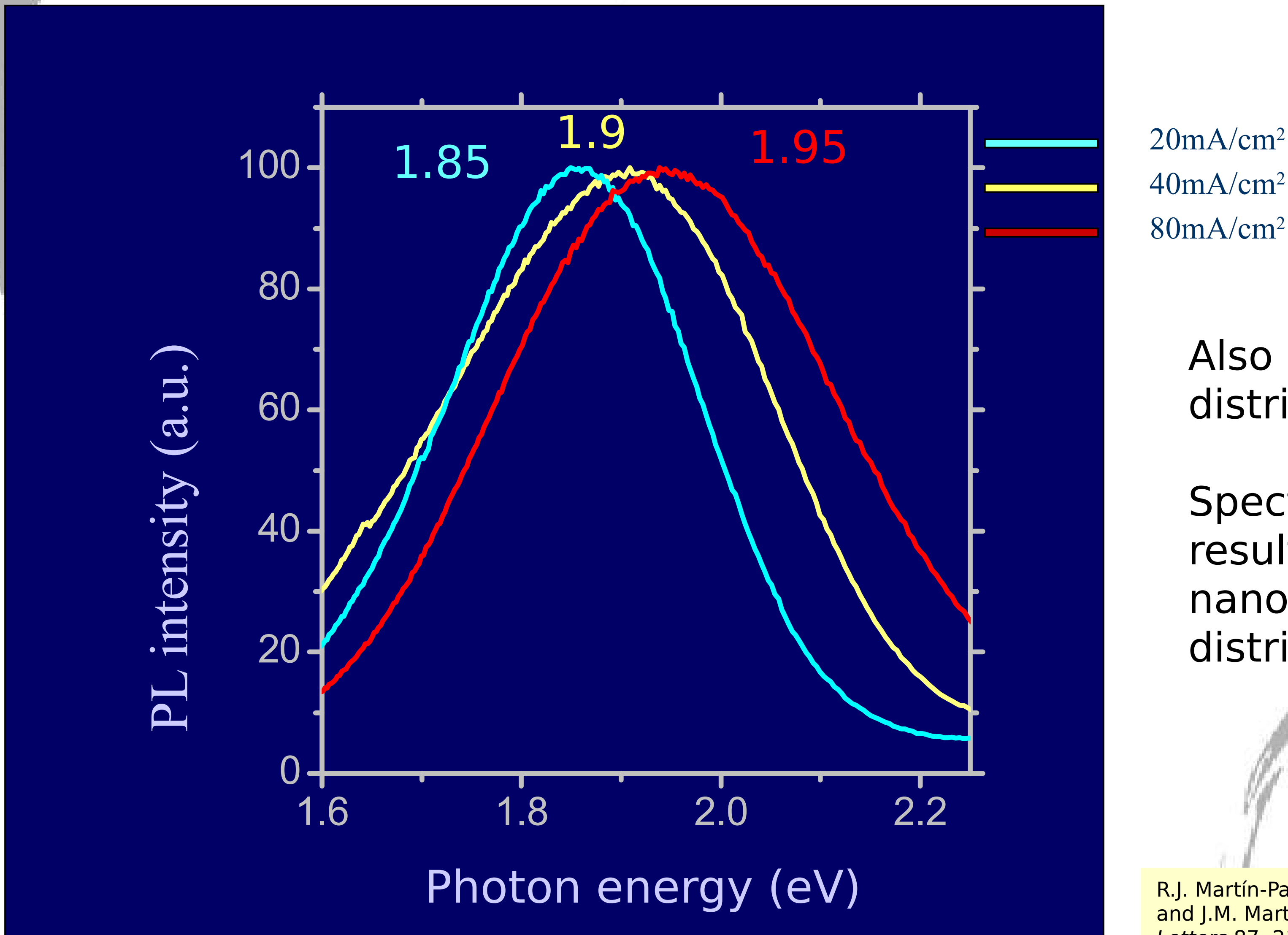

Also Gaussian distribution!!!

Spectral width result of the nanocrystal size distribution

R.J. Martín-Palma, L. Pascual, P. Herrero and J.M. Martínez-Duart, *Applied Physics Letters* 87, 211906 (2005).

Porous SiGe

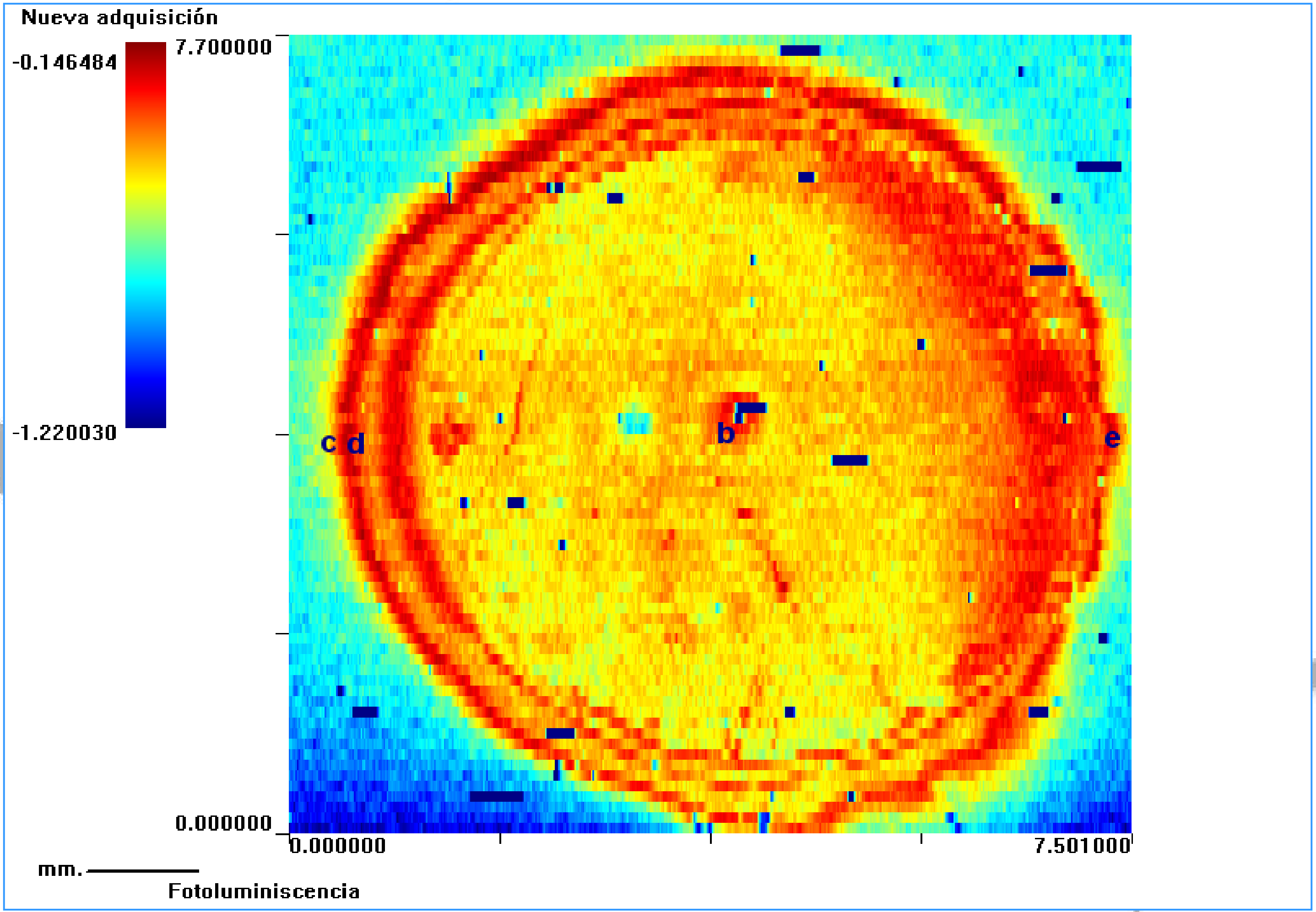

T. Del Caño, L. F. Sanz, P. Martín, M. Avella, J. Jiménez, A. Rodríguez, J. Sangrador, T. Rodríguez, V. Torres-Costa, R. J. Martín-Palma, and J. M. Martínez-Duart, *Journal of The Electrochemical Society* 151, C326 (2004).

PS/Si interface

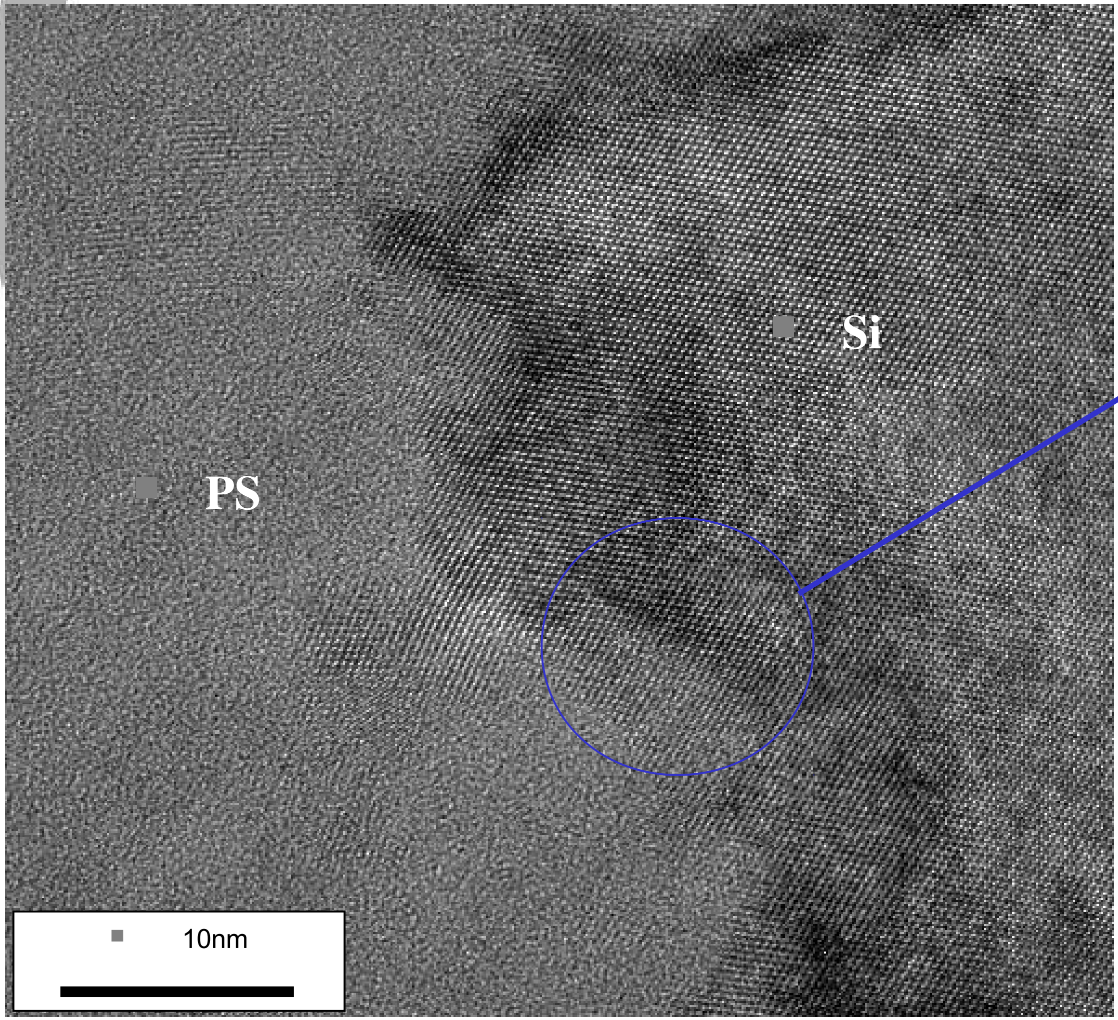

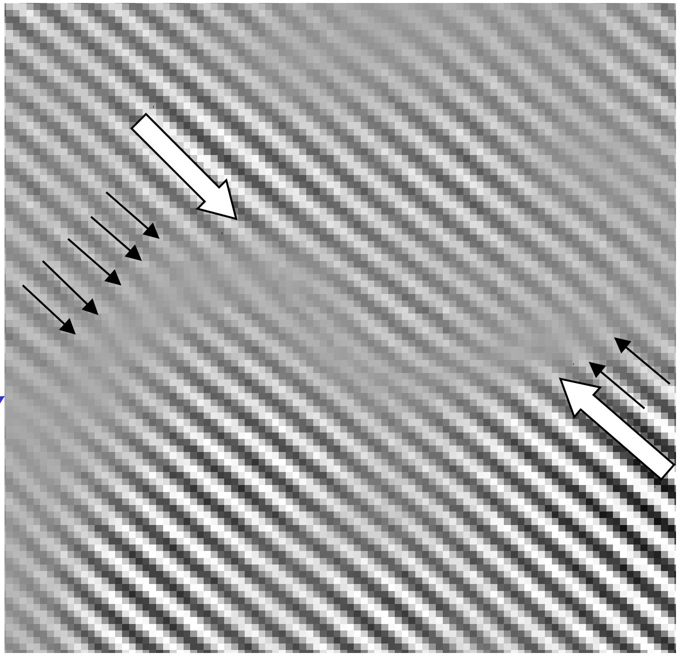

- High density of dislocations.
- Significant effect on the overall behavior (anomalous absorption, leak currents, etc.).

R.J. Martín-Palma, L. Pascual, A. Landa, P. Herrero and J.M. Martínez-Duart, *Applied Physics Letters* 85, 2517 (2004).

Multilayers

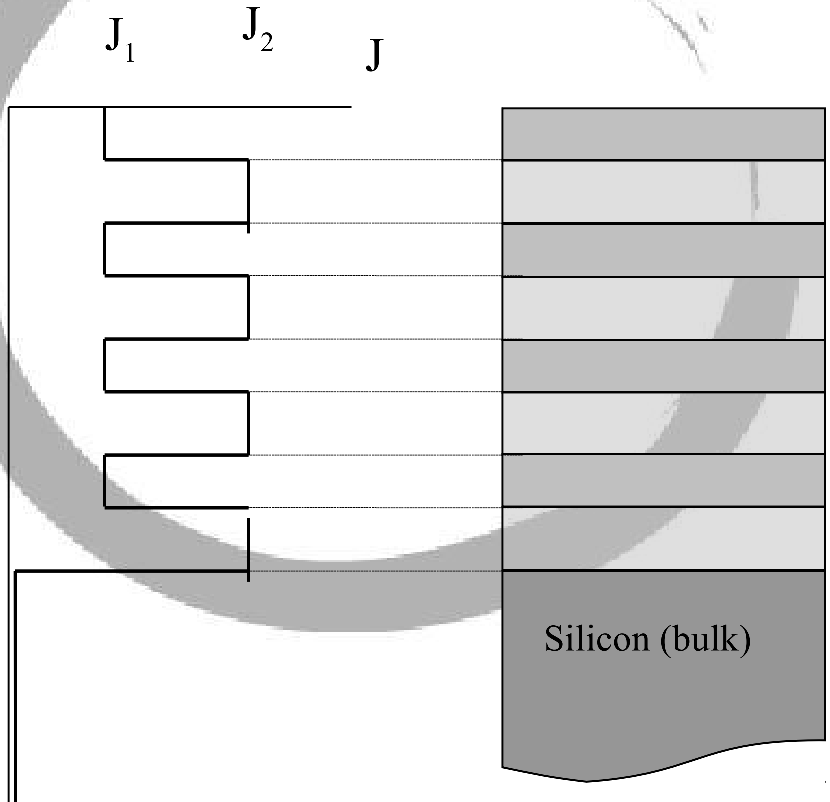

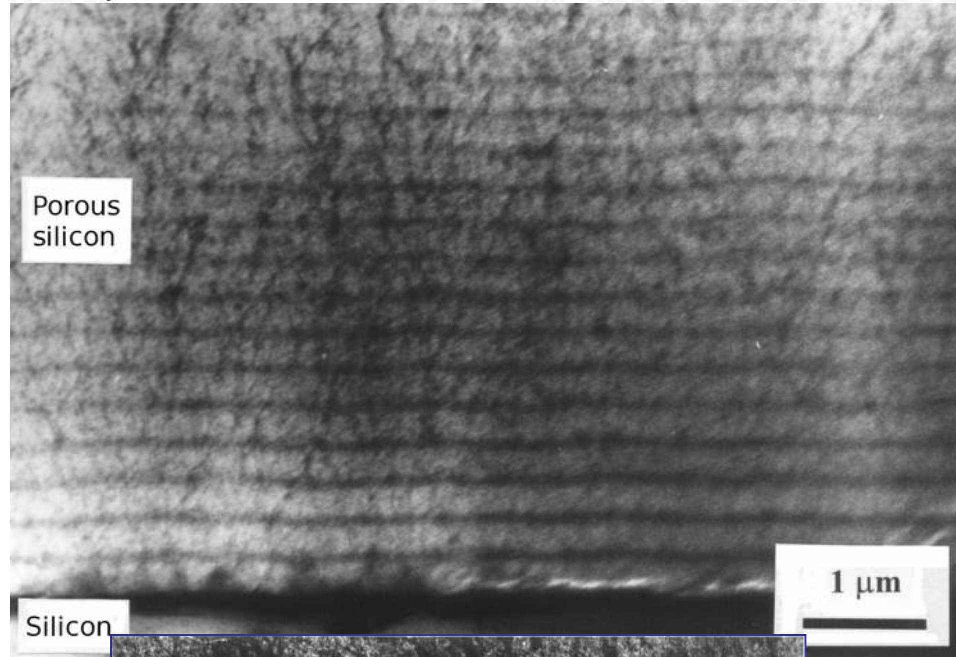

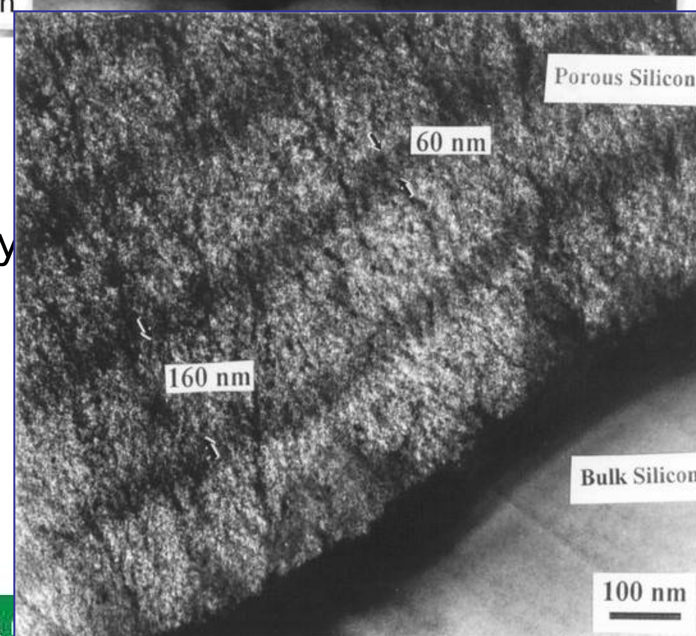

Produced by variations of the current density
Periodic variations of porosity.

air / (HL)^p / Si

- H = high *n*, low porosity
- L = low *n*, high porosity
- p = number of periods

1D, 2D, & 3D patterns

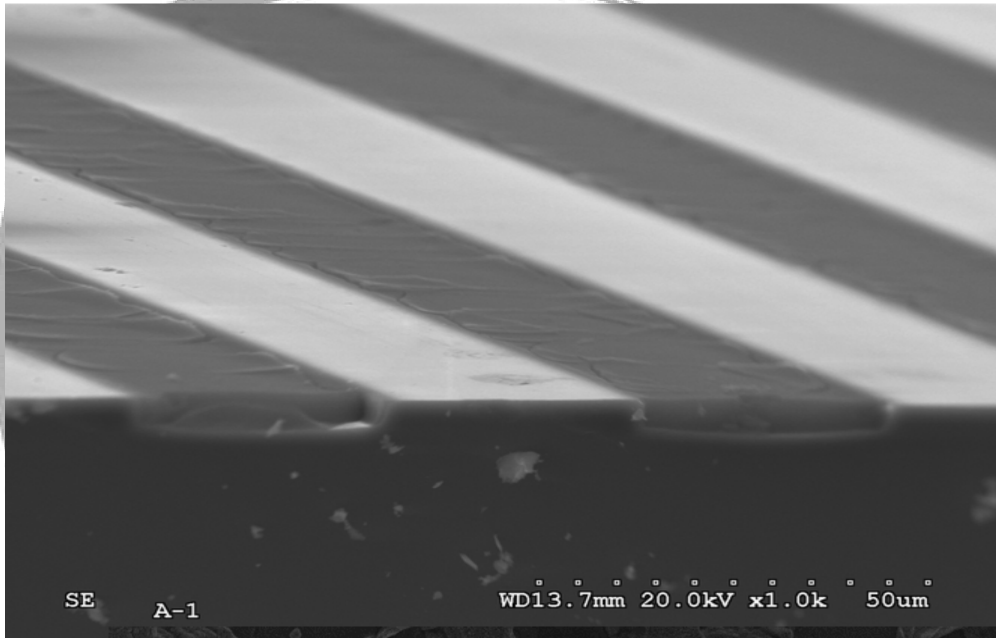

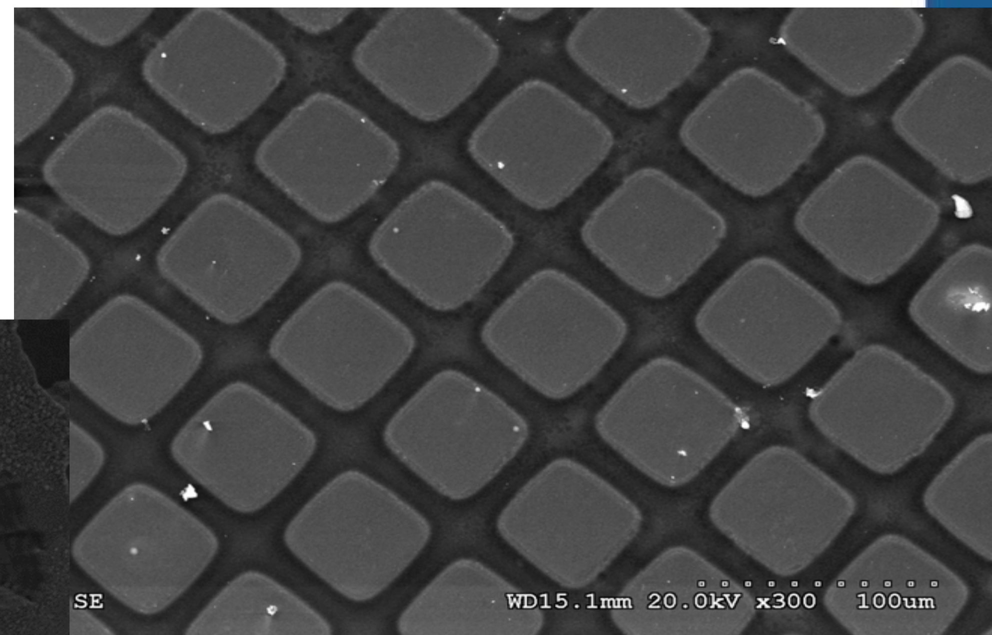

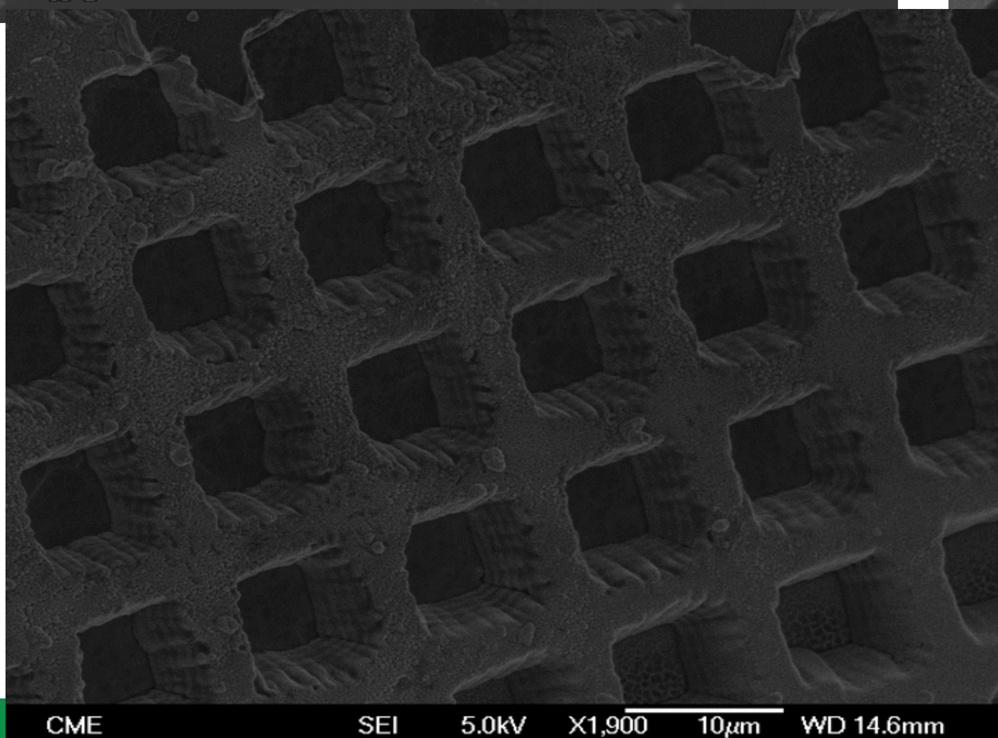

Key properties

- Formed by (electro-)chemical dissolution of Si: cheap to fabricate.
- Light emission from Si (quantum size effects).
- Can be fabricated as a thin film or as powder.
- Large surface area (200-1000 m^2/cm^3).
- Can be passivated by SiO_2, Si_3N_4, …
- The ability to electrochemically tune the pore diameters and nanocrystals size, and to chemically modify the surface provides control over the size and type of molecules adsorbed.
- Its behavior can be altered from bio-inert to bioactive to resorbable.
- Other porous semiconductors: SiC, GaP, SiGe, Ge, GaAs, InP.

VOLUME 87, NUMBER 6 PHYSICAL REVIEW LETTERS 6 AUGUST 2001

Strong Explosive Interaction of Hydrogenated Porous Silicon with Oxygen at Cryogenic Temperatures

D. Kovalev, V. Yu. Timoshenko, N. Künzner, E. Gross, and F. Koch

Technische Universität München, Physik-Department E16, D-85747 Garching, Germany

(Received 12 March 2001; published 19 July 2001)

We report new types of heterogeneous hydrogen-oxygen and silicon-oxygen branched chain reactions which have been found to proceed explosively after the filling of pores of hydrogen-terminated porous silicon (Si) by condensed or liquid oxygen in the temperature range of 4.2–90 K. Infrared vibrational absorption spectroscopy shows that, while initially Si nanocrystals assembling the layers have hydrogen-terminated surfaces, the final products of the reaction are SiO_2 and H_2O. Time-resolved optical experiments show that the explosive reaction develops in a time scale of 10^{-6} s. We emphasize the remarkable structural properties of porous Si layers which are crucial for the strong explosive interaction.

DOI: 10.1103/PhysRevLett.87.068301 PACS numbers: 81.65.–b, 68.03.Fg, 82.33.Vx

- “Hydrogenated porous silicon reacts explosively with oxygen at cryogenic temperatures, releasing several times as much energy as an equivalent amount of TNT, at a much greater speed”.
- Although hydrogenated porous silicon would probably not be effective as a weapon, due to its functioning only at low temperatures, other uses can be explored.

Outline

- Introduction: What is Nanotechnology? Examples and applications.
- What is porous silicon? Why is it interesting?
- How is porous silicon fabricated?, how does it look like?
- Key properties.
- Applications: From photonics to biomedicine
- Summary

Applications

- AR coating, Bragg reflectors, waveguides, microcavities,…
- Photonic crystals
- Light emitting diodes
- Photodiodes, solar cells
- Chemical sensors
- Biological sensors

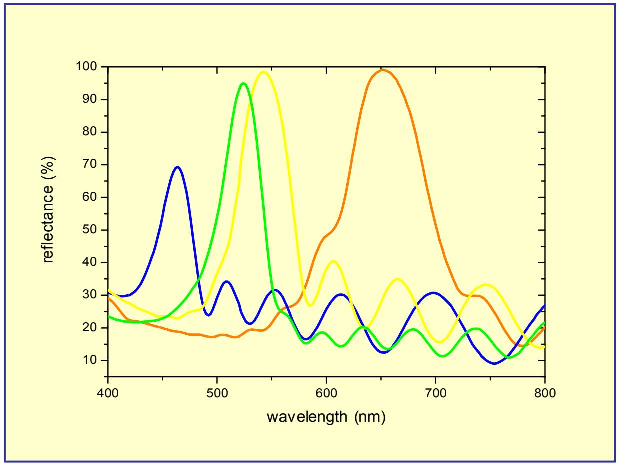

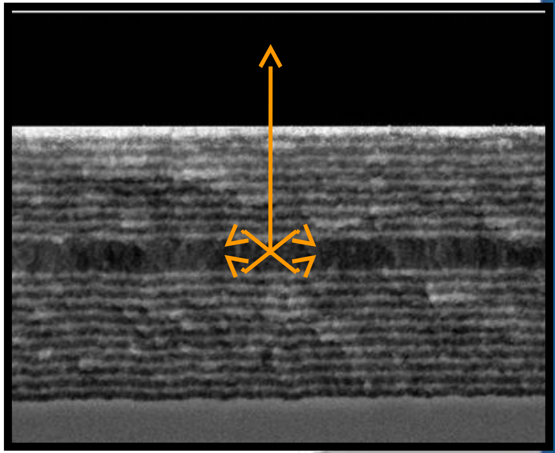

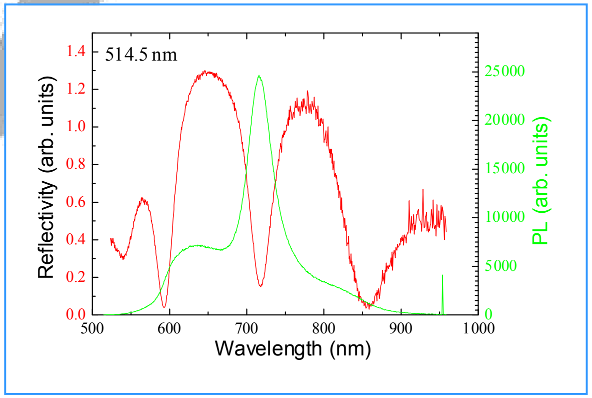

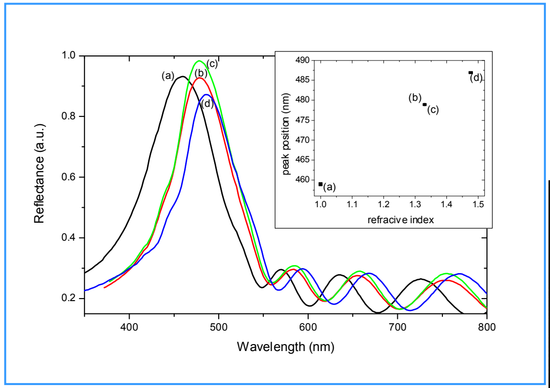

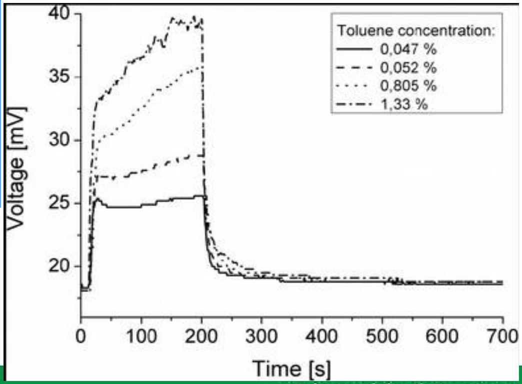

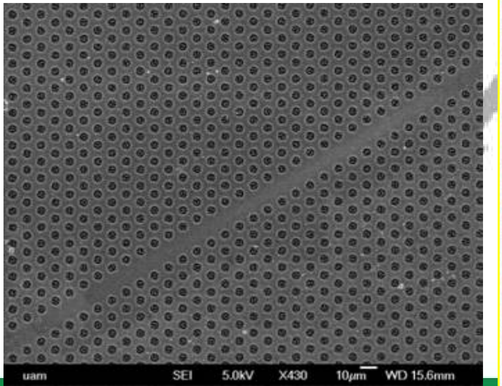

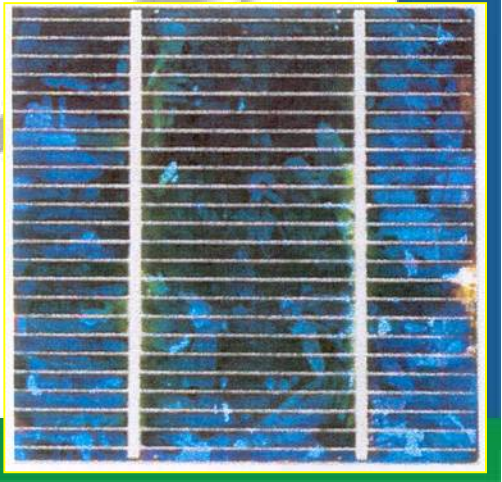

AR coatings

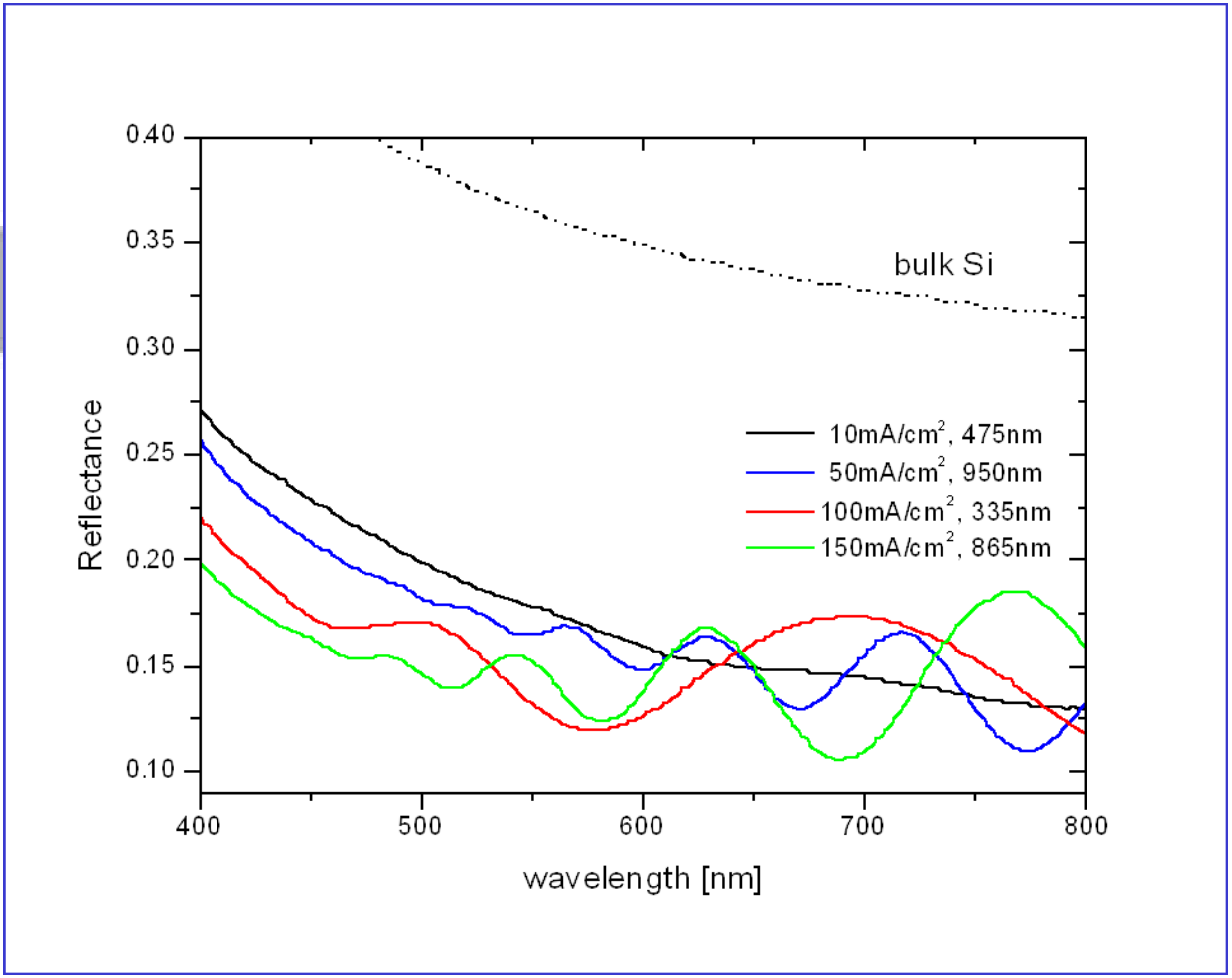

- Notable reduction of *R*.
- R depends on the formation parameters → Structure of PS.

Optical constants (*n* and *k*)

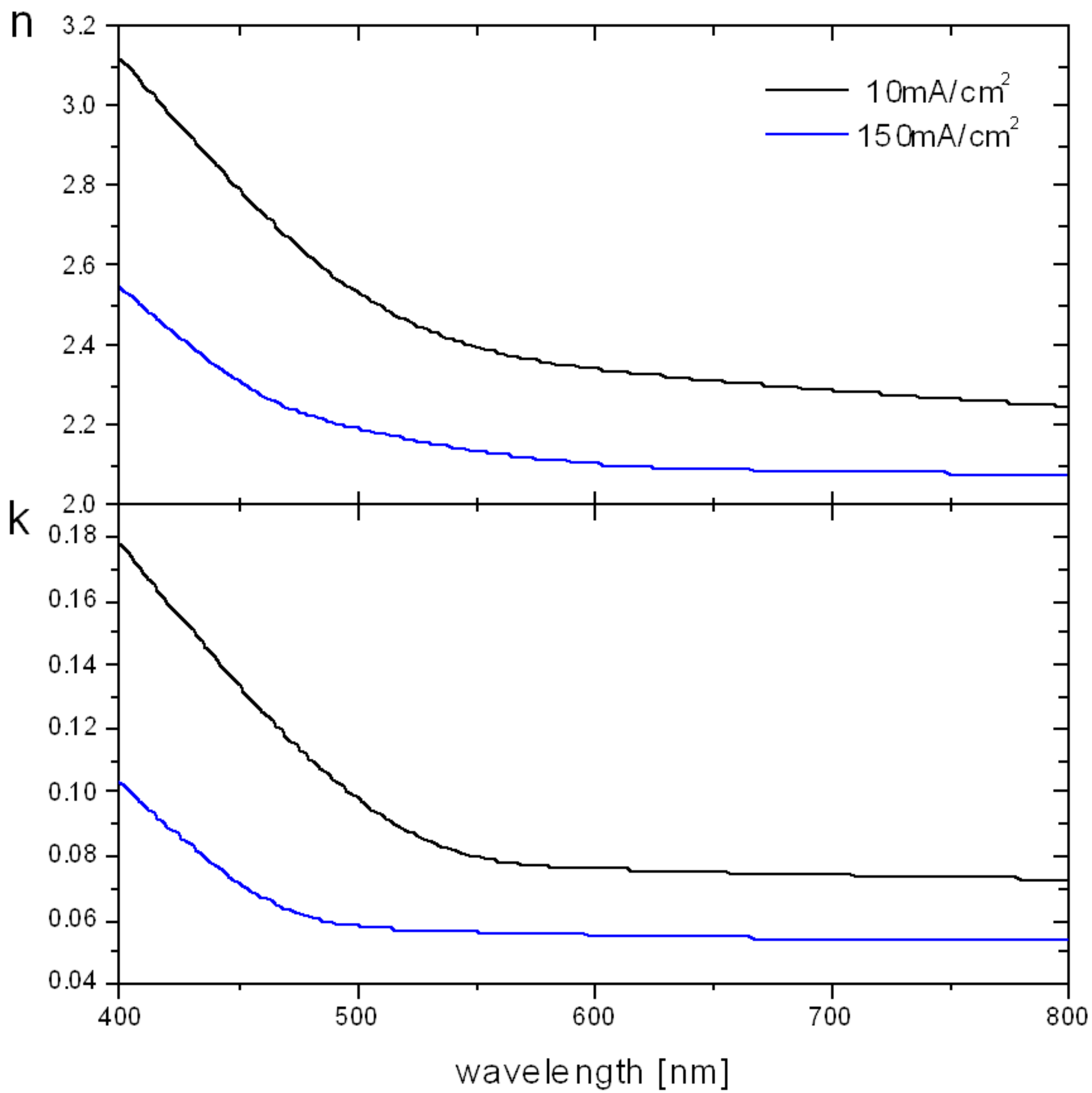

The optical constants (*n* and *k*) and layer thickness are determined from the reflectance spectrum by means of a self-adaptive genetic algorithm.

Thickness inhomogeneity and absorption processes lead to high values of *k*, since the value of this “effective” k stands for the overall coherency loss.

V. Torres-Costa, R.J. Martín-Palma and J.M. Martínez-Duart, *Journal of Applied Physics* 96, 4197 (2004).

PS multilayer stacks

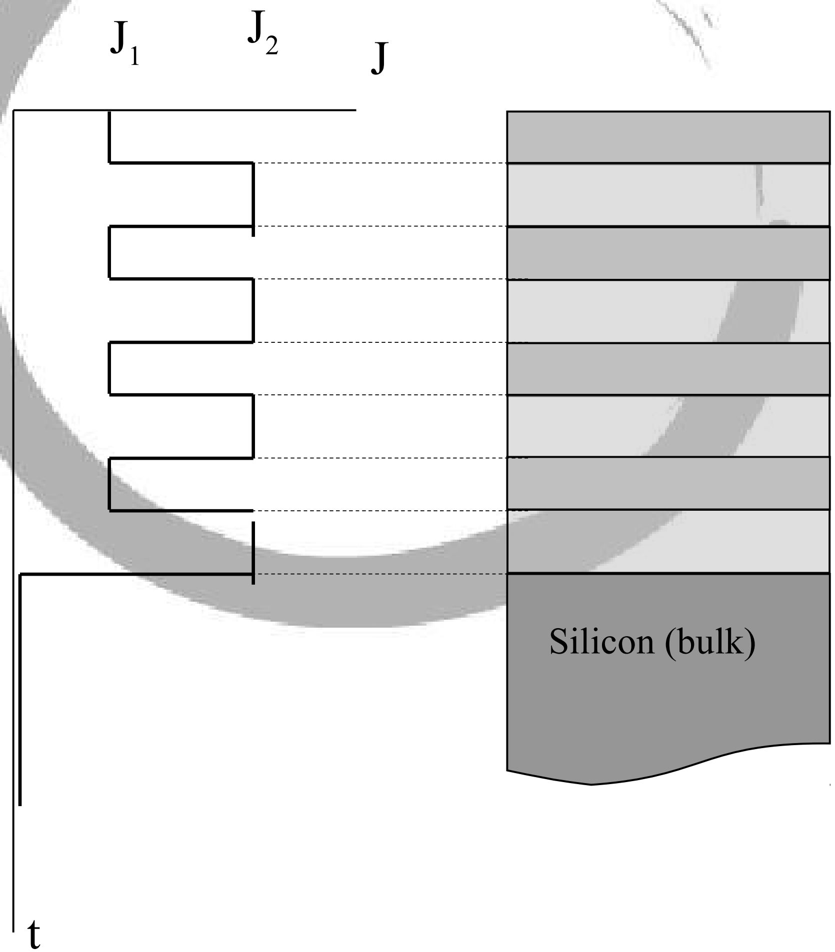

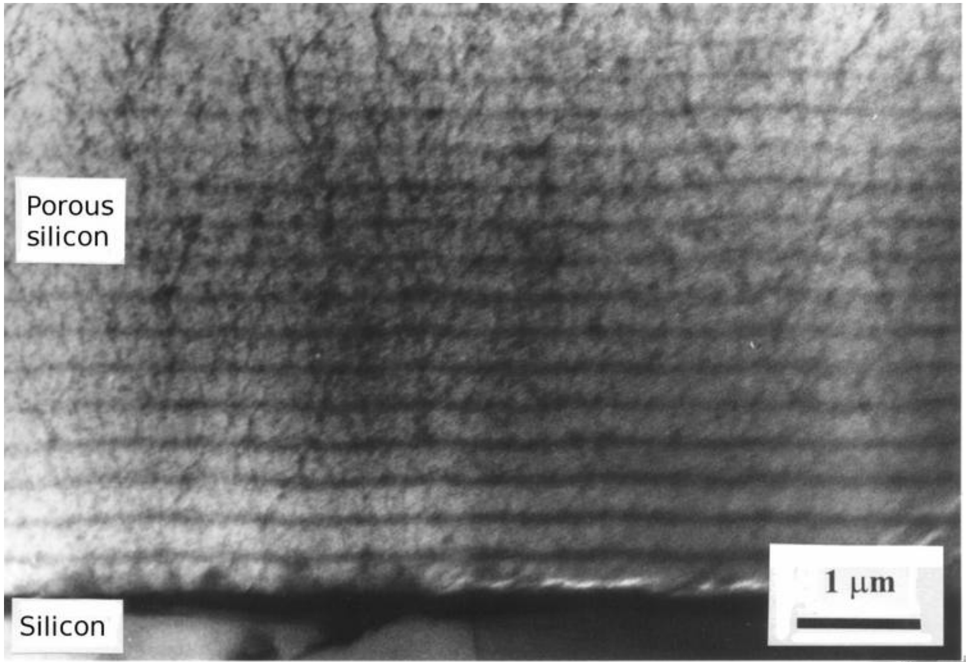

Produced by variations of the current density: Periodic variations of porosity.

air / $(HL)^p$ / Si
- H = high *n*, low porosity
- L = low *n*, high porosity
- p = number of periods.

PS multilayer stacks (cont'd)

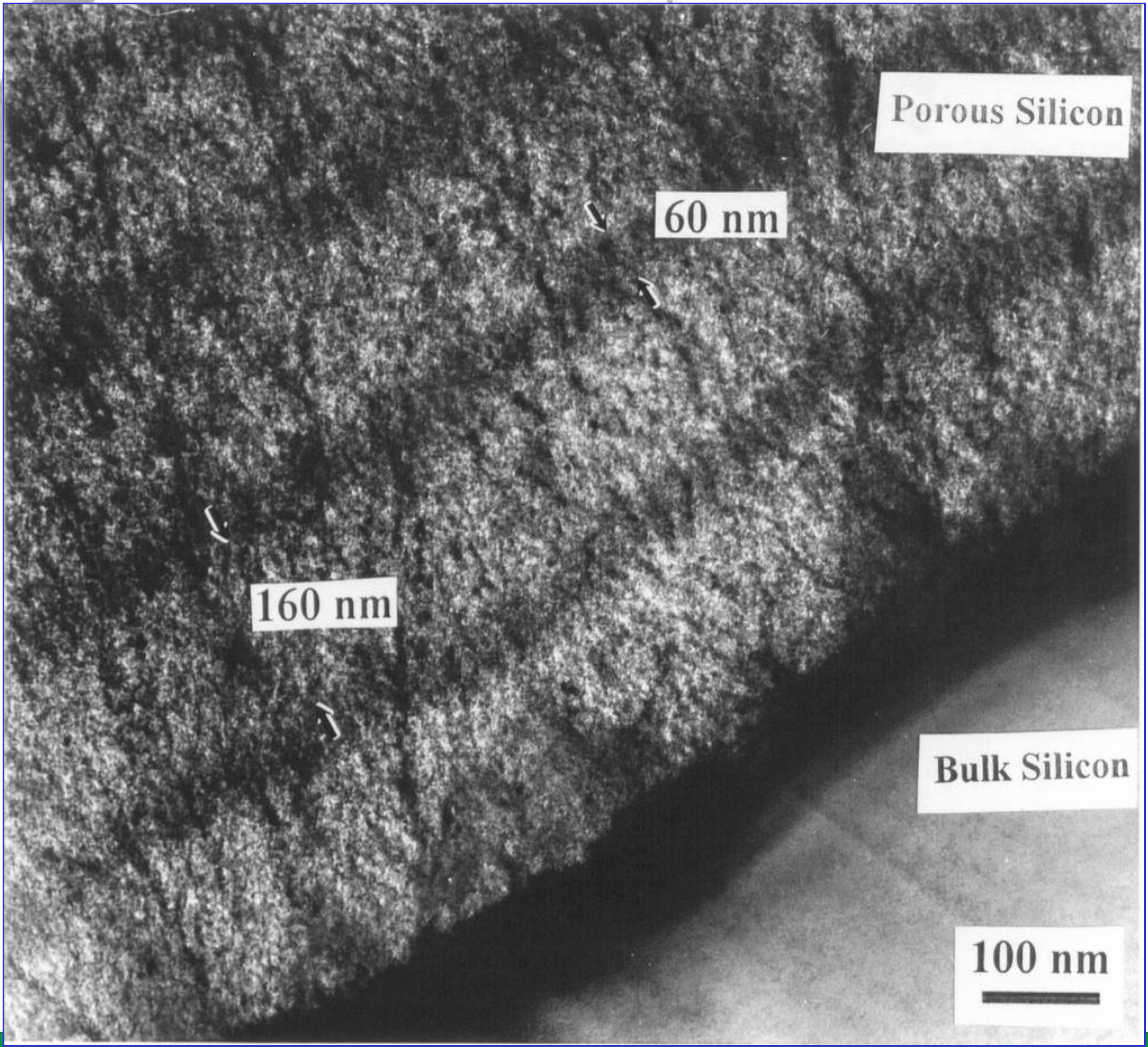

A change of ρ does not affect the already etched parts of the sample

⇓

Only the newly produced PS grows with a different porosity according to the new ρ.

Good quality of layers and interfaces
⇓
Results in good optical properties.

R.J. Martín-Palma *et al*., *J. Mat. Sci. Lett.* 17, 845 (1998).

Multilayer design

Optical constants

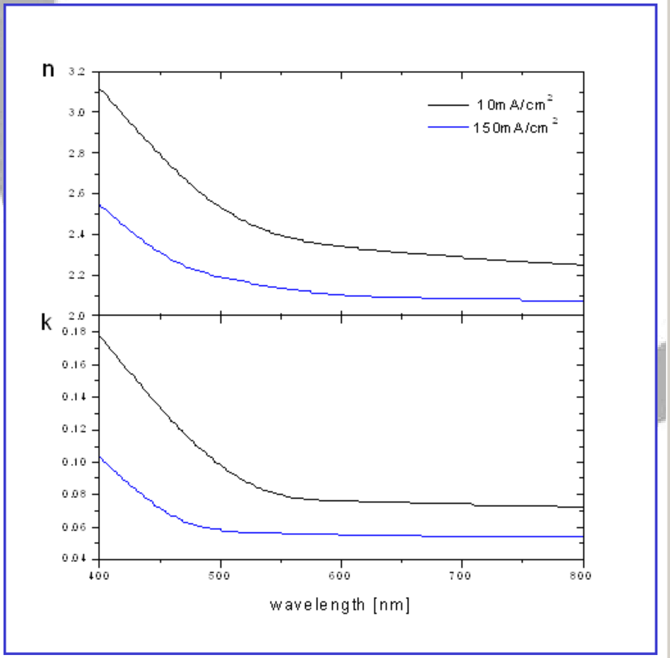

Structure desing

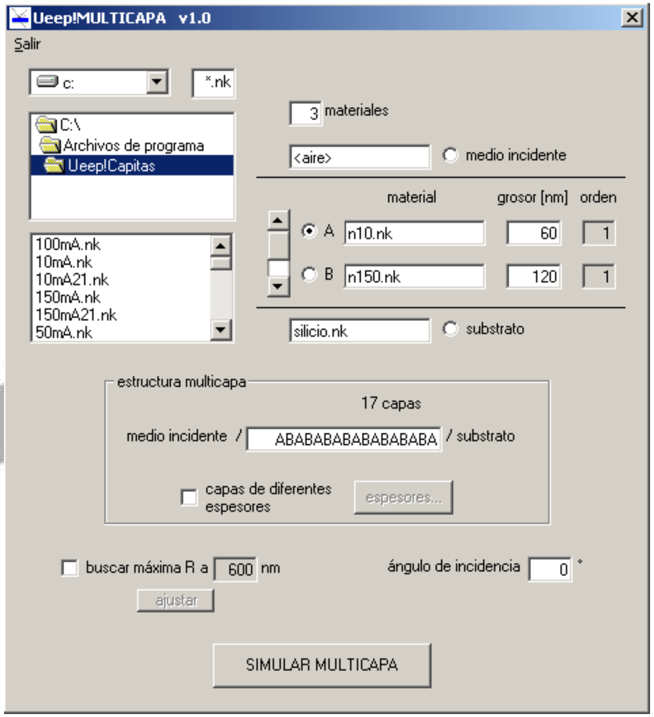

Simulation and fabrication

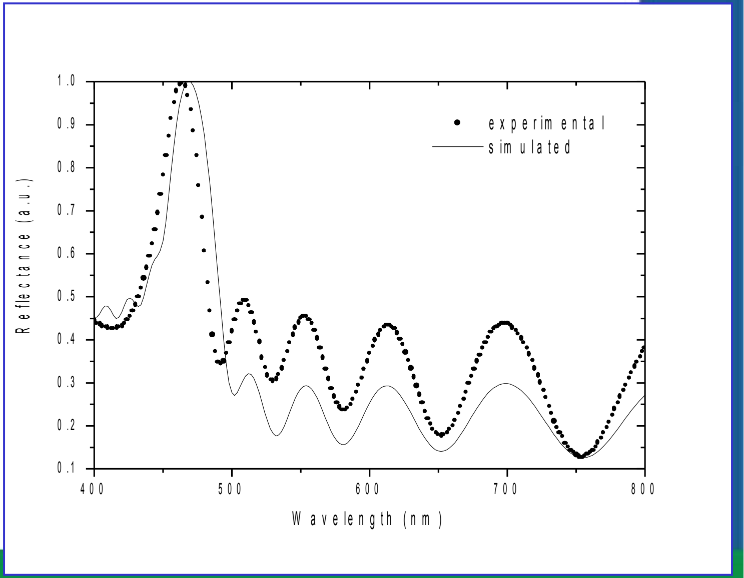

Control porosity → Control *n* (and thickness)

Coatings with the “desired” optical properties can be fabricated

V. Torres-Costa, R.J. Martín-Palma and J.M. Martínez-Duart, *Applied Physics A* 79, 1919 (2004).

Interference filters in the IR

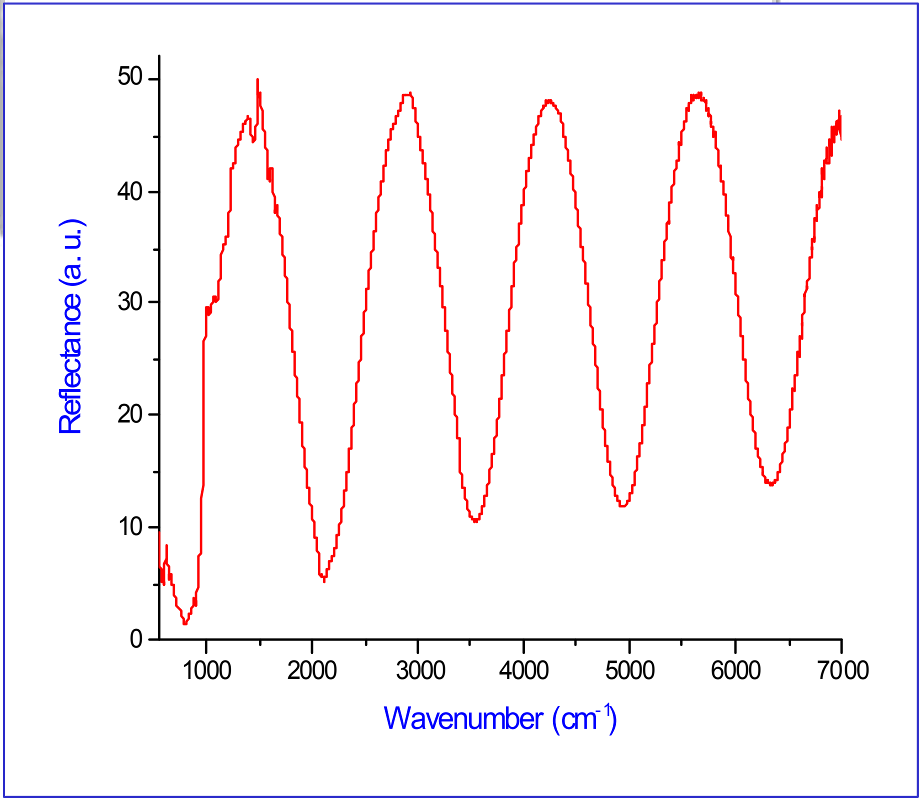

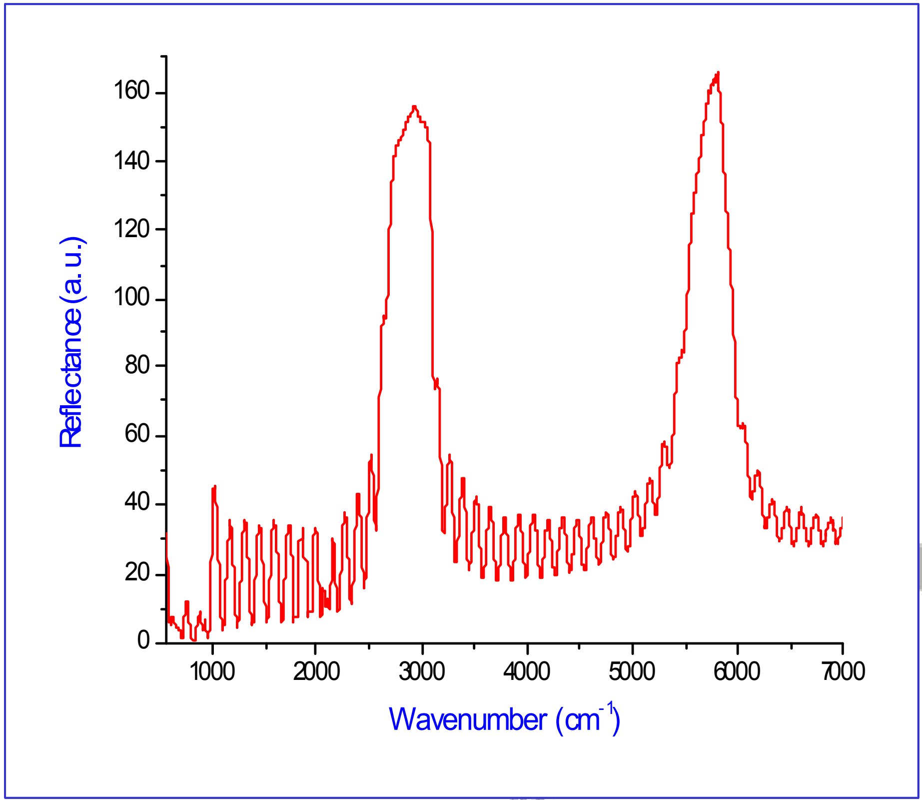

Bragg reflectors

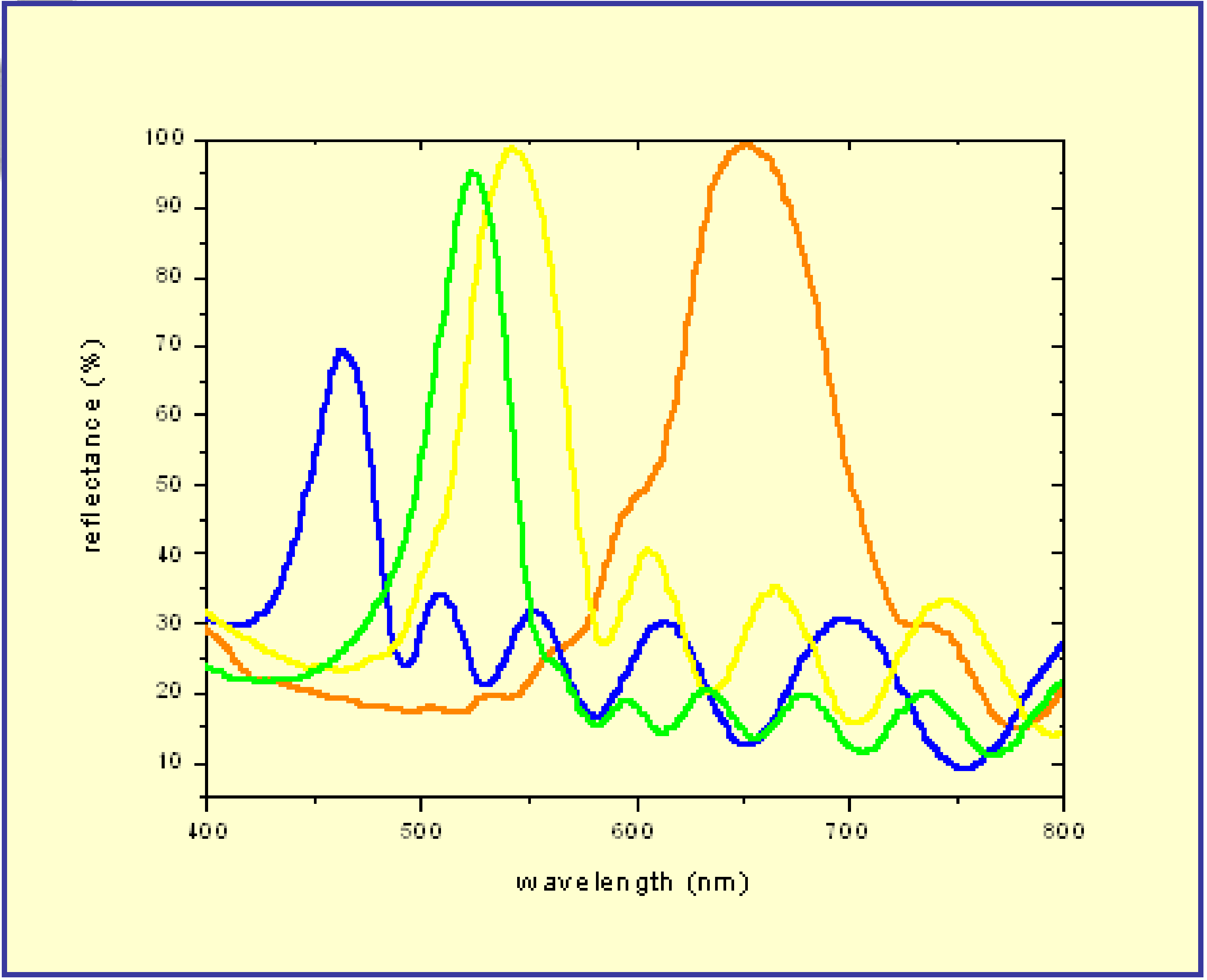

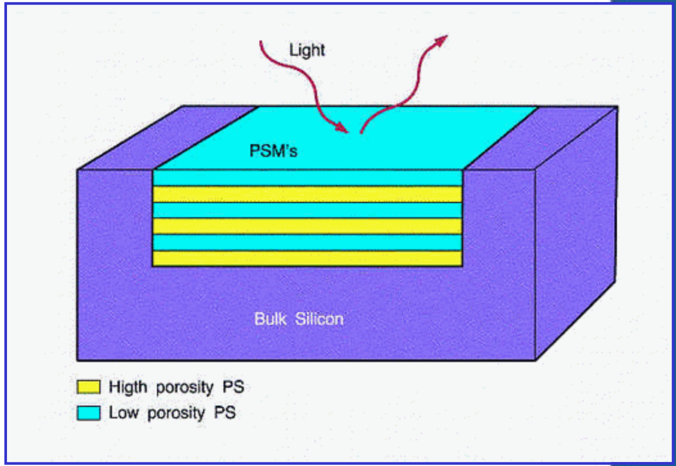

Reflectance maximum (stop-band) centered at the wavelength where the λ/2 condition is reached.

Structure infiltration by a substance of refractive index n_{liq}

↓

increase of effective refractive index:

$$\Delta n \cong p(n_{liq}-1)$$

↓

spectral shift:

$$\Delta\lambda/\lambda_0 = \Delta n = p(n_{liq}-1)$$

↓

Optical chemical sensors

Chemical sensors

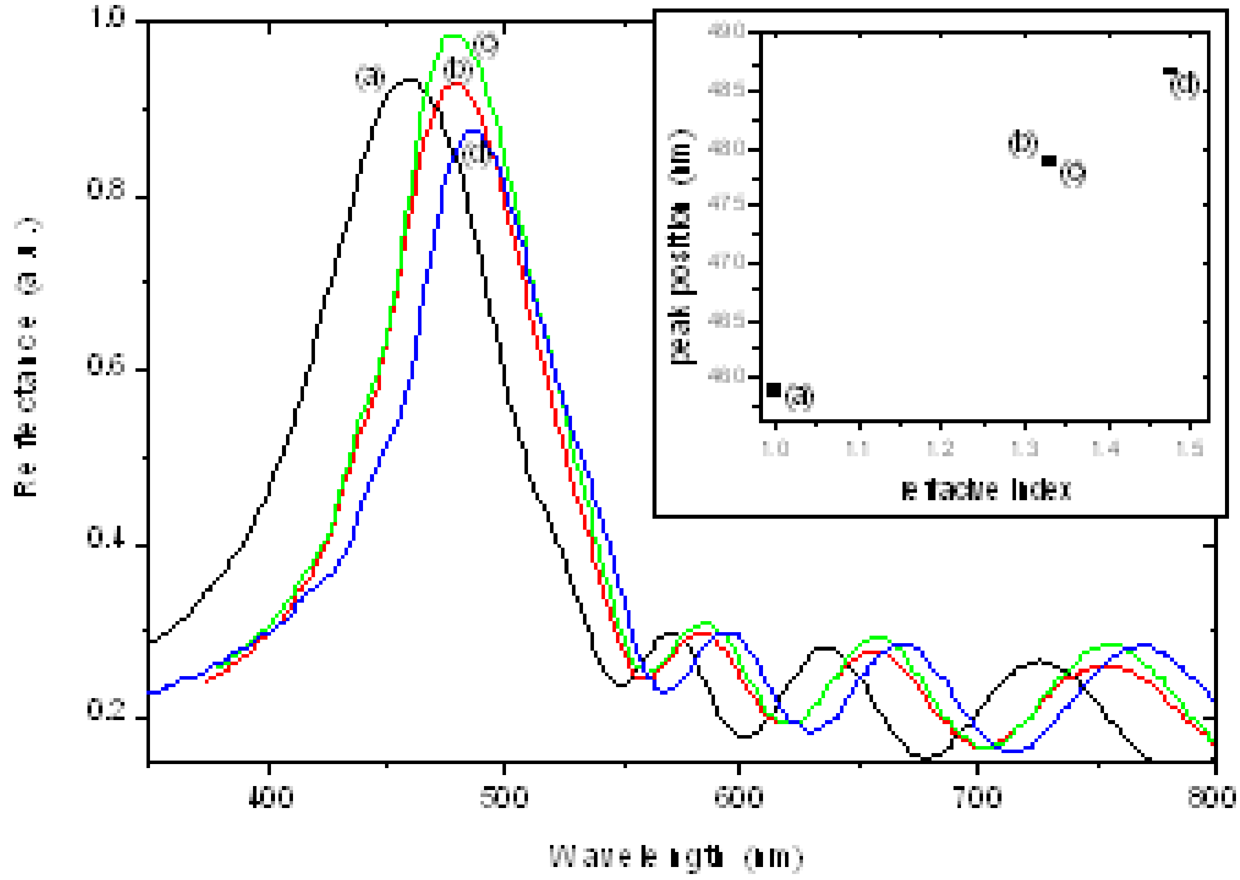

(a) As-prepared PS multilayer.
Infiltration with:
(a) Water.
(b) Ethanol.
(c) Trichloroethylene.

Reflectance peak position as a function of *n* of the filling liquid: (water n= 1.333, ethanol n= 1.329 and triclorethylene n= 1.476).

Reversible behavior!!!

V. Torres-Costa, F. Agulló-Rueda, R.J. Martín-Palma and J.M. Martínez-Duart, *Optical Materials* 27, 1084 (2005).

Gas sensors

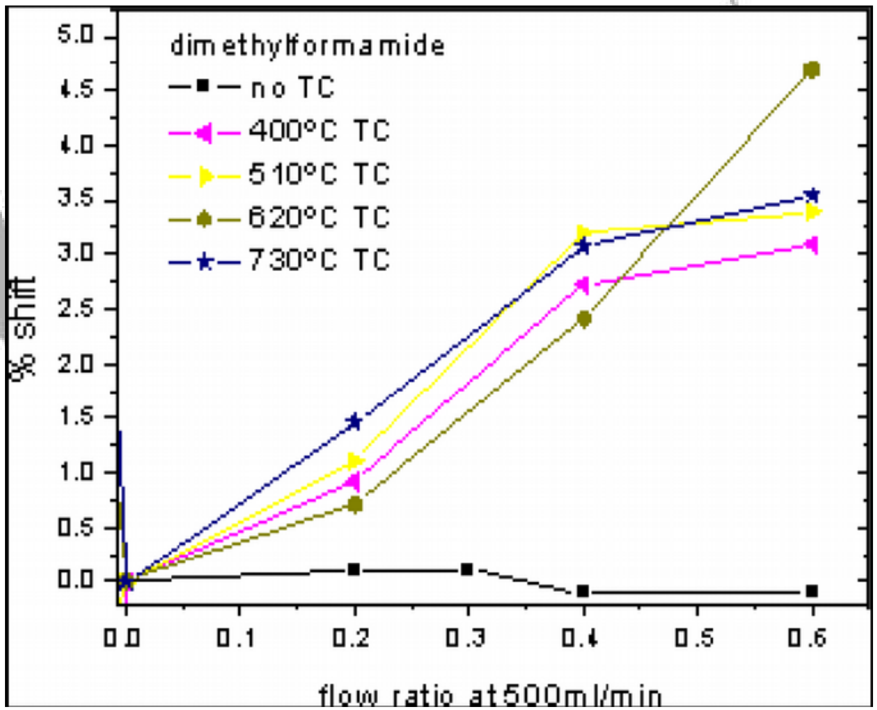

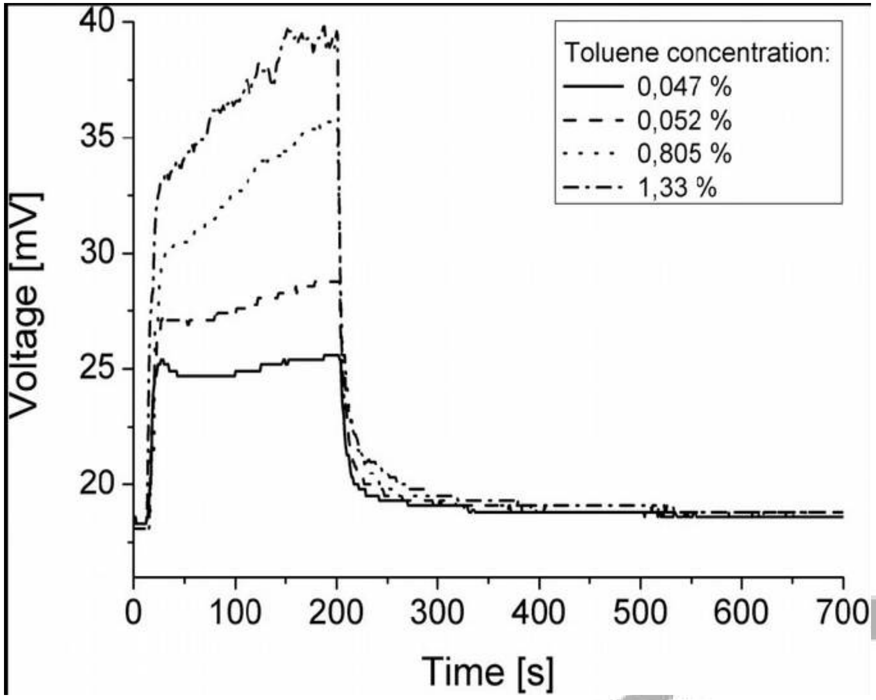

Optical response of PS as a function of dimethylformamide concentration at a constant nitrogen flow.

- Response of TC PS sensors to different toluene concentrations (R @ fixed λ).
- Toluene was introduced in the chamber with a nitrogen flow at t = 20 s and flushed away at t = 200 s.

V. Torres-Costa, J. Salonen, T. M. Jalkanen, V.-P. Lehto, R. J. Martín-Palma, and J. M. Martínez-Duart, Phys. Status Solidi A, 1– 3 (2009).

High specific surface of PS

+

Control of the physico-chemical behavior of its surface

⇓

Development of **biosensors**

Surface functionalization

- **Biofunctional surface: Functional groups** on the surface. These groups react with biomolecules (proteins, DNA, ...).
- **Thermally activated chemical vapor deposition (TA-CVD):** Activation of precursor 3-aminopropyltriethoxysilane (APTS) at high temperature.
- By TA-CVD amine groups are deposited (-NH_2). These groups react with biomolecules through a peptide bond.

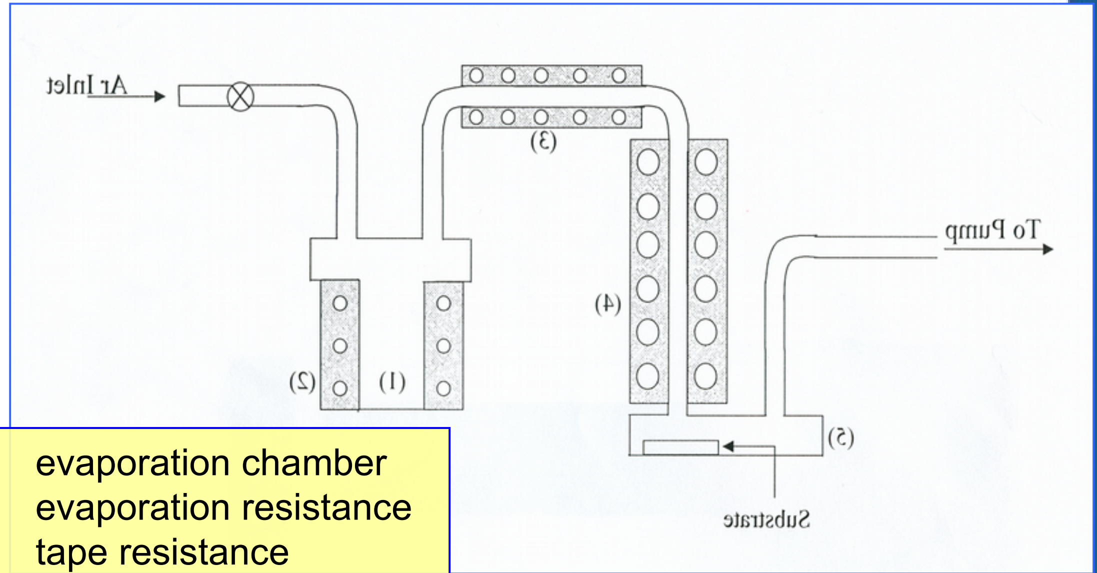

(1)	evaporation chamber
(2)	evaporation resistance
(3)	tape resistance
(4)	activation furnace
(5)	treatment chamber.

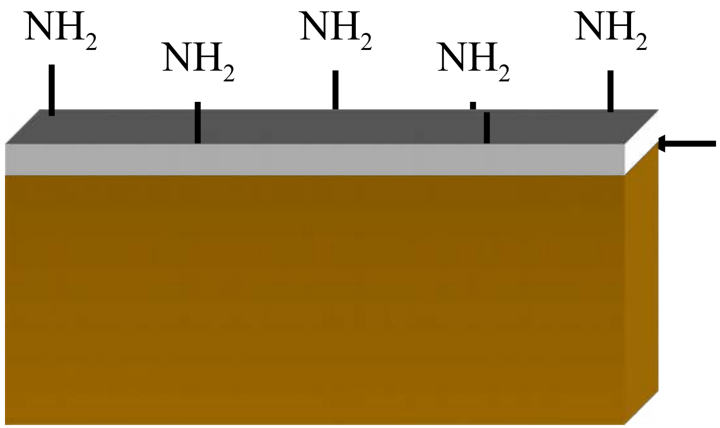

- Metalorganic precursor:

  3-aminopropyltriethoxysilane (APTS).

- Evaporation temperature: 100ºC to 200ºC.

- Activation temperature: 700ºC to 850ºC.

- Pressure: 0.6mb to 3mb.

R.J. Martín-Palma, M. Manso, J. Pérez-Rigueiro, J.P. García-Ruiz and J.M. Martínez-Duart, *Journal of Materials Research* 19, 2415 (2004).

Biocompatibility of PS: Activation of the surface

- To test functionality we use a label fluorofore (**fluoresceine isotiocianate,** FITC).
- Fluorescence is measured by confocal microscopy: pinholes keep light from just one plane.

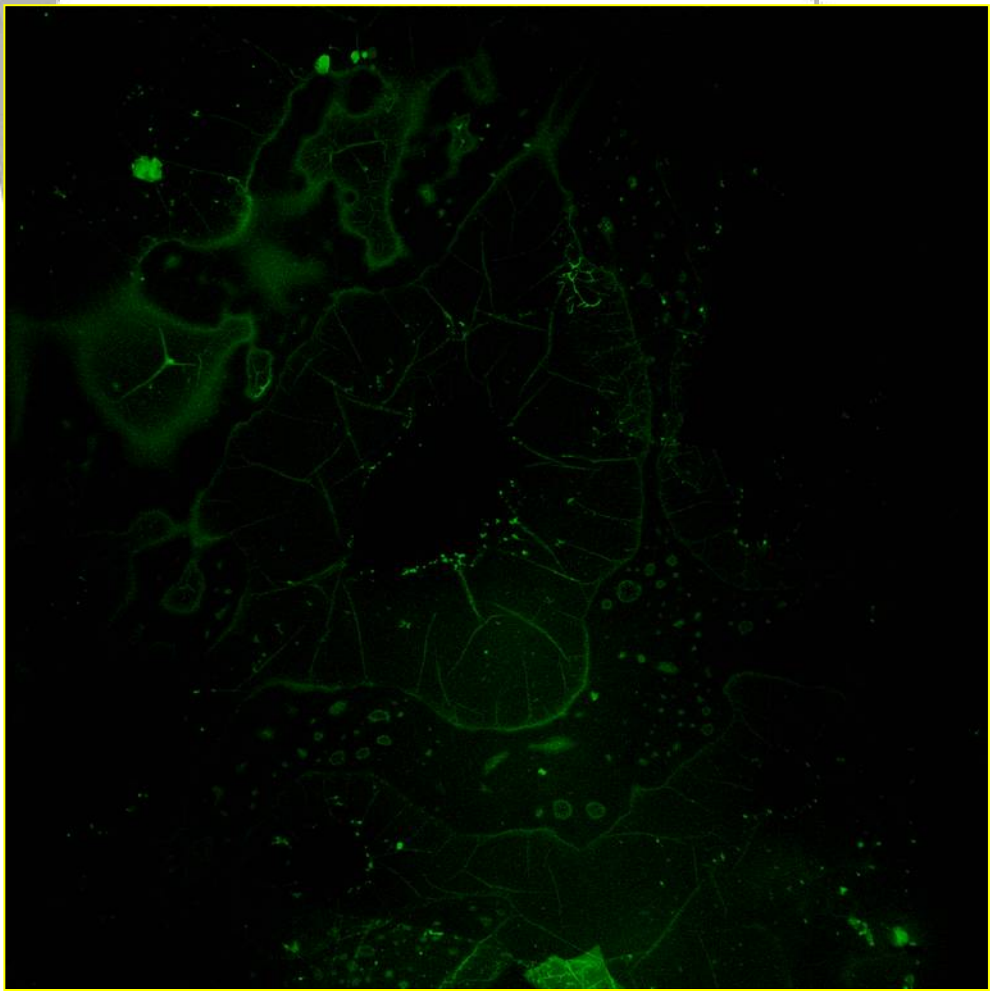

Silicon substrate

Surface 305 x 305 μm^2

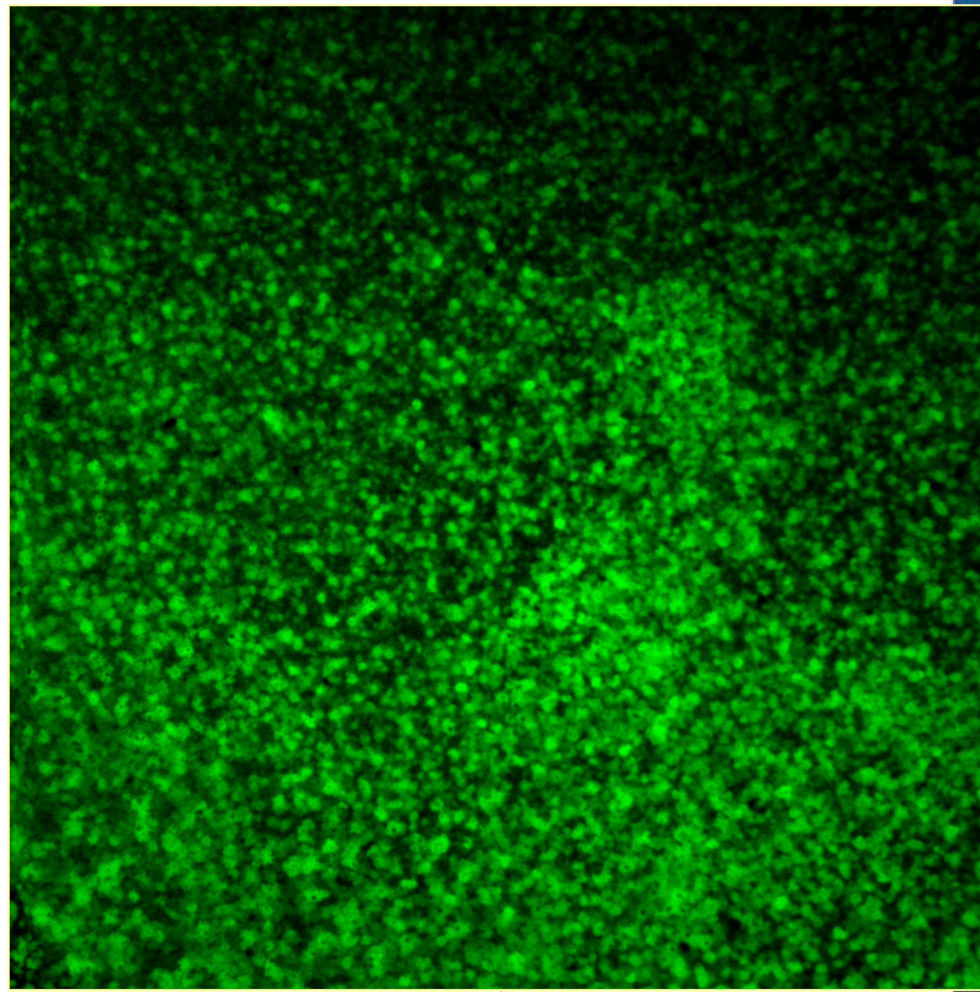

Porous silicon substrate

Functionalized surfaces with antibodies immobilized

To test the functionality of immobilized biomolecules, specific **antibody-antigen reaction** was chosen. It can be used for biosensing of antigens.

Antigens are marked with FITC that make possible its detection by confocal microscopy.

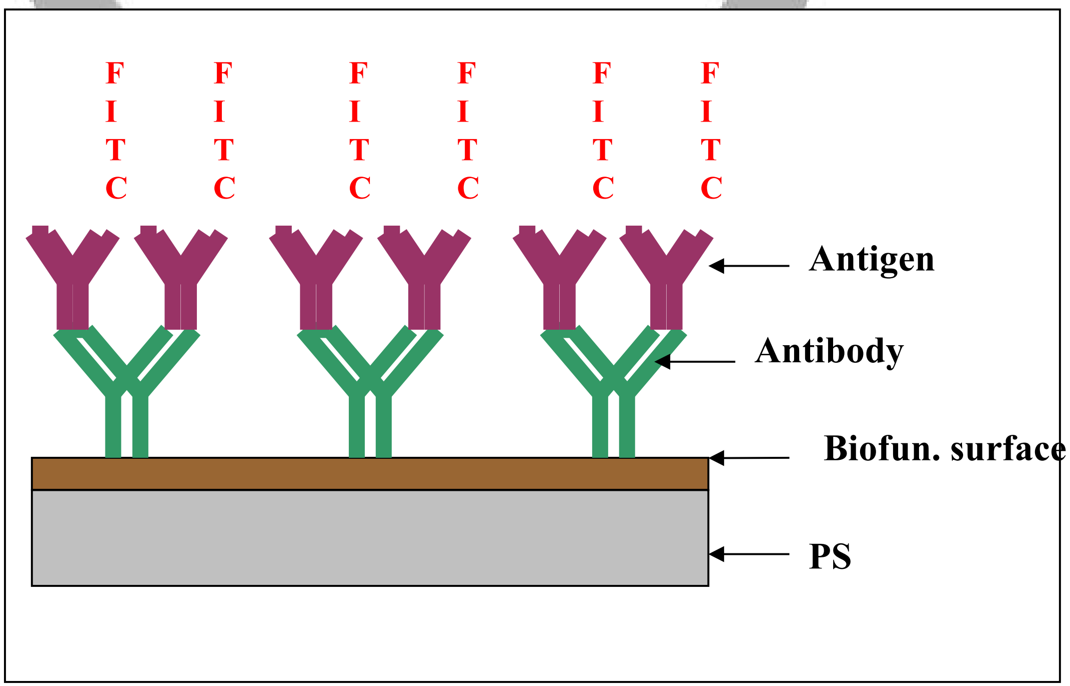

Policlonal mouse inmunoglobulines were used.

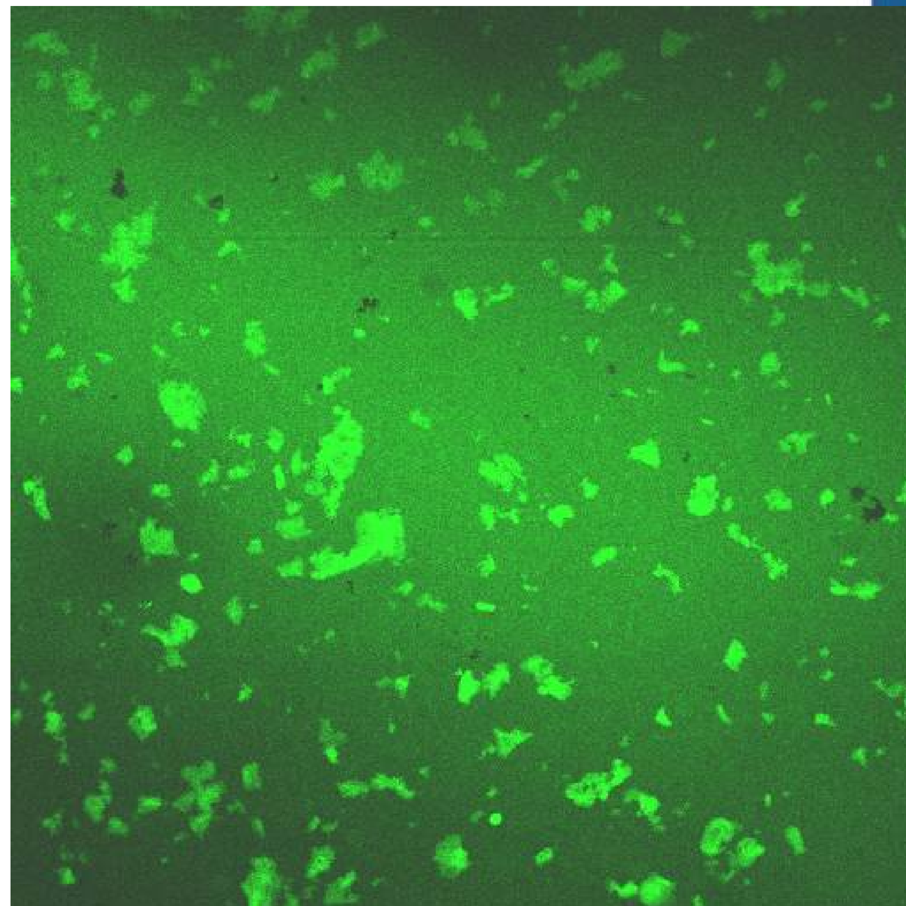

Surface 305 x 305 μm^2

Optical biosensing: reflectance spectrum

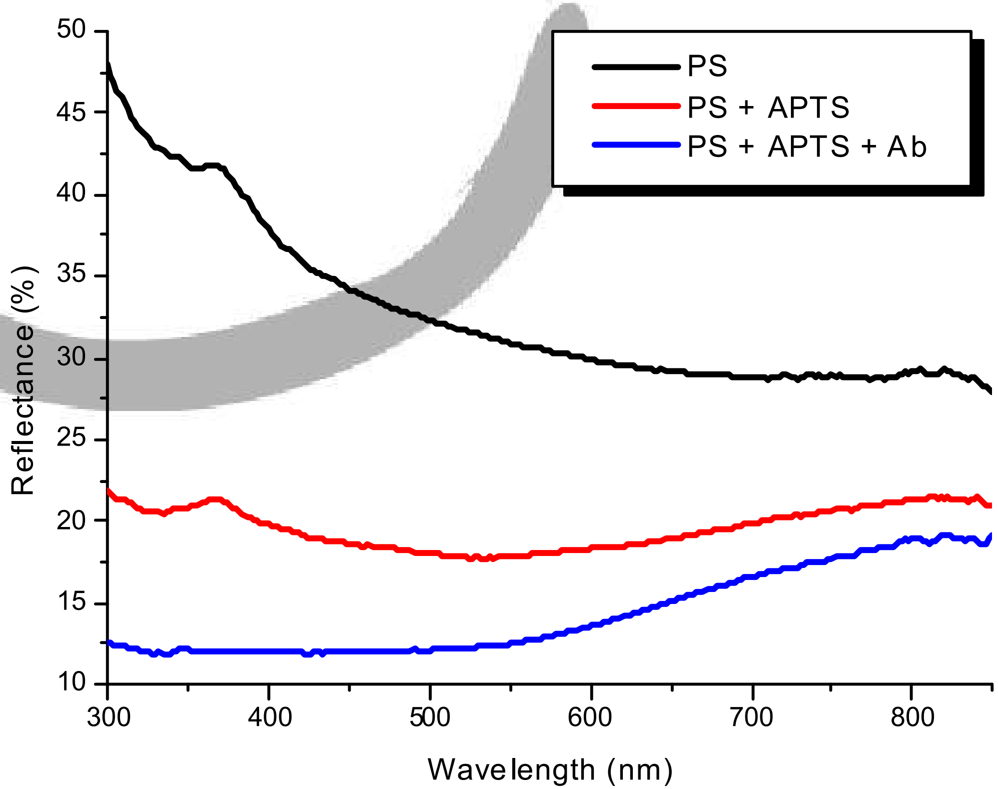

- Notable reduction of R after the bioactivation process.
- Larger reduction after immobilization of antibodies.
- R at a given wavelength can be used for detection.

R.J. Martín-Palma, V. Torres-Costa, M. Arroyo-Hernández, M. Manso, J. Pérez-Rigueiro and J.M. Martínez-Duart, *Microelectronics Journal* 35, 45 (2004).

Optical biosensing: Bragg reflectors

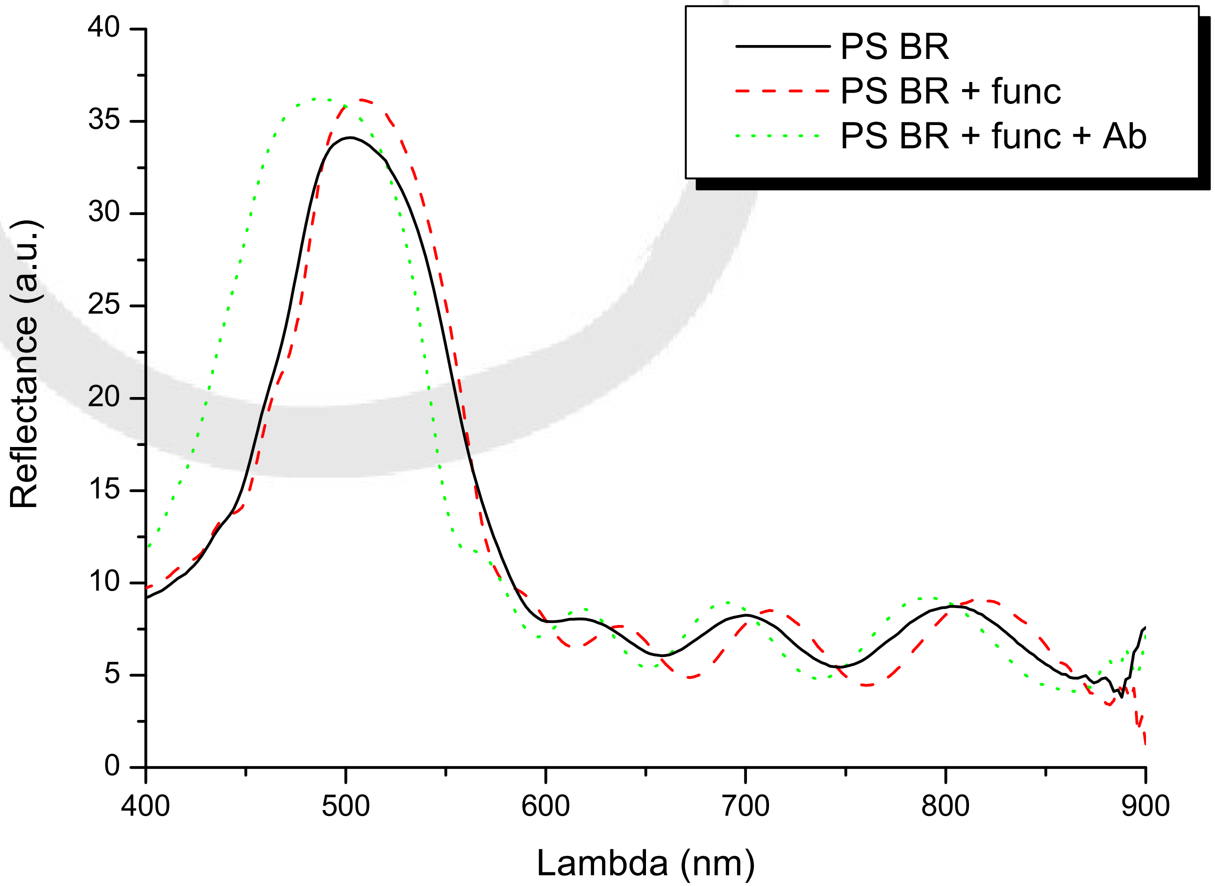

PS-based Bragg reflector:

- As formed.
- After the biofunctionalization process.
- After immobilization of polyclonal mouse antibodies.

Polyclonal mouse antibodies are detected.

It is possible to detect “any” molecule (DNA, proteins, ...) just by choosing the appropriate complementary pair.

M. Arroyo-Hernández, R.J. Martín-Palma, V. Torres-Costa, J.M. Martínez Duart, *Journal of Non-Crystalline Solids* 352, 2457 (2006).

Optical microcavities

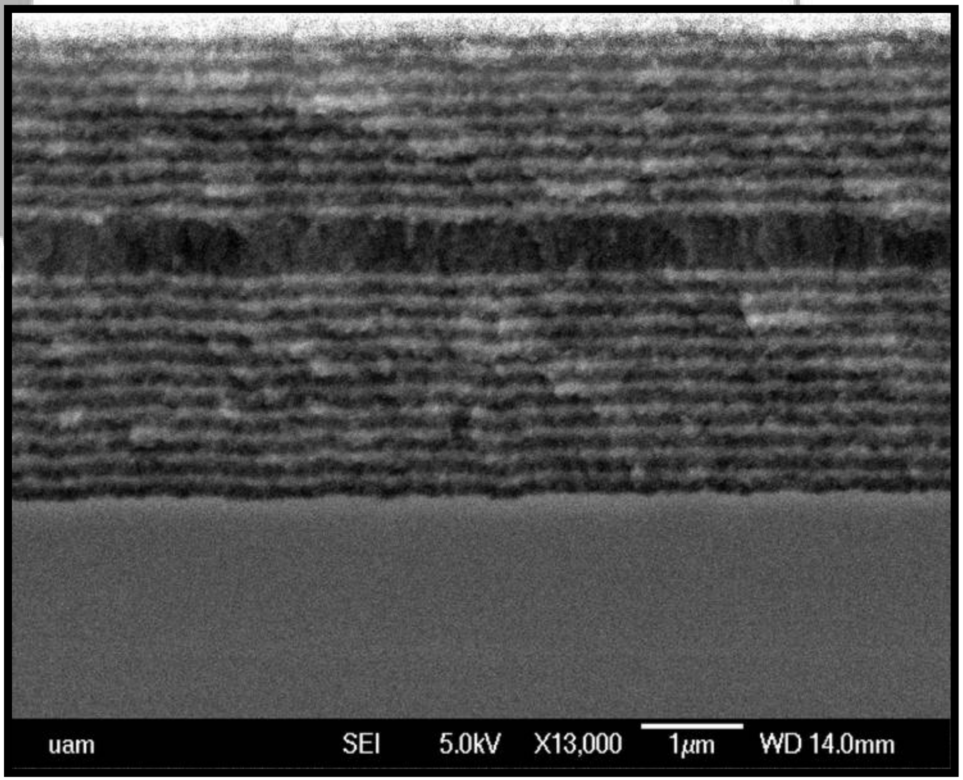

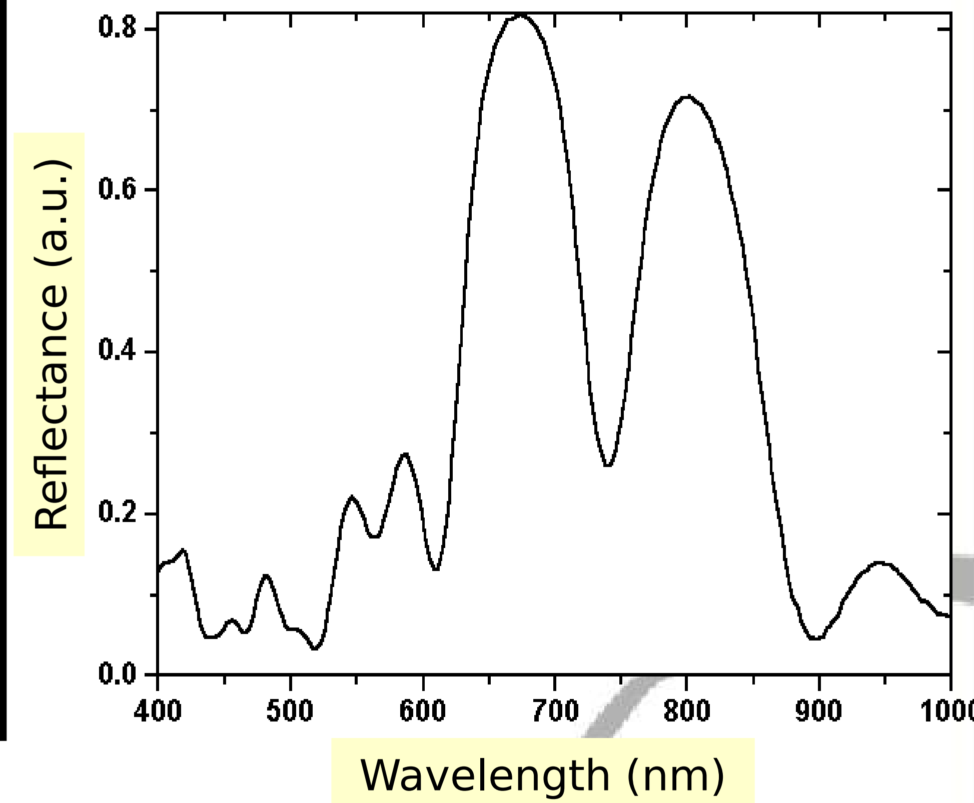

Resonant layer between Bragg reflectors

air / $(AB)^p$ B $(AB)^p$ /Si

Resonant peak at λ_0:

$$2n_s d_s \cos\theta_s = m\lambda_0 \qquad (m = 1, 2, \ldots)$$

Filtered light emitters

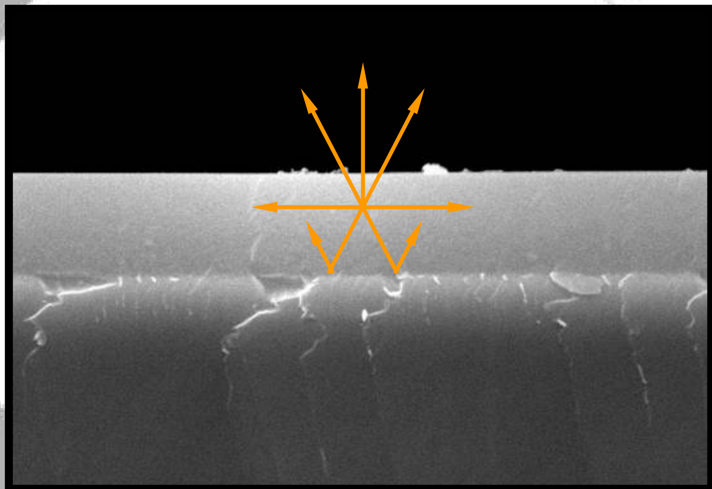

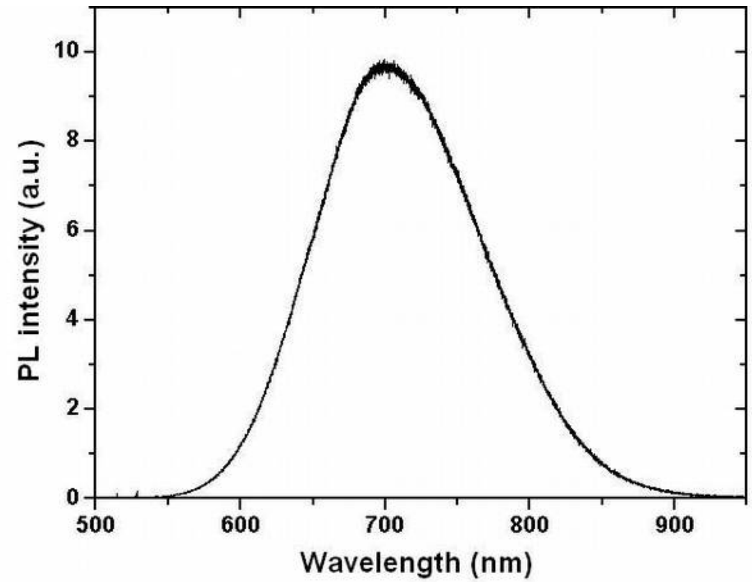

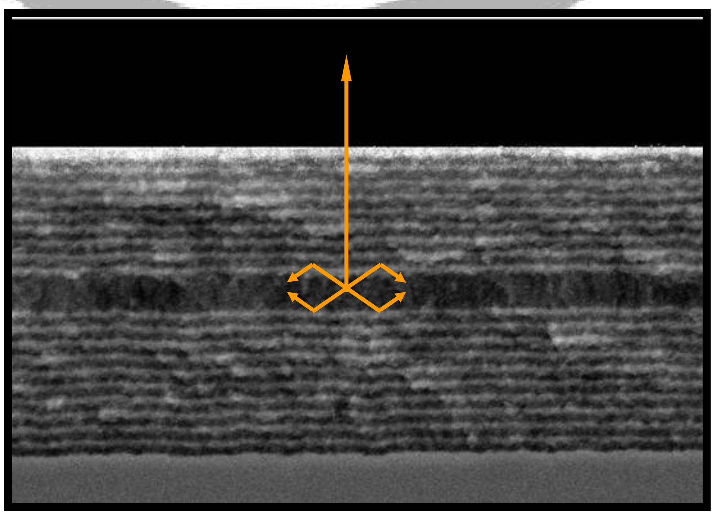

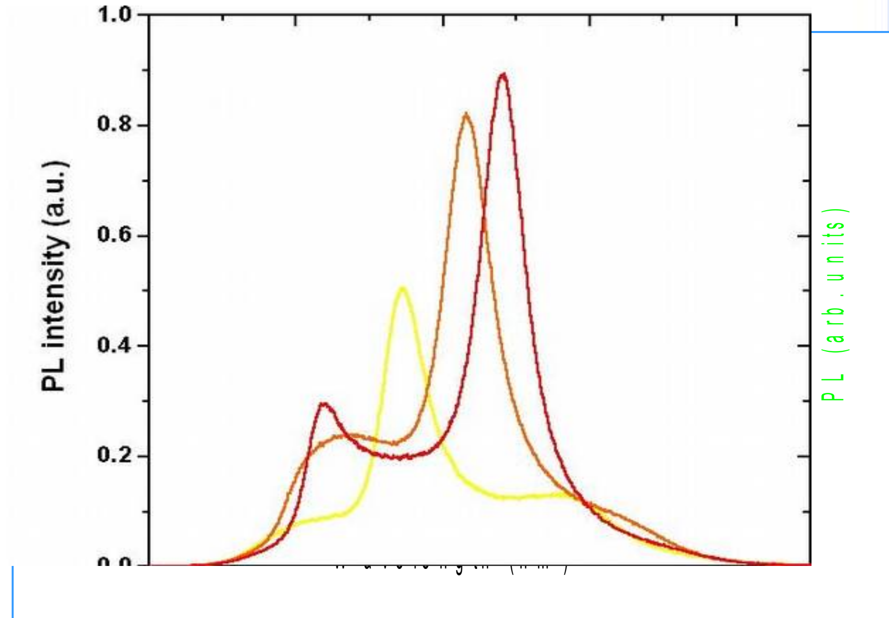

V. Torres-Costa, F. Agulló-Rueda, R.J. Martín-Palma and J.M. Martínez-Duart, *Optical Materials* 27, 1084 (2005).

PS optical microcavities can be used to filter PS luminescent emission, leading to monochromatic light emitters.

PS-based solar cells

<u>Advantages of using PS:</u>

- The highly textured morphology of PS can be used to enhance light trapping → Reduction of *R* in the visible/NIR range
- Cheap process

<u>Drawbacks:</u>

- Electrical contacts to PS (highly resistive material)
- Long-term stability

Fabrication

Surface: 50×50 mm^2.

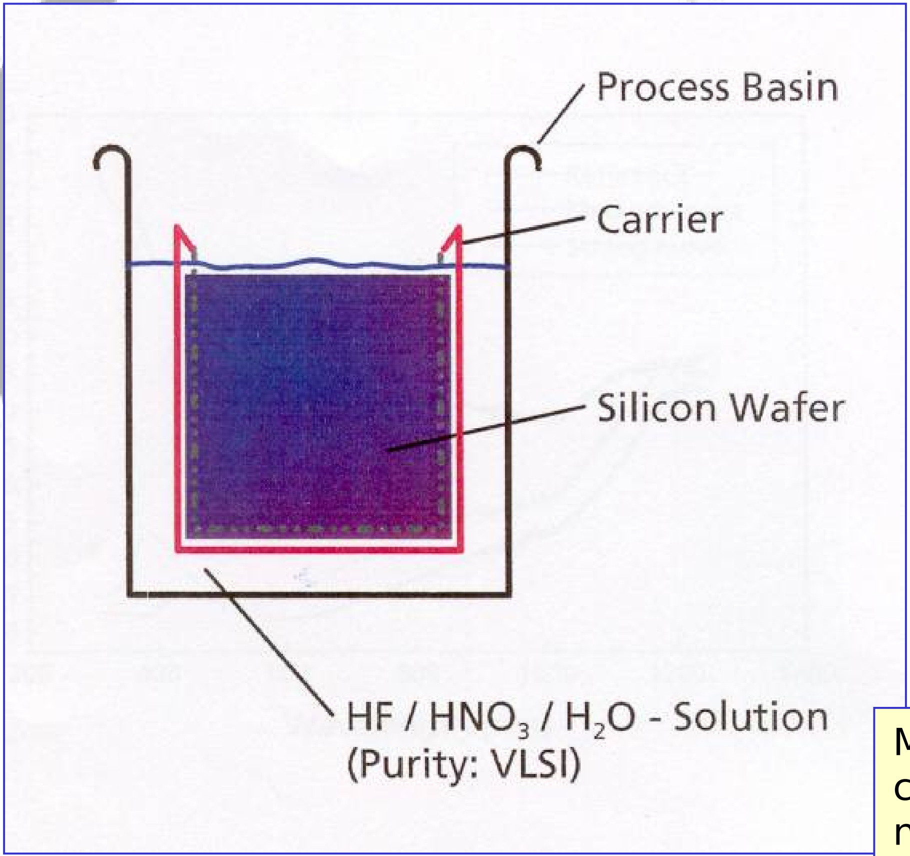

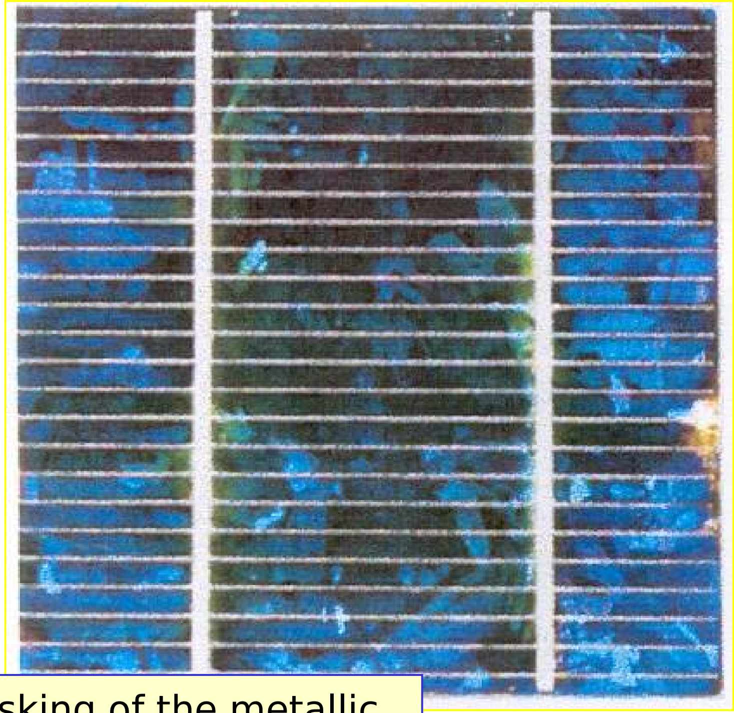

Masking of the metallic contacts is not necessary during the formation of PS.

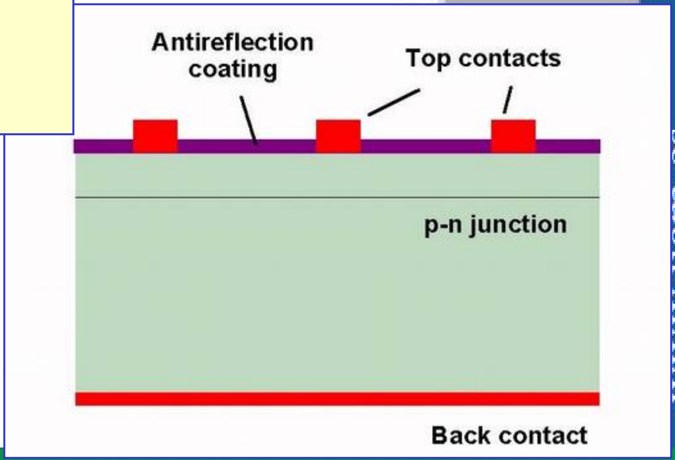

- PS formed by chemically etching ready-made industrial solar cells (emitter of the n^+/p junctions), after the deposition of the front and back contacts.
- HF/HNO_3-based solution.
- No protection of contacts.

Simple and inexpensive PS formation process.

Optical properties

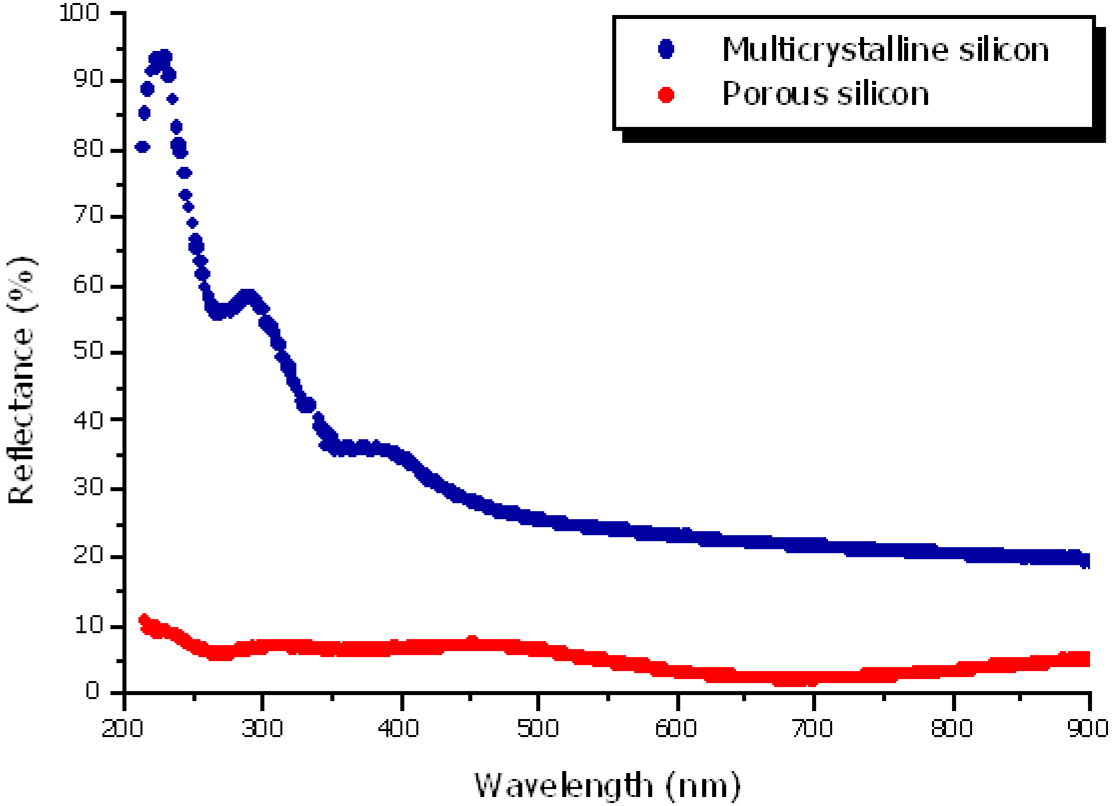

Average reflectance: 26.8 % (Multicrystalline silicon) → 5.0 % (PS, stain etched)

R.J. Martín-Palma, L. Vázquez, P. Herrero, J.M. Martínez-Duart, M. Schnell and S. Schaefer, *Optical Materials* 17, 75 (2001).

Characteristic solar cell parameters before/after PS

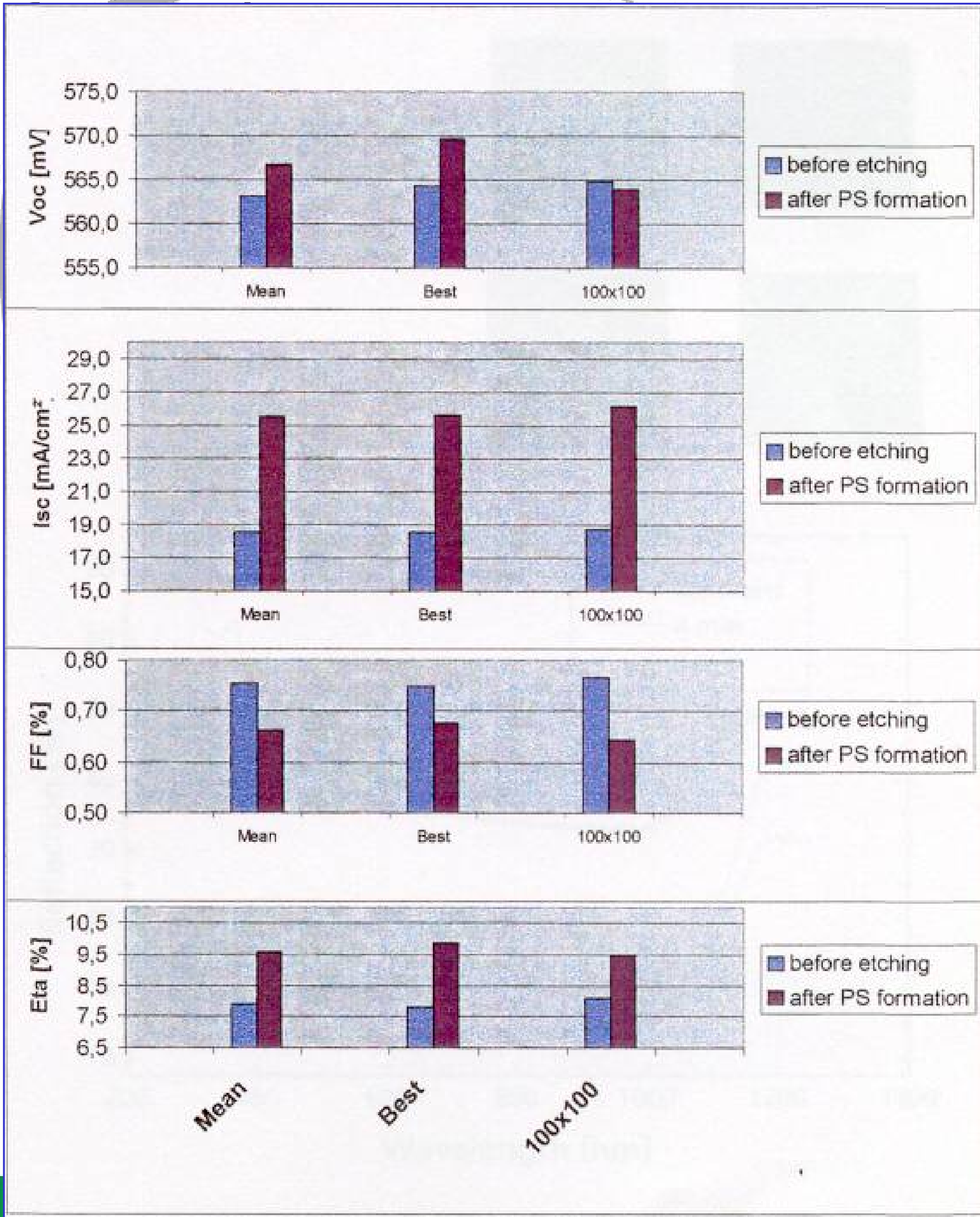

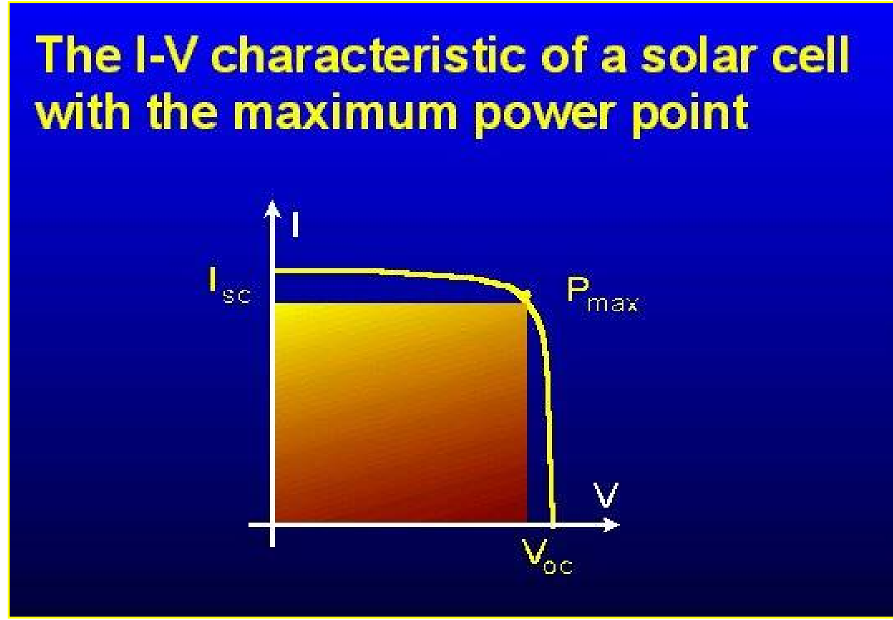

$$FF = \frac{V_{oc} - \ln(V_{oc} + 0.72)}{V_{oc} + 1} \qquad \eta = \frac{P_{out}^{max}}{P_{in}}$$

The overall effect of PS formation on the solar cells is a notable rise of the efficiency from about 7.5 % to around 9.6 %.

R.J. Martín-Palma, L. Vázquez, J.M. Martínez-Duart, M. Schnell and S. Schaefer, *Semiconductor Science and Technology* 16, 657 (2001).

Effect of extended exposure to the atmosphere and long periods of irradiation on the I-V characteristics

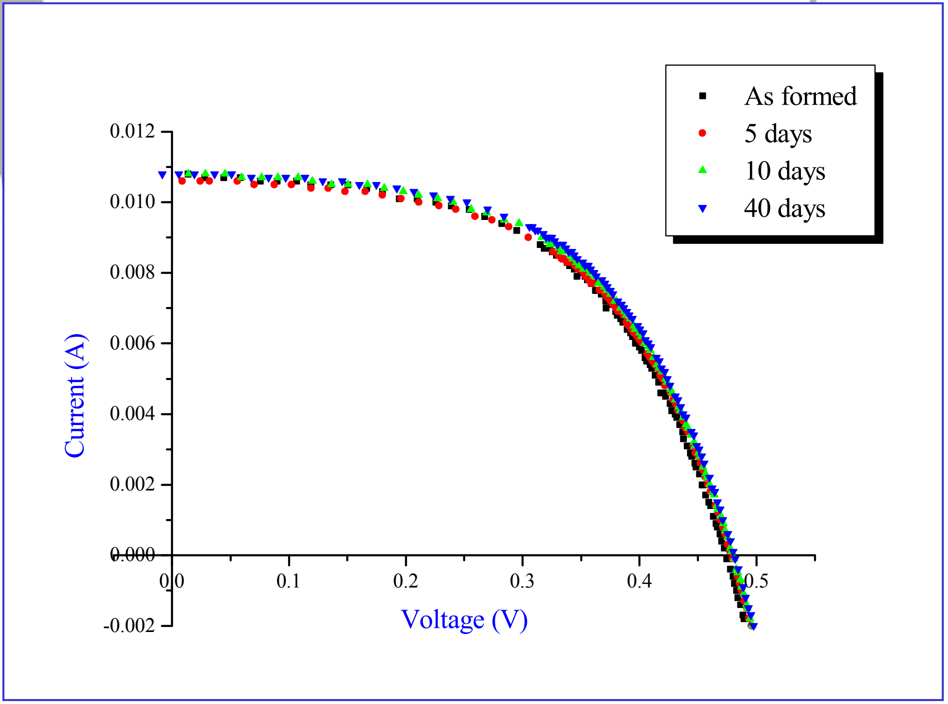

In both cases:

→ I_{sc} remains almost constant.

→ Slight increase of V_{oc}.

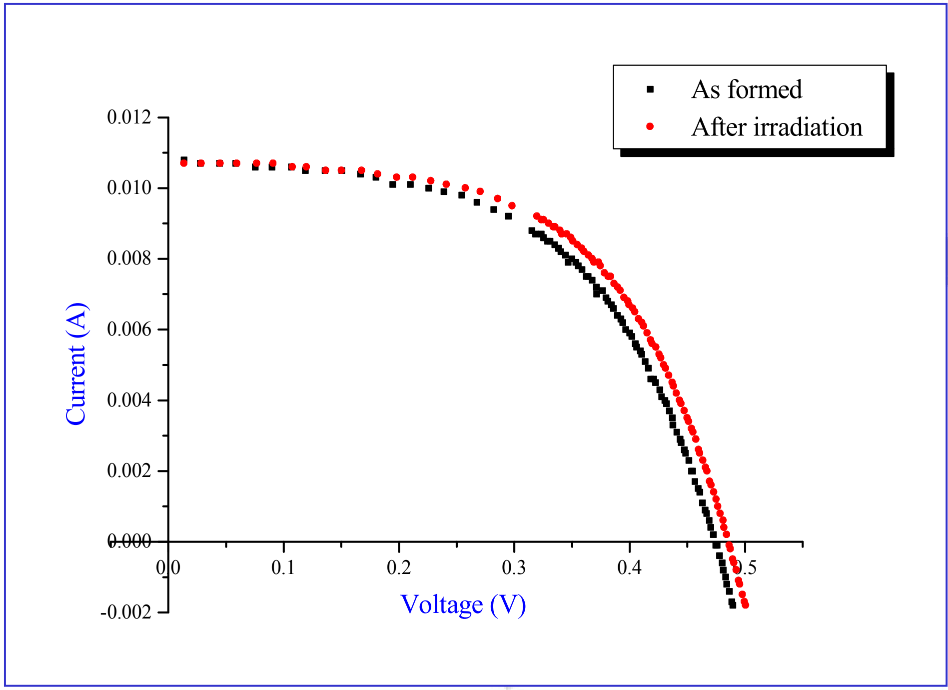

R.J. Martín-Palma, R. Guerrero-Lemus, J.D. Moreno, J.M. Martínez-Duart, A.Gras and D. Levy, *Materials Science & Engineering B* 69, 87 (2000).

Electrical characterization: temperature coefficients

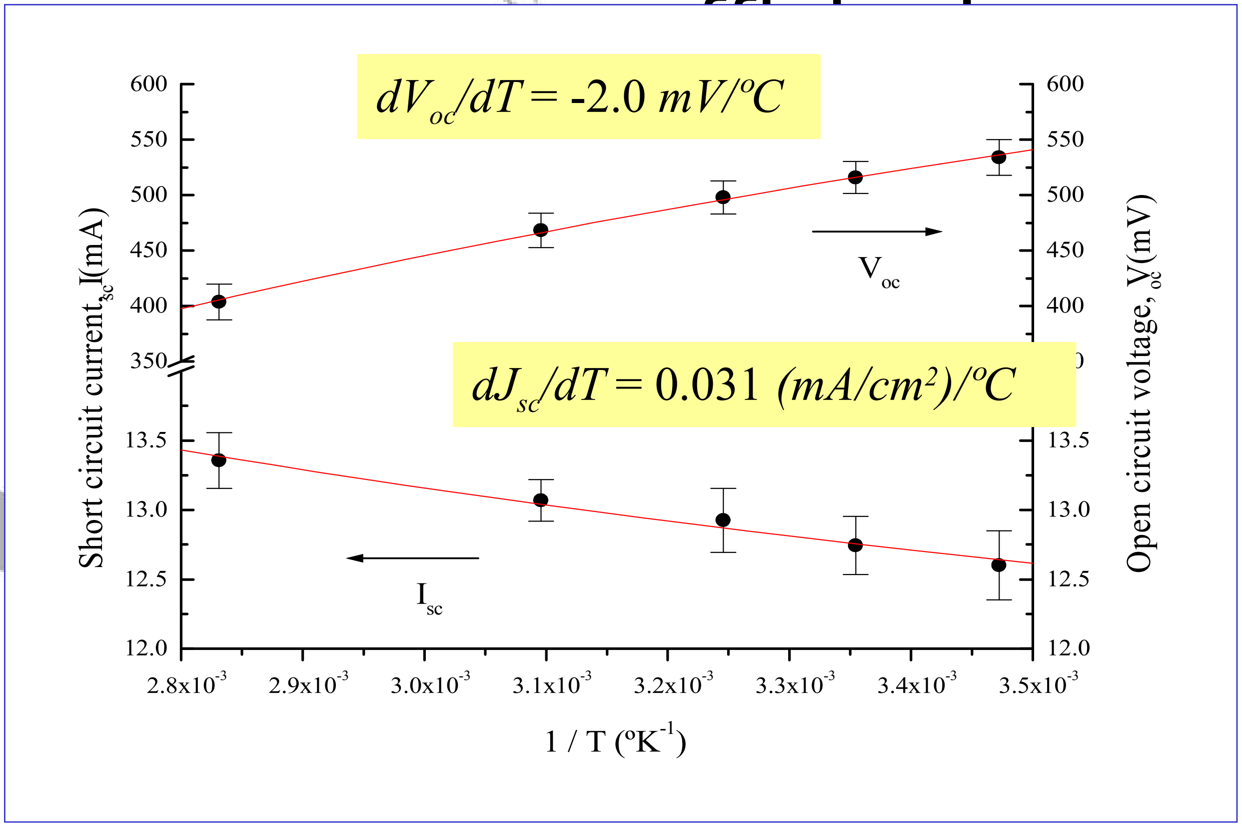

R.J. Martín-Palma, R. Guerrero-Lemus, J.D. Moreno, J.M. Martínez-Duart, A.Gras and D. Levy, *Materials Science & Engineering B* 69, 87 (2000).

- The variation of I_{sc} and V_{oc} vs. T (10 ºC to 80 ºC) was determined.
- I_{sc} rises with T (0.011 mA/K) → Increment of L_{dif} for minority carriers.
- V_{oc} decreases with T (-2 mV/K) → $I_o \propto T$.
- Temperature coefficients close to that of standard Si solar cells → PS is not degrading the electrical behavior at different T of the solar cells.

NANOSAT program


Una nueva filosofía en proyectos espaciales

Promover líneas de Investigación y Desarrollo en el área de las Nanotecnologías en el INTA y en las otras Instituciones participantes.

Desarrollar un sistema de comunicaciones en diferido para enlazar estaciones científicas remotas, como la Base Antártica Española y otras ubicaciones, para la centralización de los datos y la tele-operación de los equipos.

Calificar una pequeña plataforma para la demostración en órbita de nuevos sensores, componentes comerciales y nuevas tecnologías como las comunicaciones ópticas intra-satélite.

Photonic crystals

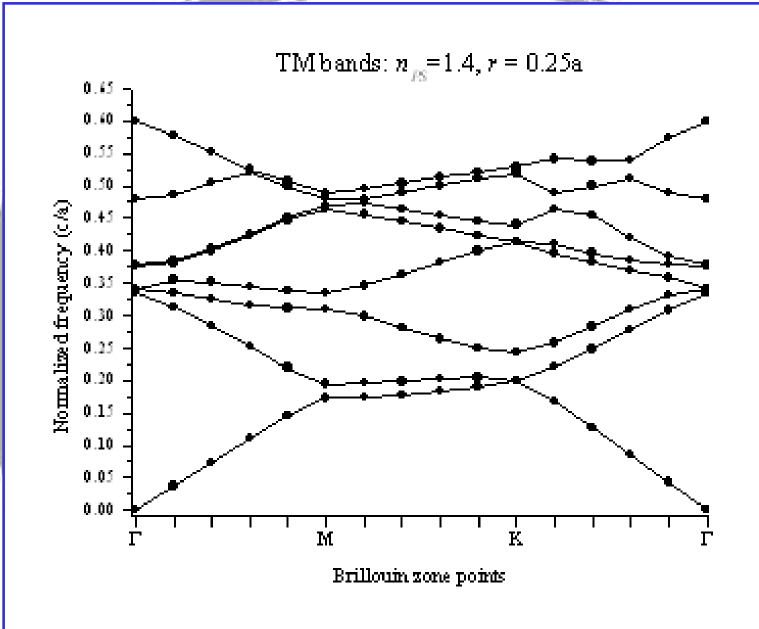

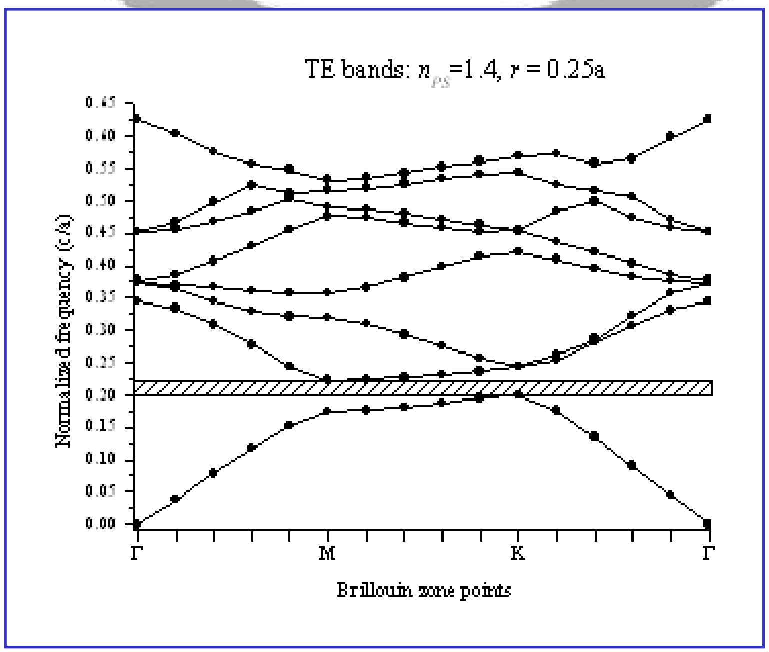

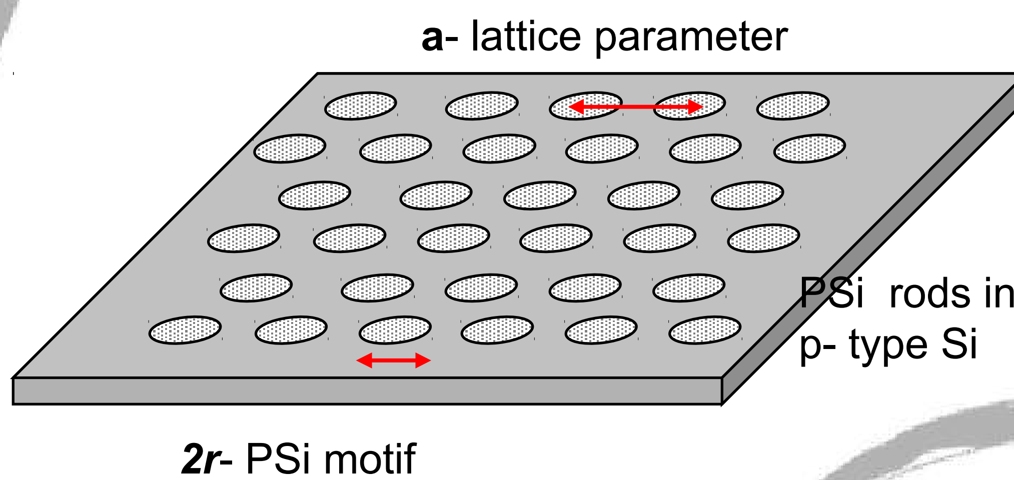

R.J. Martín-Palma, M. Manso, M. Arroyo-Hernández, V. Torres-Costa and J.M. Martínez-Duart, *Applied Physics Letters* 89, 053126 (2006).

Photonic crystals

Colloidal lithography

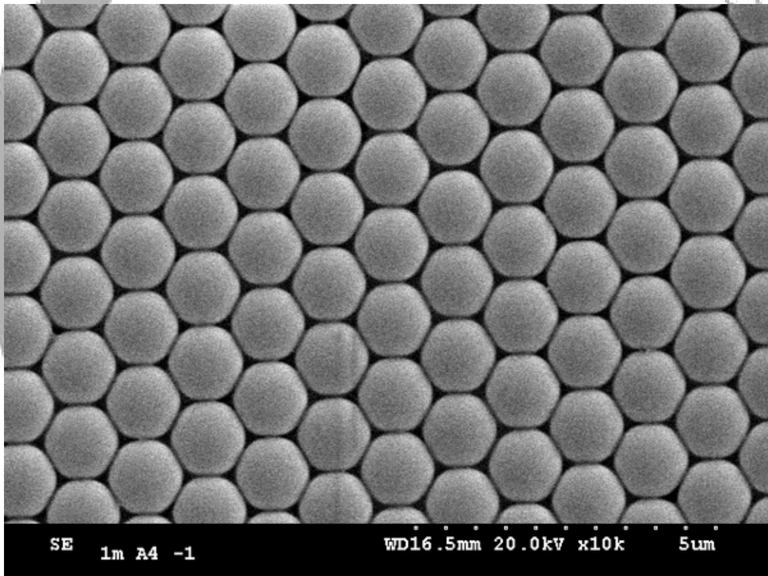

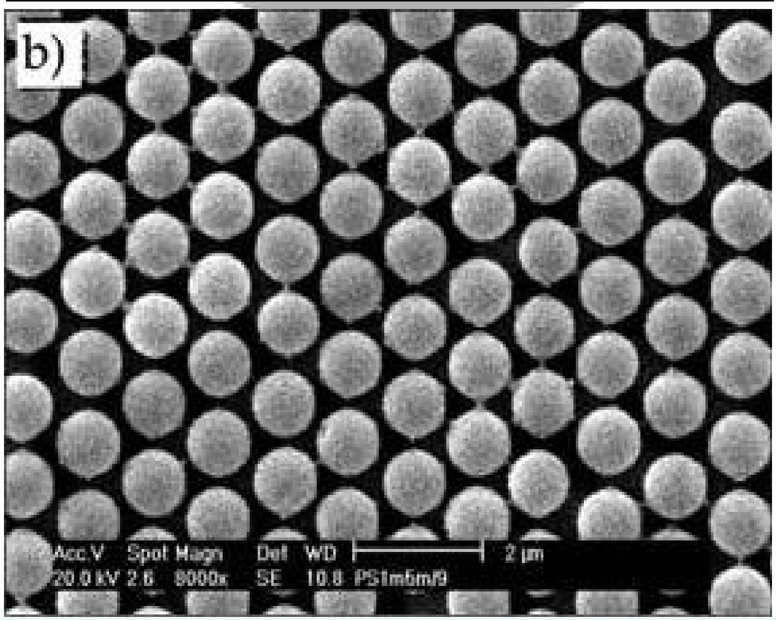

Traditional lithography

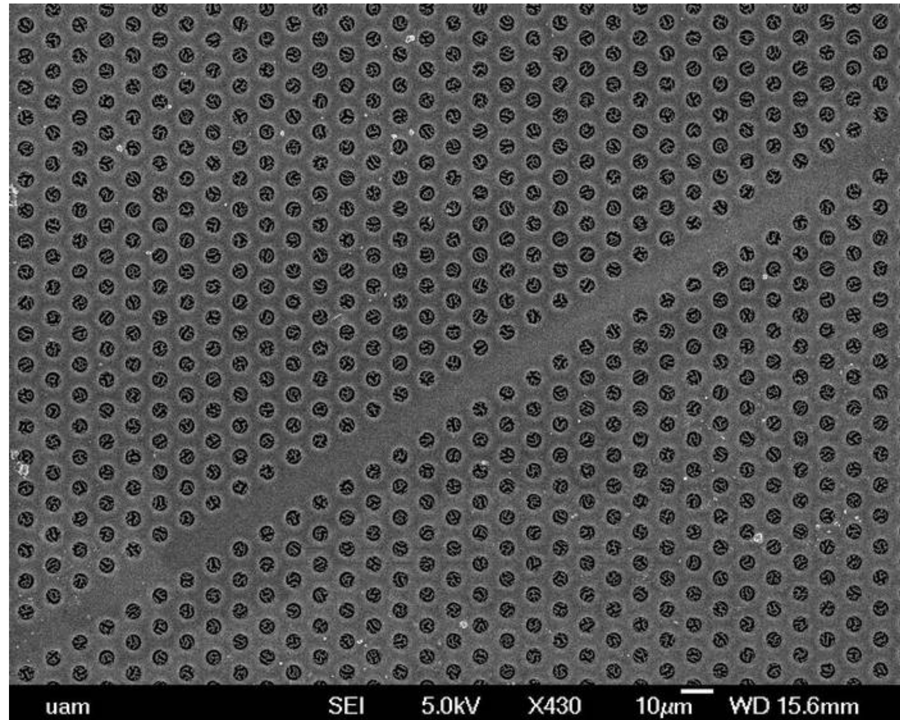

R.J. Martín-Palma, V. Torres-Costa, M. Manso, and J.M. Martínez-Duart, *Journal of Nanophotonics* 3, 031504 (2009).

M. Manso Silvan, M. Arroyo Hernandez, V. Torres Costa, R.J. Martin Palma, J.M. Martinez Duart, *Europhysics Letters* 76, 690 (2006).

Photonic crystals (cont'd)

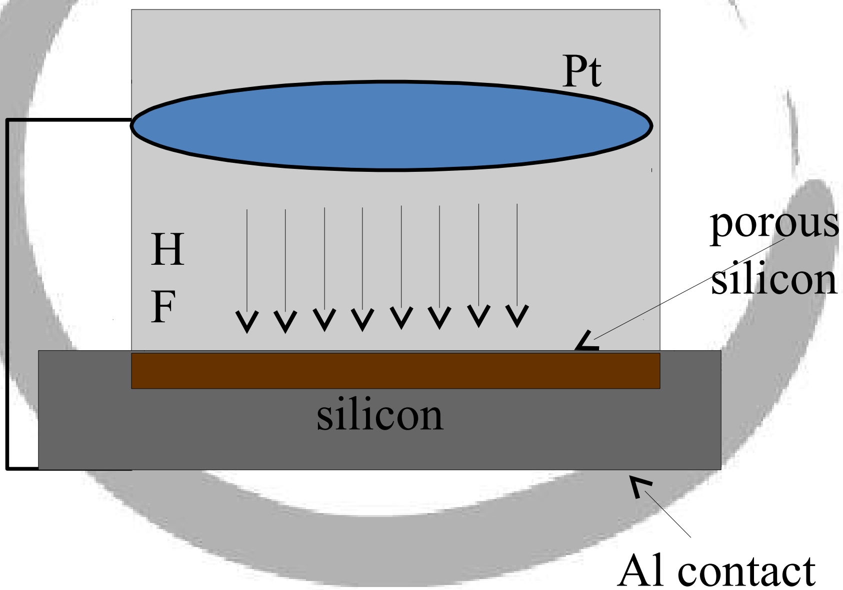

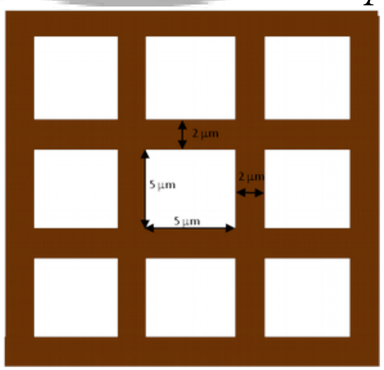

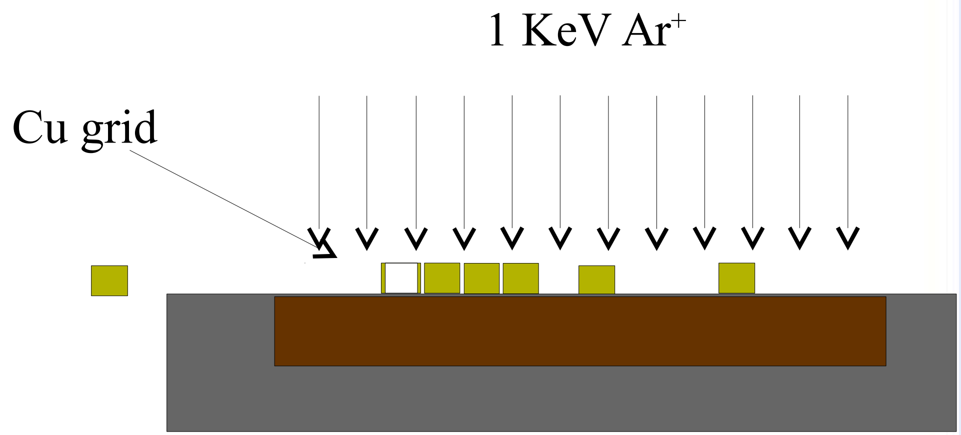

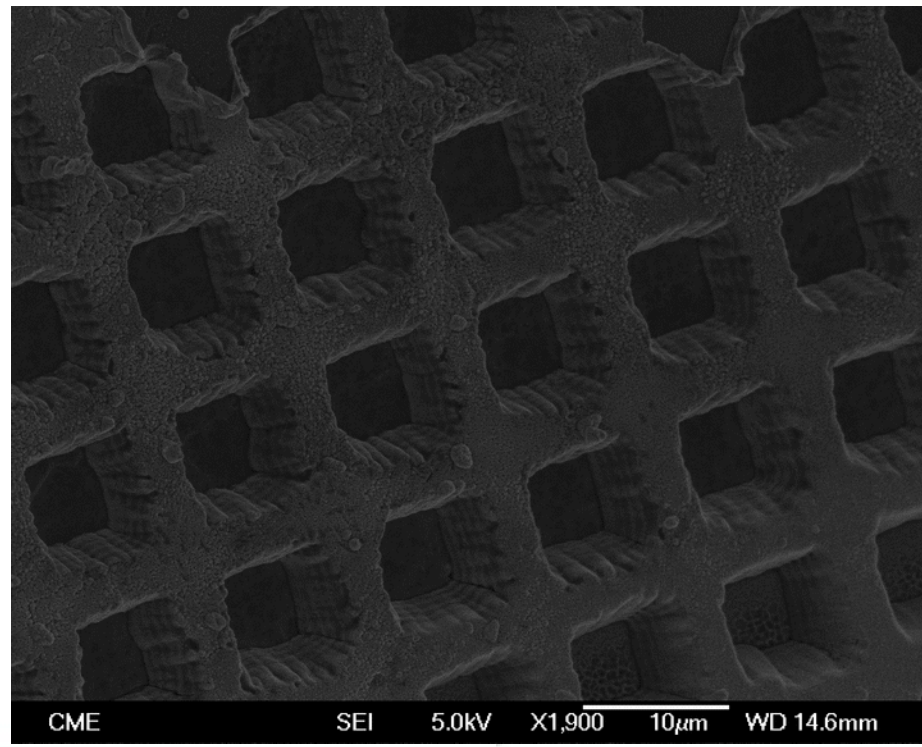

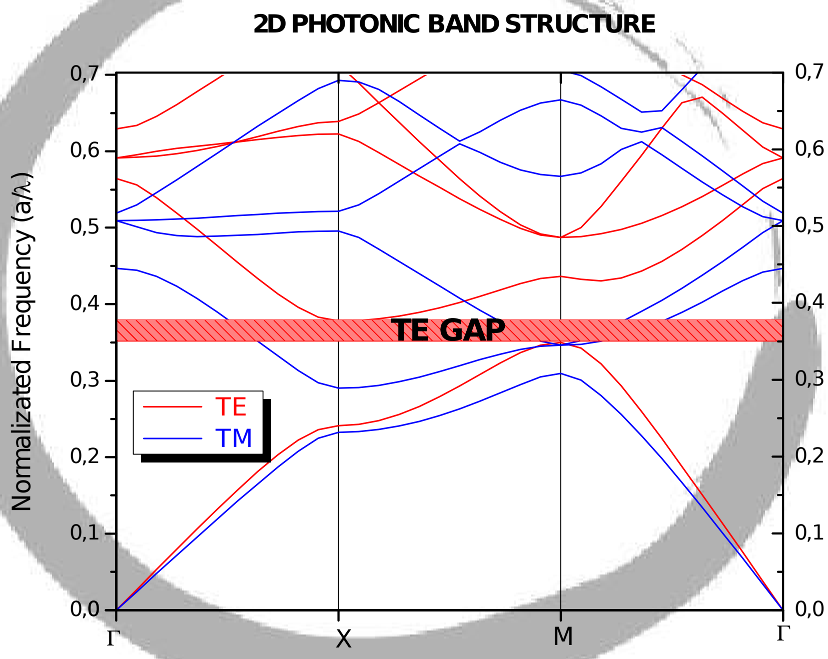
2D PHOTONIC BAND STRUCTURE
Normalizated Frequency (a/λ)
0,0
0,1
0,2
0,3
0,4
0,5
0,6
0,7
Γ
X
M
Γ
TE GAP
TE
TM

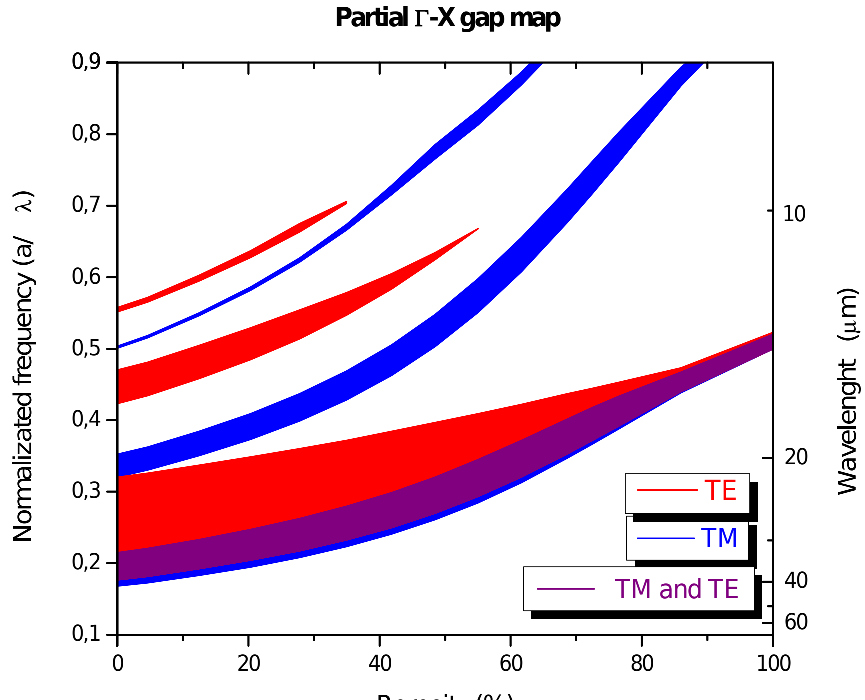
Partial Γ-X gap map
Normalizated frequency (a/ λ)
0,1
0,2
0,3
0,4
0,5
0,6
0,7
0,8
0,9
Wavelenght (μm)
10
20
40
60
Porosity (%)
0
20
40
60
80
100
TE
TM
TM and TE

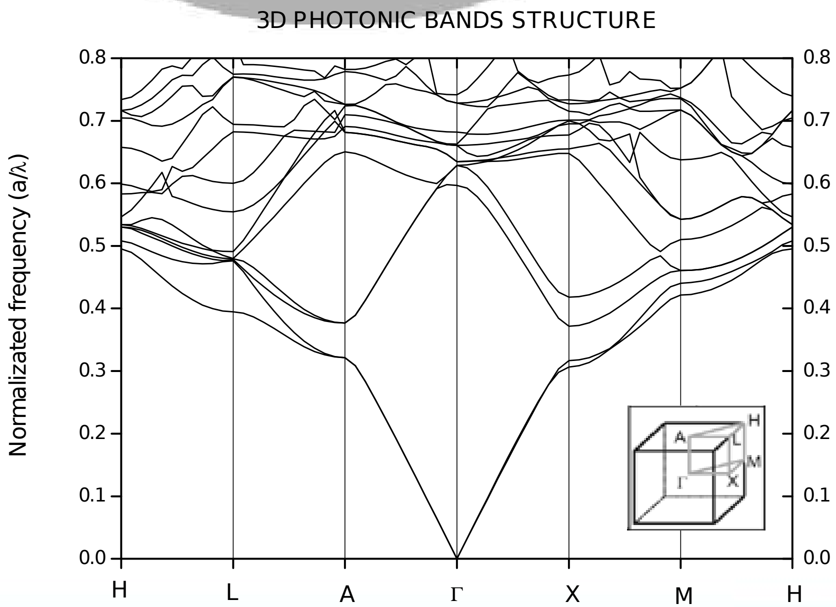
3D PHOTONIC BANDS STRUCTURE
Normalizated frequency (a/λ)
0.0
0.1
0.2
0.3
0.4
0.5
0.6
0.7
0.8
H
L
A
Γ
X
M
H

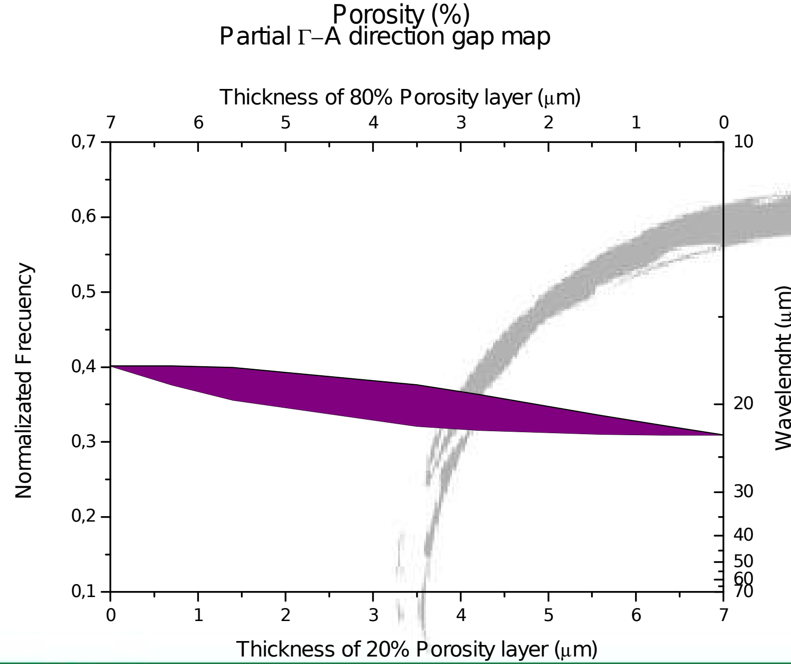
Partial Γ–A direction gap map
Thickness of 80% Porosity layer (μm)
7
6
5
4
3
2
1
0
Normalizated Frecuency
0,1
0,2
0,3
0,4
0,5
0,6
0,7
Wavelenght (μm)
10
20
30
40
50
60
70
Thickness of 20% Porosity layer (μm)
0
1
2
3
4
5
6
7

www.uam.es

Hybrid gold/porous Si thin films for plasmonic solar cells

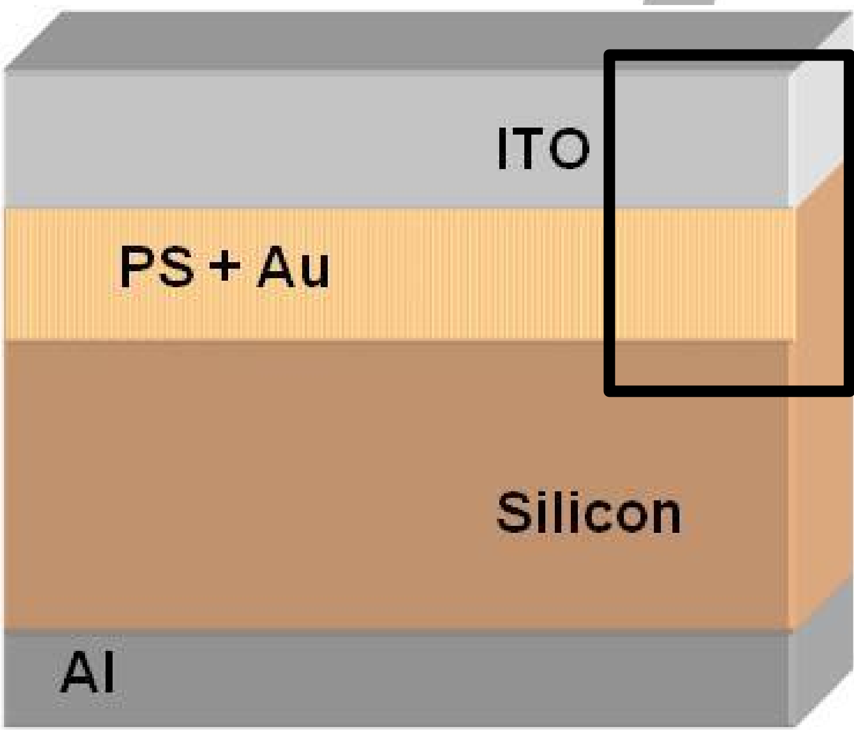

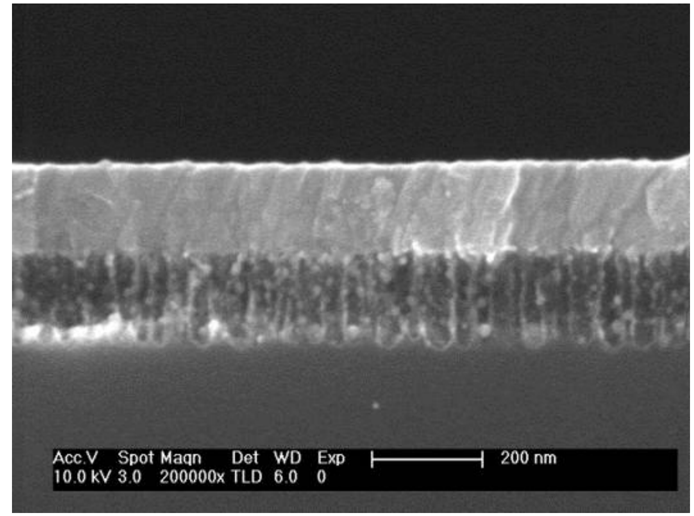

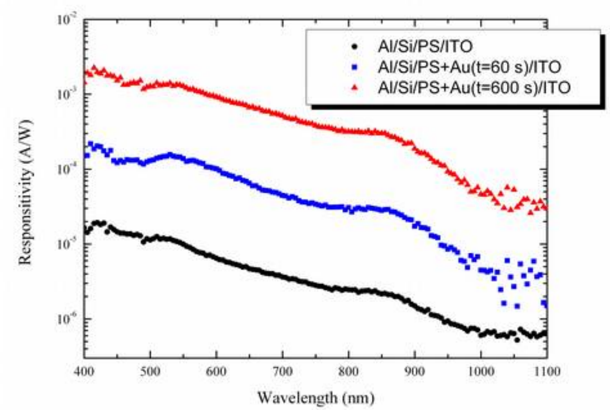

www.uam.es

Biomedical applications:
nanoPS-based multifunctional particles

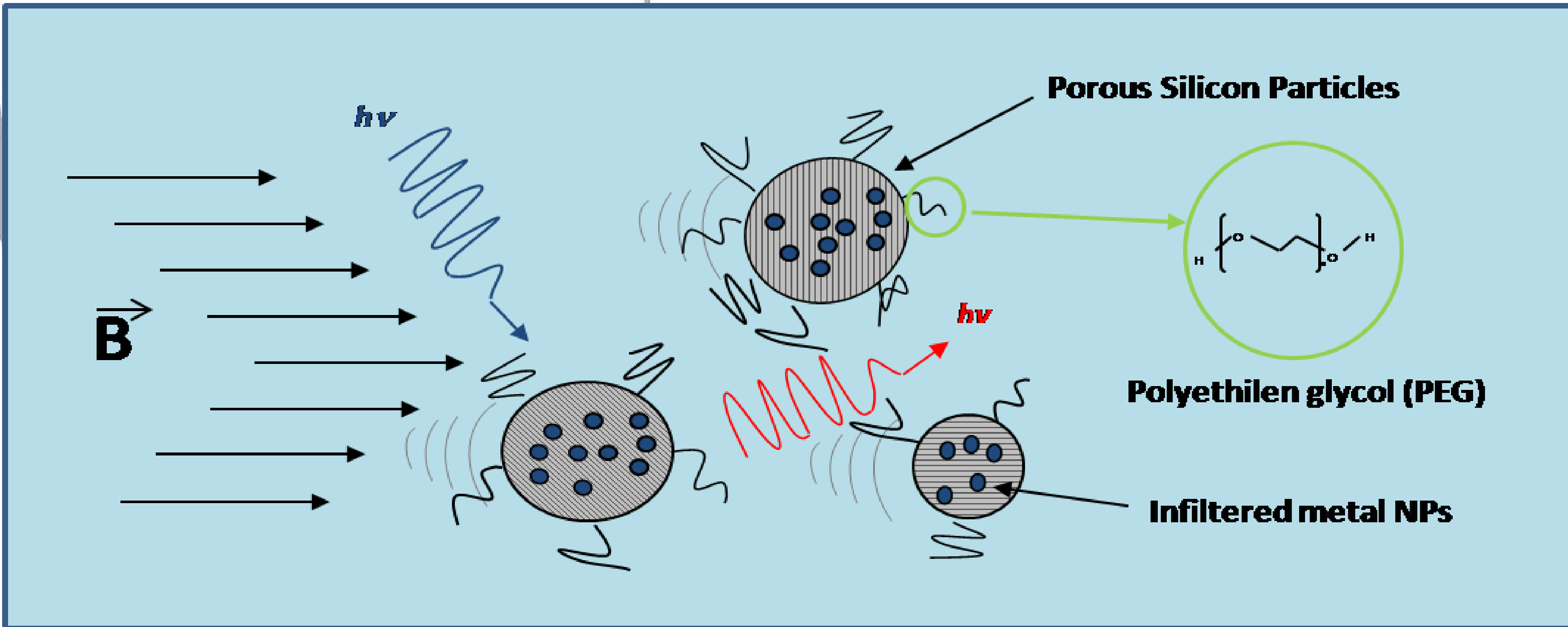

- A porous SiO_2 matrix hosts Si nanocrystals and metal NPs.
- Luminescent + magnetic + biocompatible.

NanoPS-based multifunctional particles in action

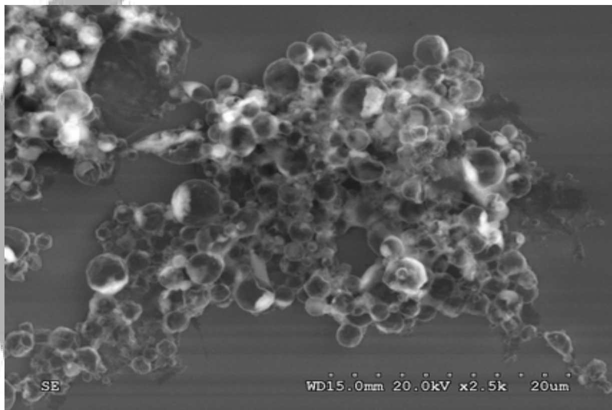

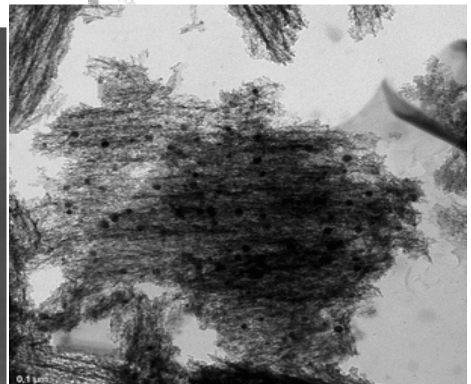

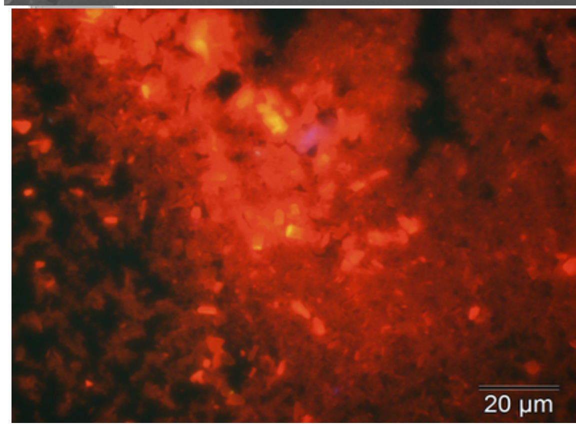

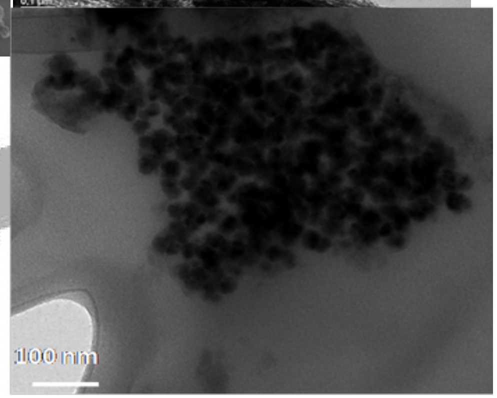

- The blue emission of the nanoPS particles allowed tracking the cellular cytosol of hMSCs.
- Studies of proliferation up to 72h showed no apoptosis response in the cells.

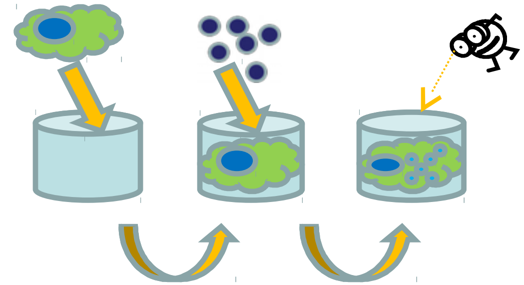

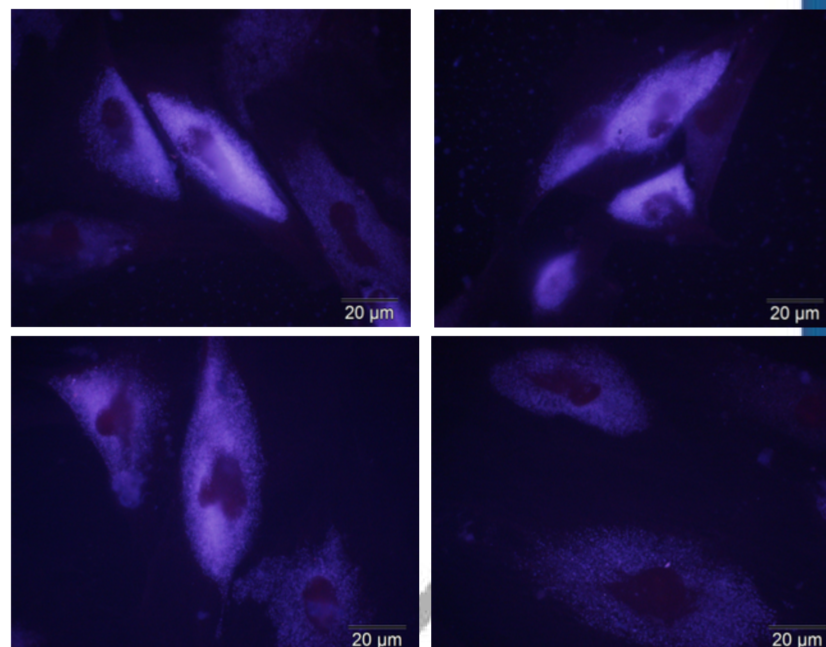

Potential applications:
Cellular & molecular imaging, cell labeling & tracking, diagnosis, targeted delivery of therapeutic compounds, magnetic resonance imaging contrast agents, probes & sensors, …

Magnetic PS flakes as retina pressure actuators

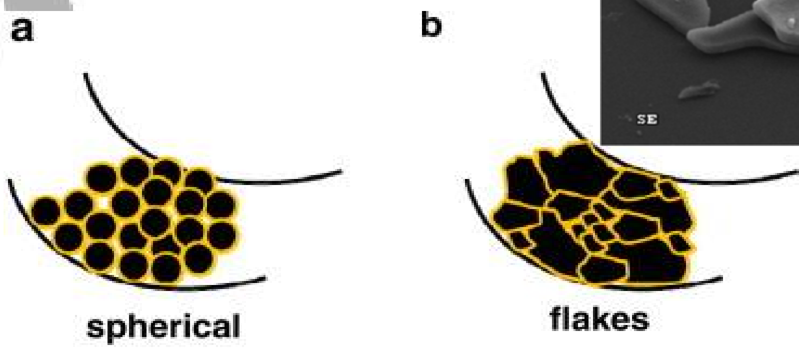

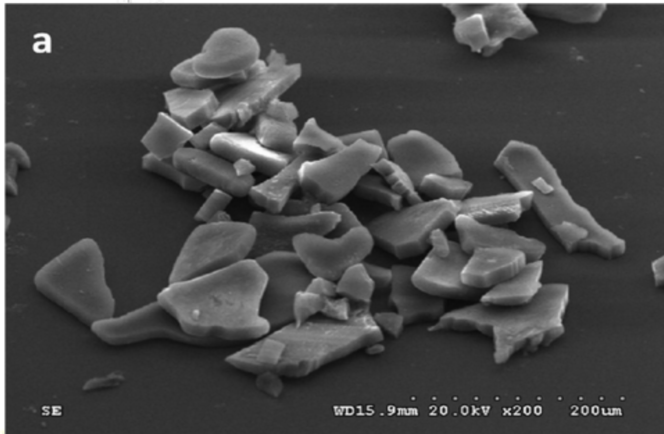

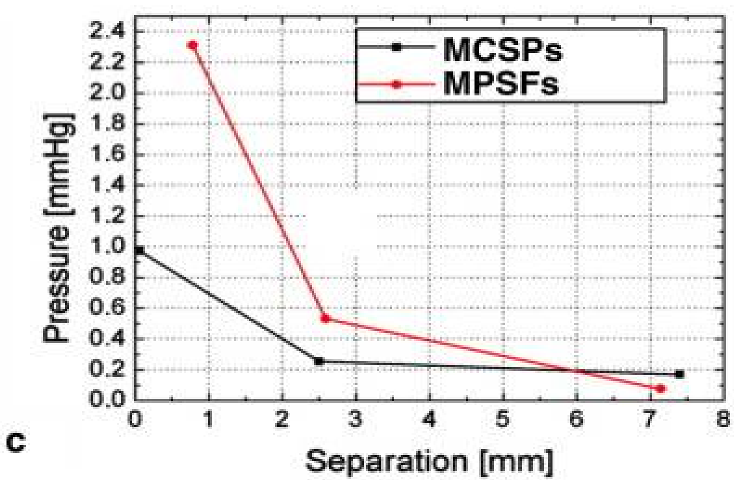

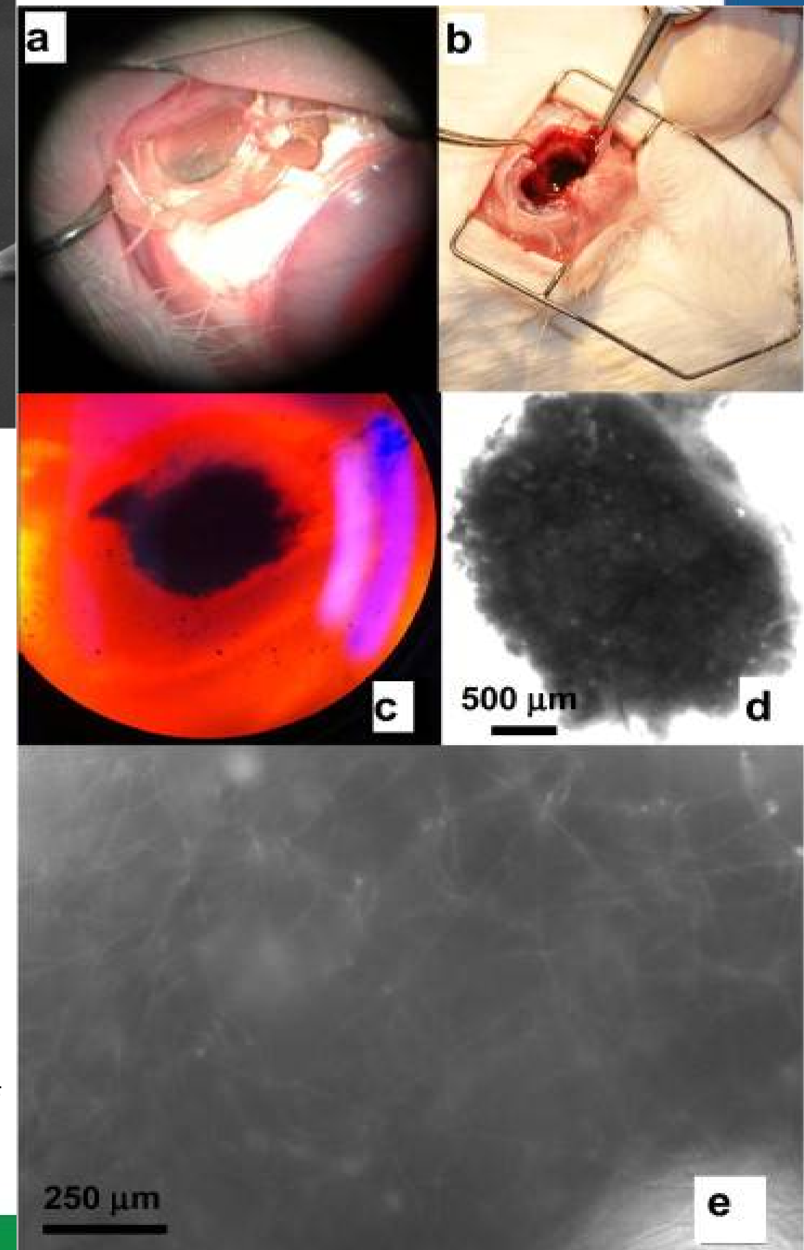

Low inflammatory response and no necrosis effects

Images after 1 month post mortem inspection of rabbits: (a) area of the sclera after explanation of the permanent magnet; (b) Eye dissection for extraction of the MPSF agglomerate from the eye wall; (c) in situ retinal tissue with attached MPSF; (d) explanted MPSF; (e) magnification from (d).

WO/2013/011176. Publication date Jan. 24, 2013

Silicon/nanoPS surface micropatterns for the control of cell behavior

www.uam.es

Fabrication

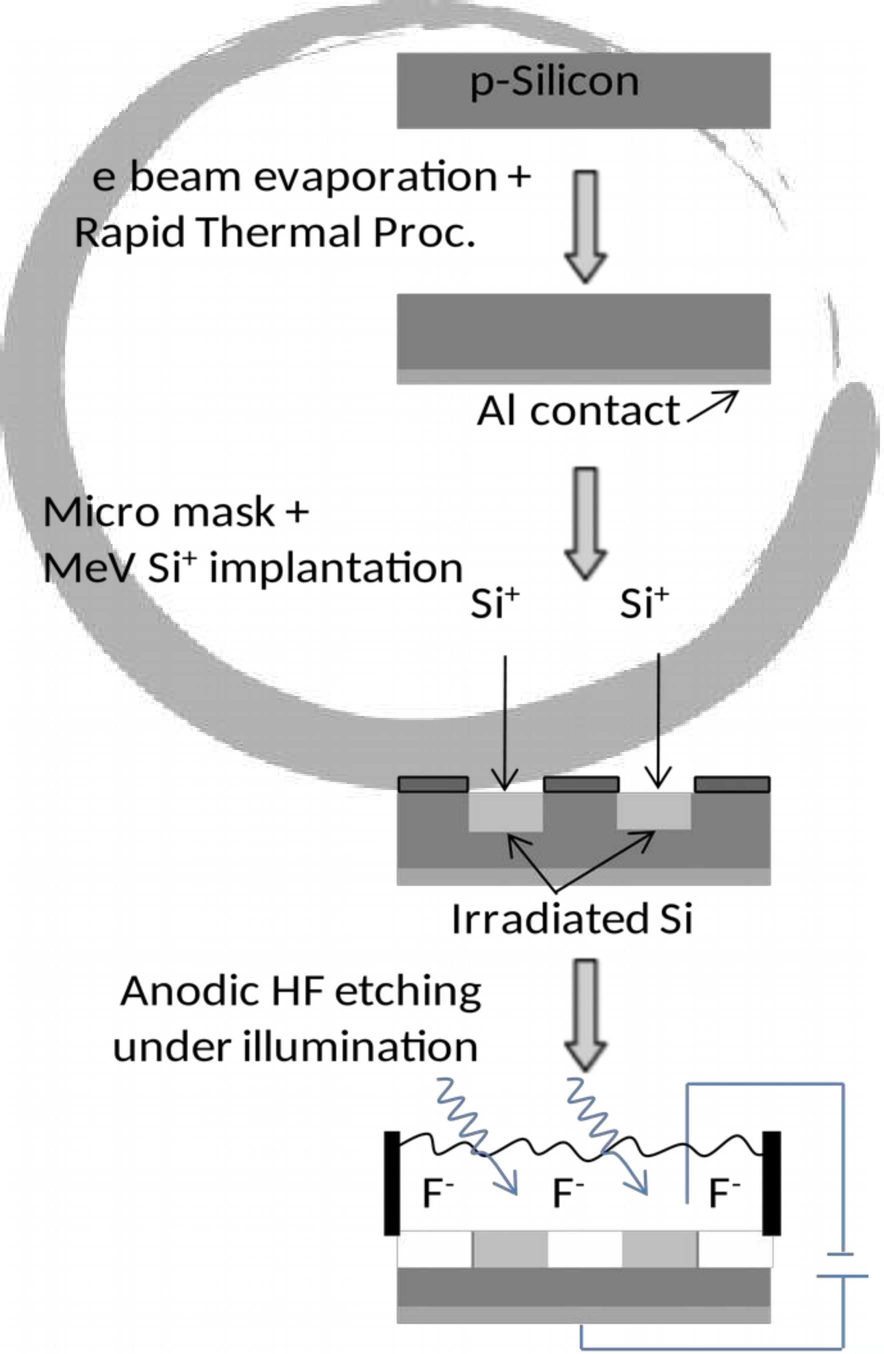

- Ohmic Al contact (e-beam evaporation + rapid thermal annealing).
- MeV implantation with Si^+ ions.
- Anodic etching.

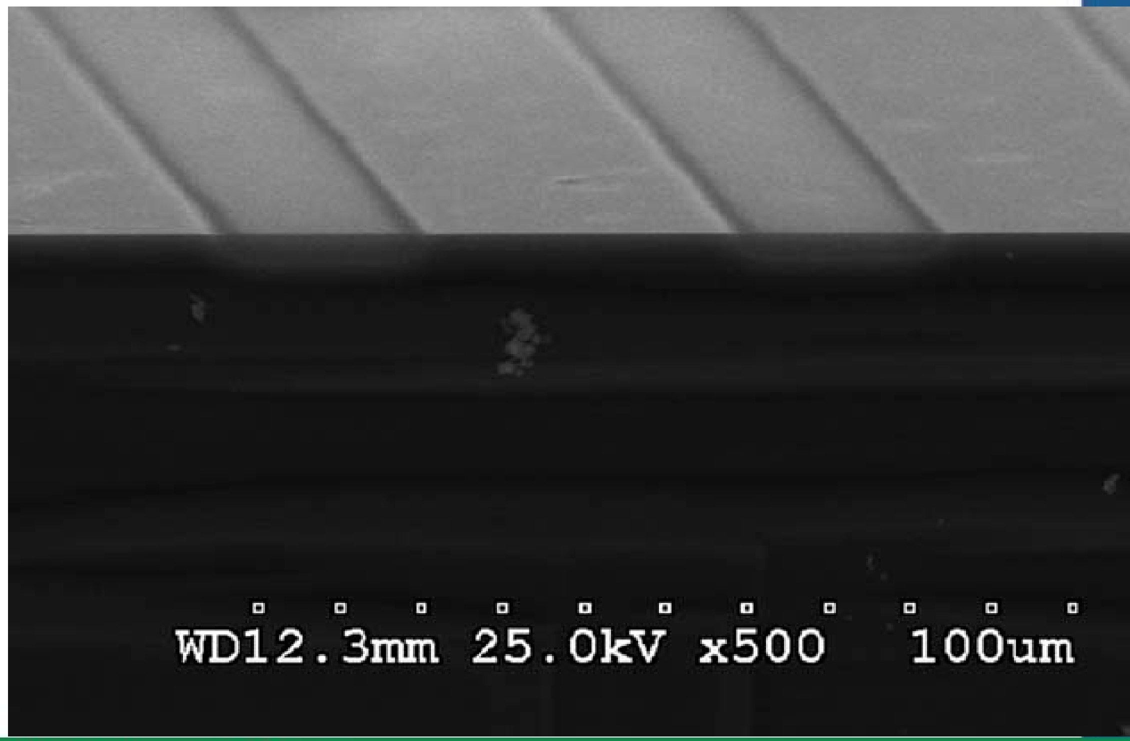

1D and 2D Si/nanoPS surface micropatterns

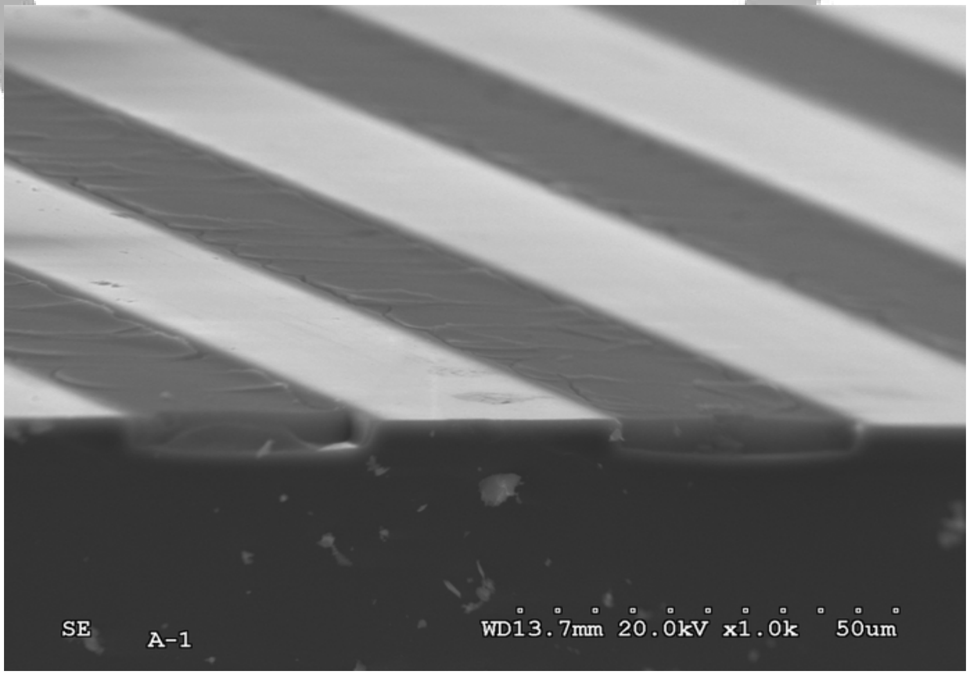

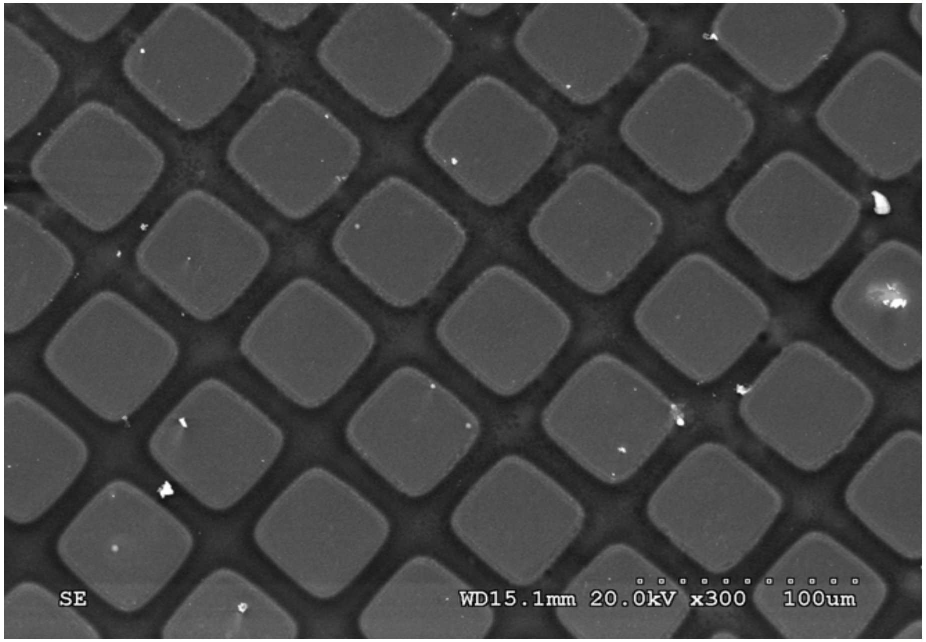

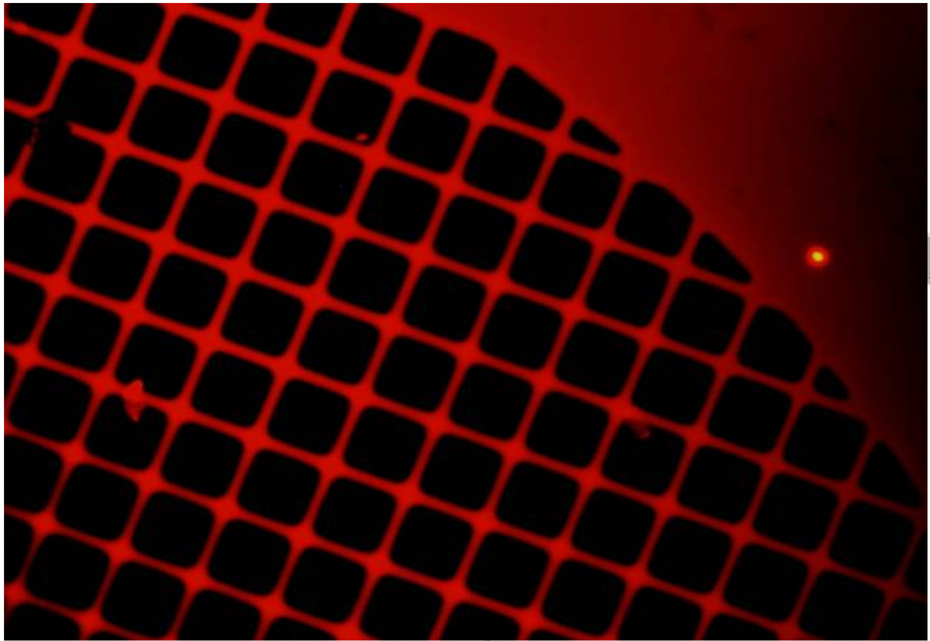

Cell culture on 1D Si/nanoPS micropatterns

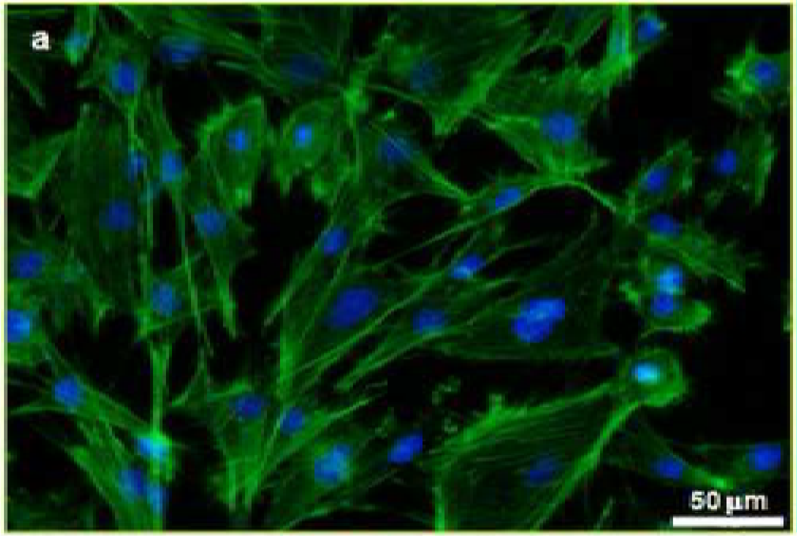

Fluorescence microscopy (actin is stained green, nuclei are stained blue):

(a) Glass control.

(c) 75 μm Si/25 μm nanoSi stripes: Cells preferentially located on Si (Several cells appear in a final stage of cellular division) → Proliferative state)

(d) 50 μm Si/25 μm nanoPS stripes: Cells predominantly located in Si areas, occasionally in nanoPS areas

(e) 40 μm Si/20 μm nanoPS stripes: Actin skeleton on Si areas, nuclei on nanoPS areas.

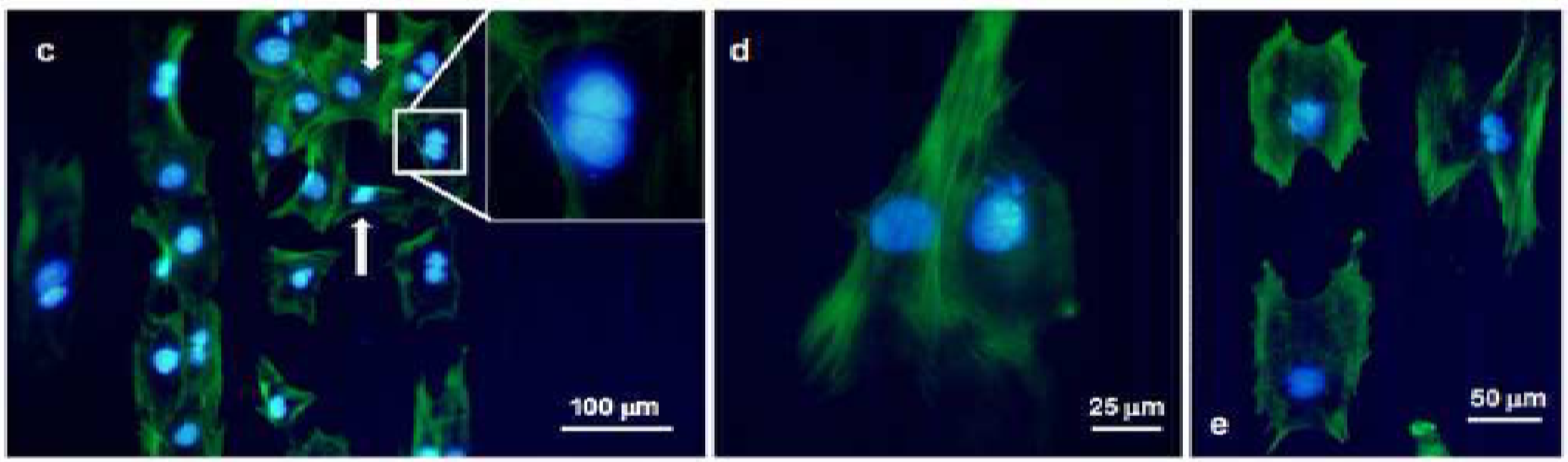

Response of hMSCs depends on the Si/nanoPS ratio

A. Muñoz-Noval *et al.*, Journal of Biomedical Materials Research: Part A 100A(6), 1615 (2012).

Cell surface distribution

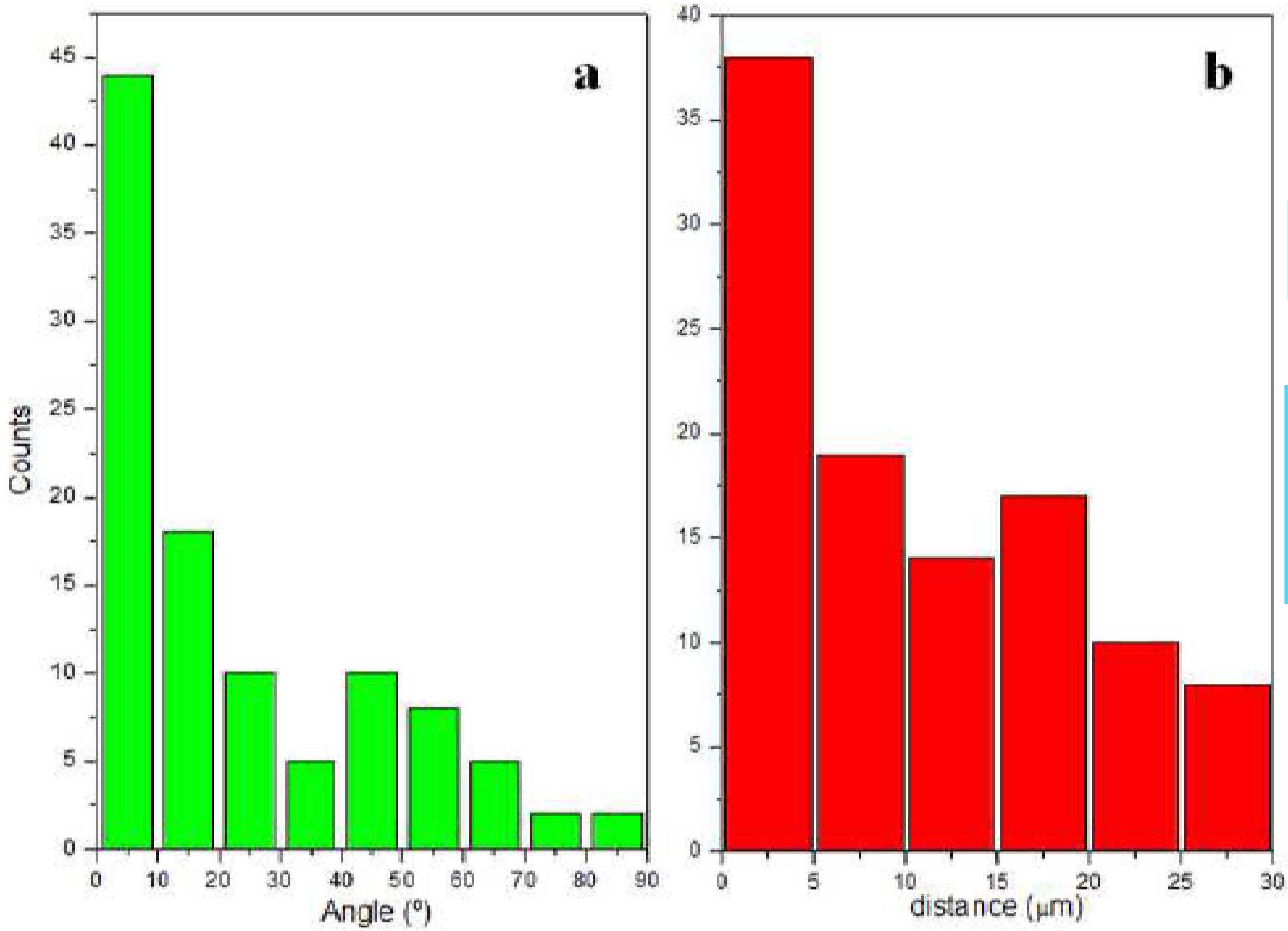

Actin fiber orientation with respect to the stripes (average 12º±5º)

Nucleus distance with respect to the center of the closest nanoPS microstripe center

40 μm Si/20 μm nanoPS 1D structures

54% of hMSCs population on the surface of nanoPS (nanoPS represents 33% of the total area!).

Cell culture on 2D Si/nanoPS micropatterns

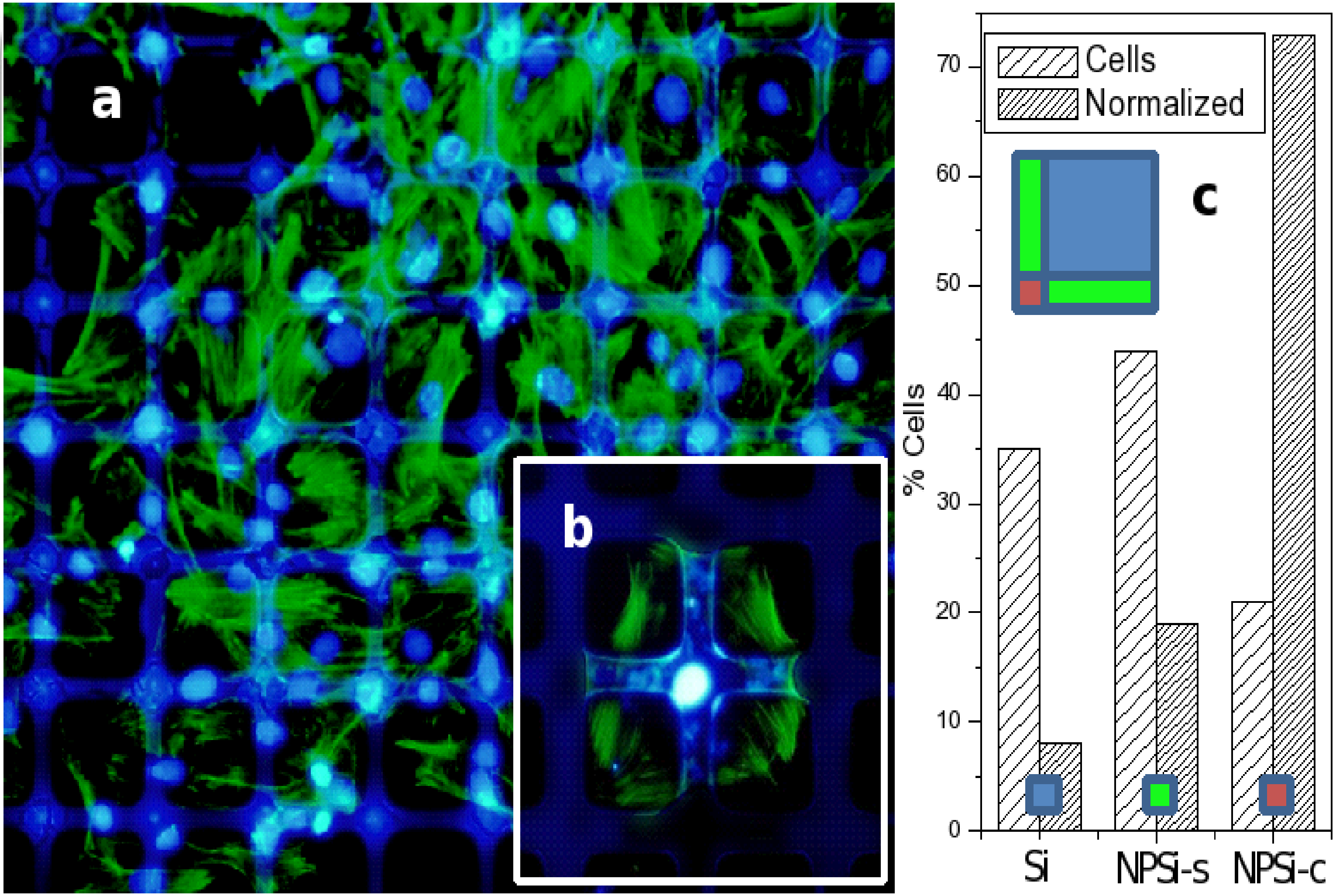

Actin is stained green
Nuclei are stained blue

V. Torres-Costa, *et al.*, International Journal of Nanomedicine 7, 623 (2012).

100 μm Si/ 25 μm nanoPS squares:

(a) General view

(b) Detail of an intersection: cells adhere and extend their cytoskeleton quasi-symmetrically

(c) histogram of hMSC population: absolute % and area-normalized

Potential applications:
Basic studies (cell adhesion and migration), tool in regeneration, healing, or cancer propagation studies.

1D and 2D patterns of Si and nanoPS were engineered by ion-beam irradiation and subsequent electrochemical etch aiming at studying the mechanisms of cell adhesion and migration.

Lessons learned: hMSCs are sensitive to surface patterns and migration can be controlled → Cells arrange in response to the particular surface topography.

Drawbacks: Relatively complex technique for the fabrication of the surface micropatterns textured at the nanoscale.

Laser fabrication of Si/nanostructured porous silicon surface micropatterns

NanoPS layers

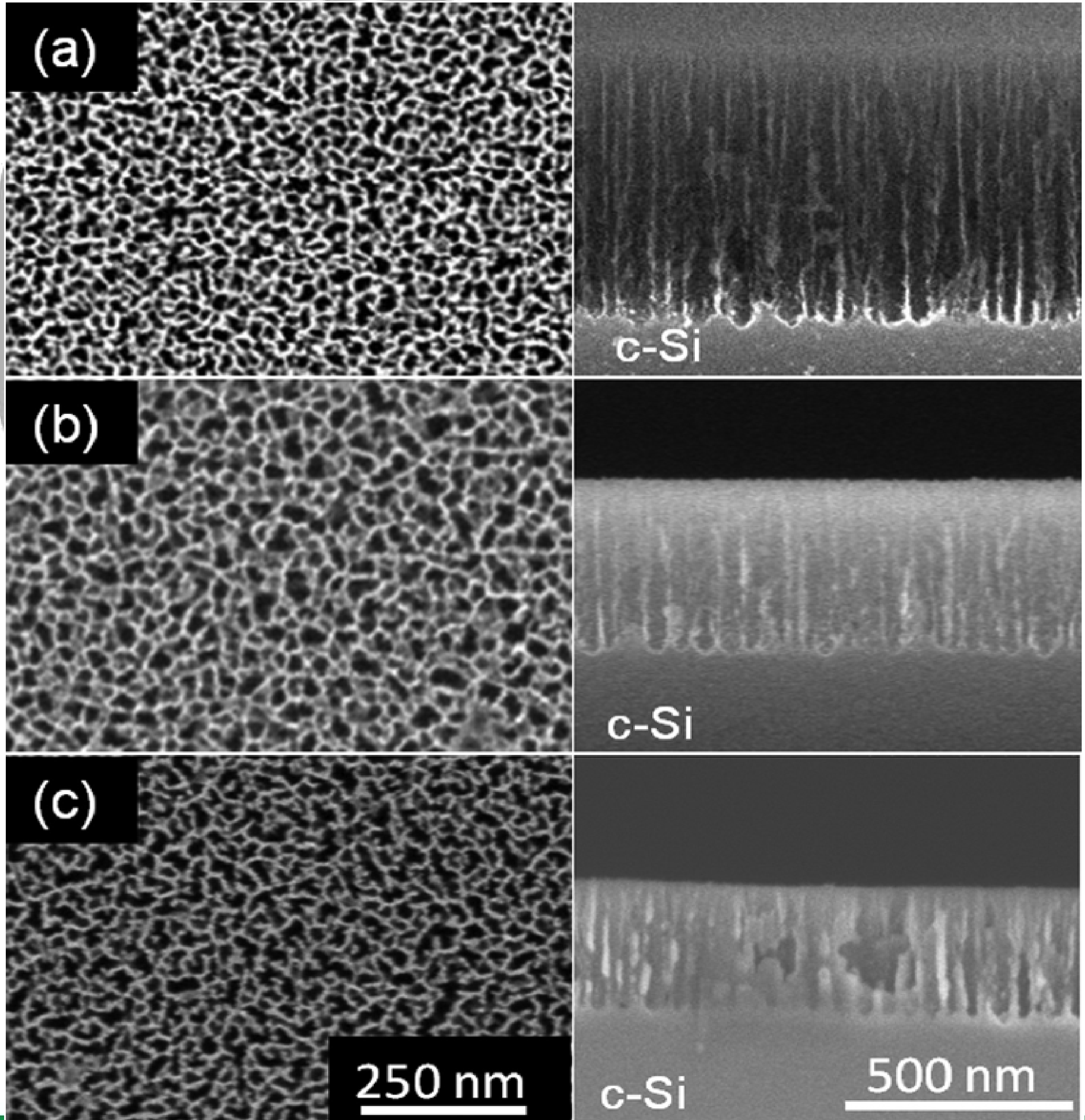

Thicknesses:

(a) 563 nm
(b) 372 nm
(c) 290 nm

Patterning method

Interferential process:

Single pulses of an excimer laser (λ = 193 nm, τ = 20 ns)

The nanoPS surface thus becomes exposed to a modulated intensity formed by the maxima and minima of interference.

The period of the modulation is modified by using different combinations of projection lenses.

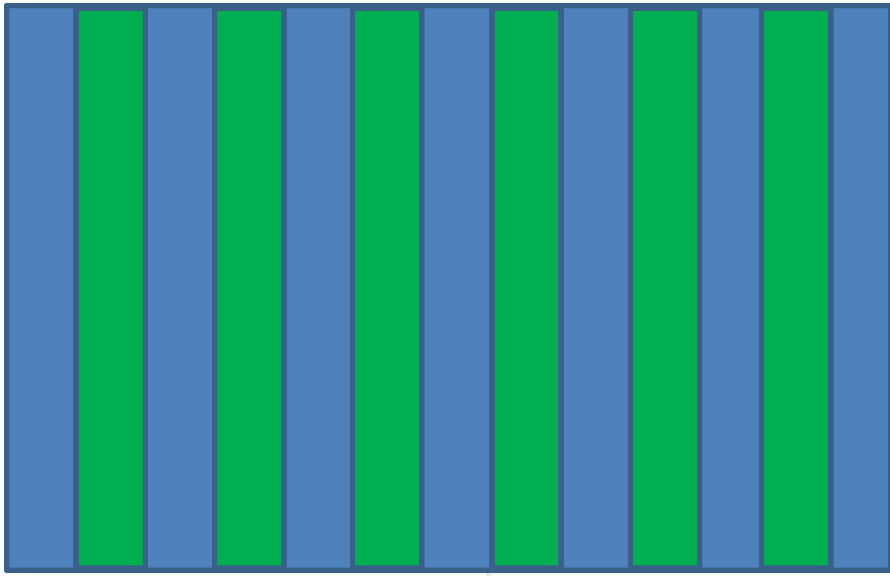

Fluence:

- constant along the *y* axis
- *x* axis: $F(x) = F \cdot (1 + \cos(2\pi x/\Delta))$

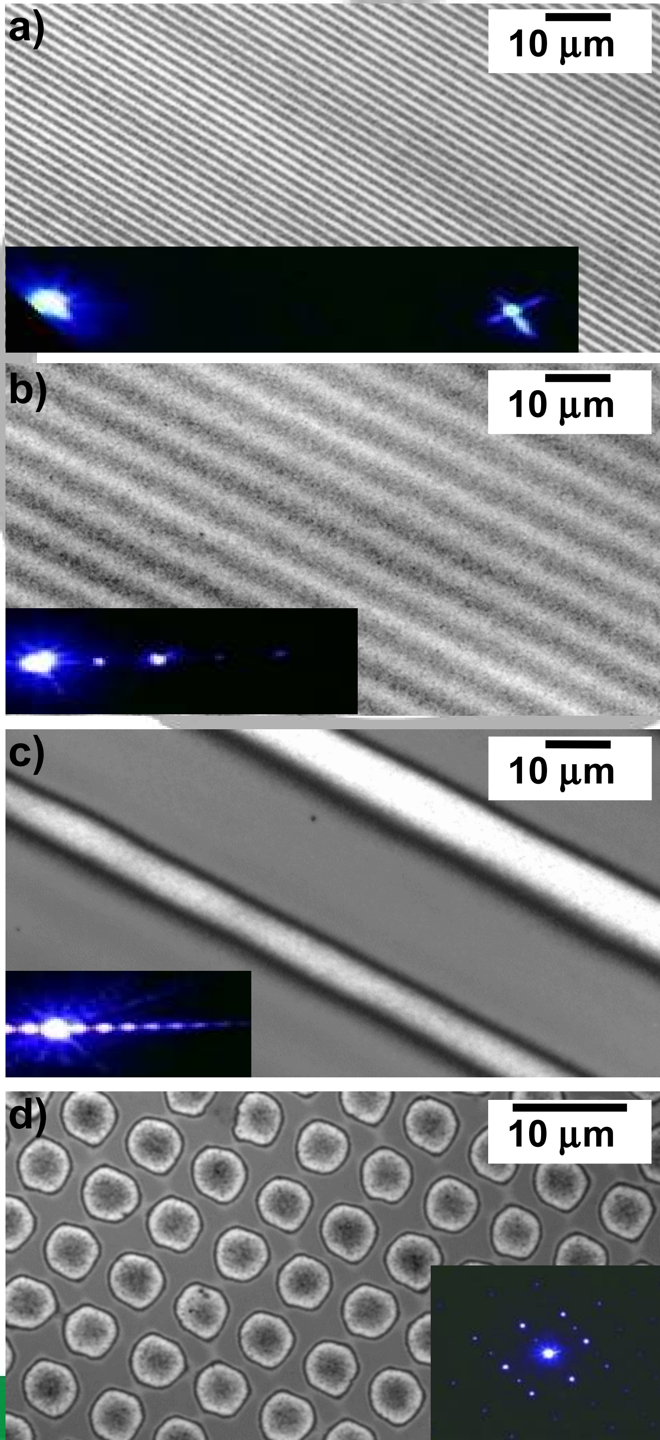

Structure of the patterns

By using different projection optics the effective laser fluences and periods achieved are different:

(a) 198 mJ/cm^2 and 1.7 μm
(b) 50 mJ/cm^2 and 6. 3 μm
(c) 11 mJ/cm^2 and 31 μm
(d) 19 mJ/cm^2 and 6.3 μm.

The insets show the experimental diffraction patterns

Structure of the patterns (cont'd)

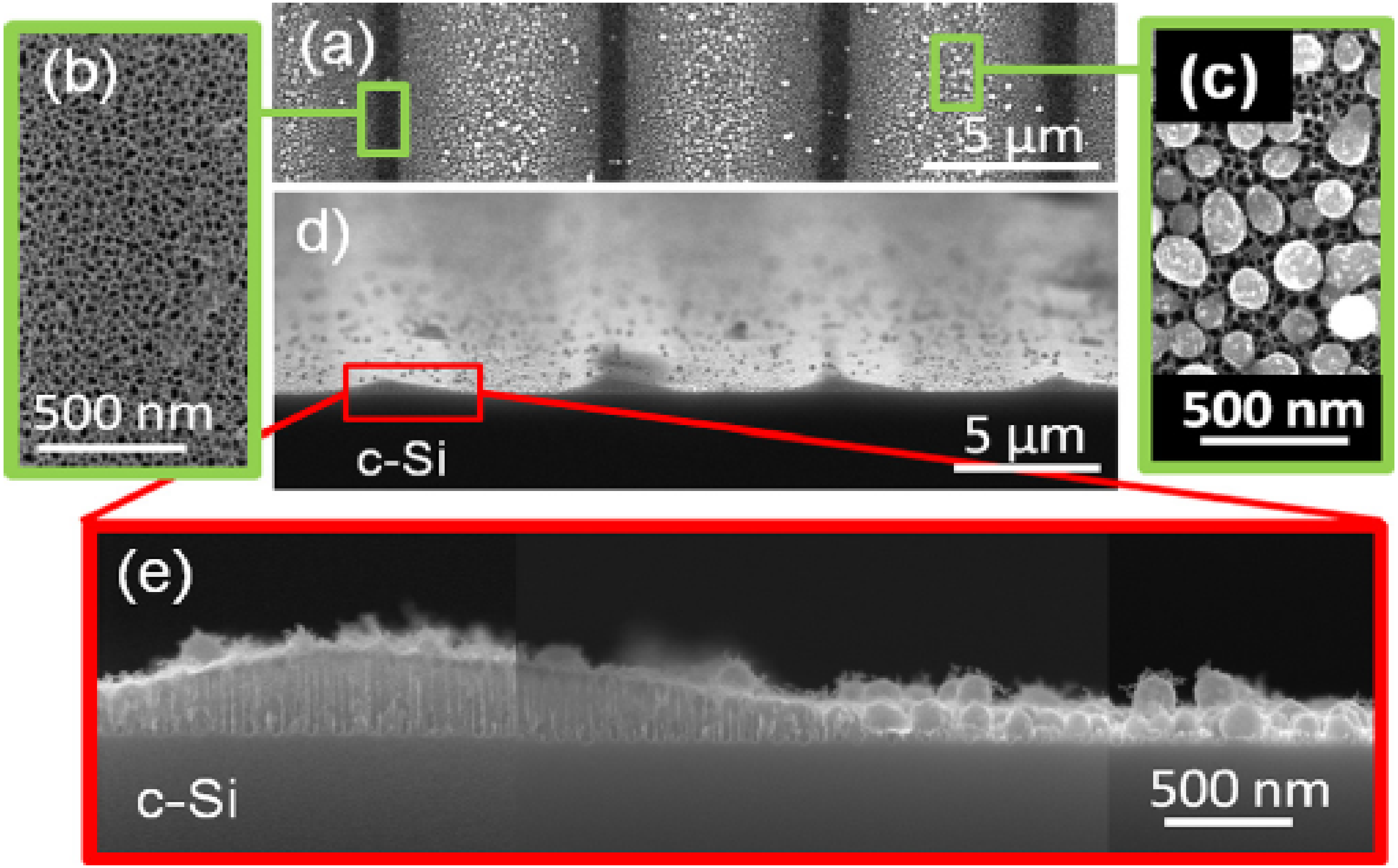

Pattern with a period of 6.3 mm (372 nm-thick nanoPS layer) using 44 mJ cm^{-2}

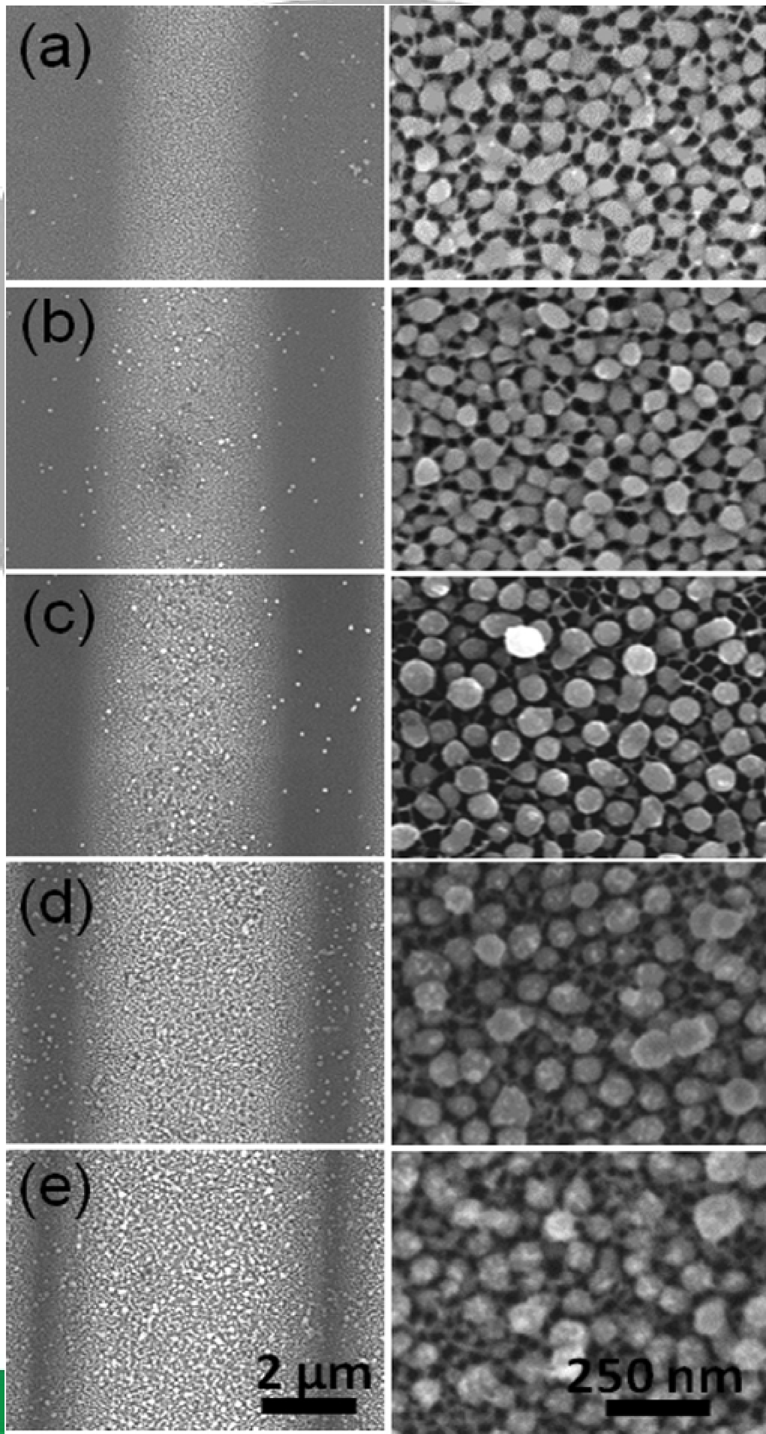

Effect of fluence

Patterns with a period of 6.3 μm / 290 nm-thick nanoPS layer

<u>Fluence:</u>

(a) 11 mJ·cm^{-2}
(b) 18 mJ·cm^{-2}
(c) 28 mJ·cm^{-2}
(d) 42 mJ·cm^{-2}
(e) 80 mJ·cm^{-2}

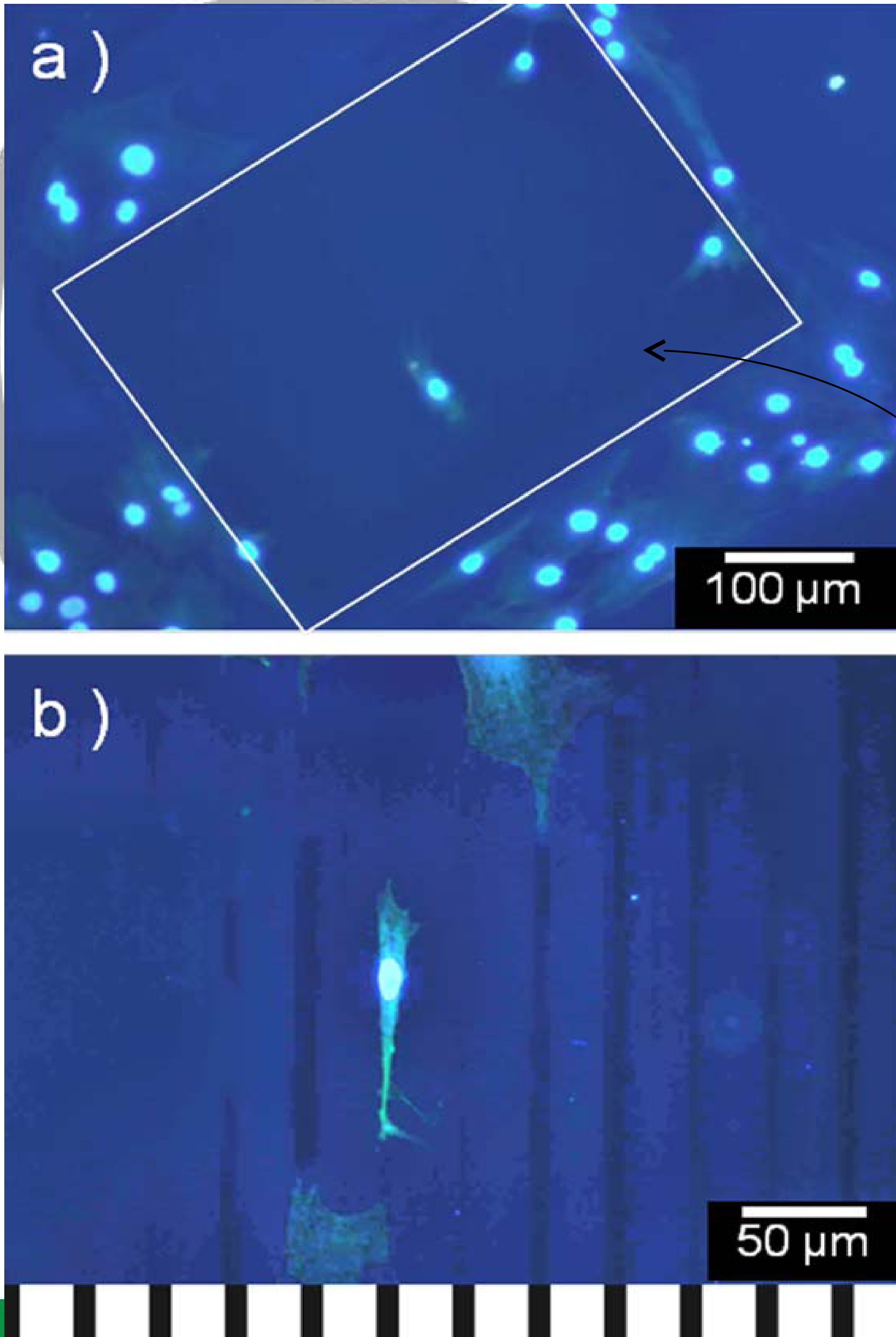

Cell culture

Blue fluorescence images of hMSCs on two patterns:

(a) 1.7 µm
(b) 31 µm

Patterned region

The hMSCs bind directly and align along the transformed regions of the pattern whenever the width of the trenches on these regions compares with the dimensions of the hMSCs.

Position of the trenches in the pattern

Lessons learned: Phase-mask UV laser interference has been proved as a powerful and versatile technique for the fabrication of 1D and 2D patterns on nanoPS in short time (ns) and over relatively large areas (mm^2).

Conclusions and outlook

Porous silicon allows the development of a wide variety of low-cost devices, entirely based on silicon, and fully compatible with nowadays CMOS technology.

Acknowledgments

UNIVERSIDAD AUTONOMA DE MADRID

GOBIERNO DE ESPAÑA
MINISTERIO DE ECONOMÍA Y COMPETITIVIDAD

cïber-bbn

Instituto de Salud Carlos III

FONDO EUROPEO DE DESARROLLO REGIONAL
"Una manera de hacer Europa"

UNION EUROPEA
FONDO SOCIAL EUROPEO

La Suma de Todos
CONSEJERÍA DE EDUCACIÓN
Comunidad de Madrid
www.madrid.org

POLITÉCNICA
"Ingeniamos el futuro"